THE LATE QUATERNARY ENVIRONMENTAL HISTORY OF THE LAKE HERON BASIN, MID CANTERBURY, NEW ZEALAND.

A thesis

submitted in partial fulfilment

of the requirements for the Degree

of

Master of Science in Geology

in the

University of Canterbury

by

J. M. Pugh

University of Canterbury

2008

Abstract

The Lake Heron basin is an intermontane basin located approximately 30 kms west of Mount Hutt. Sediments within the basin are derived from a glacier that passed through the Lake Stream Valley from the upper Rakaia Valley. The lack of major drainage in the south part of the basin has increased the preservation potential of glacial phenomena. The area provides opportunities for detailed glacial geomorphology, sedimentology and micropaleontogical work, from which a very high-resolution study on climate change spanning the Last Glacial Maximum (LGM) through to the present was able to be reconstructed.

The geomorphology reveals a complex glacial history spanning multiple glaciations. The Pyramid and Dogs Hill Advance are undated but possibly relate to the Waimaungan and Waimean glaciations. The Emily Formation (EM), previously thought to be MIS 4 (Mabin, 1984), was dated using Be10 to c. 25 ka B.P. The EM was largest advance of the Last Glacial Maximum (LGM). Ice during the LGM was at least 150m thicker than previously thought, as indicated by relatively young ages of high elevation moraines. Numerous moraine ridges and kame terraces show a continuous recession from LGM limits, and, supported by decreasing Be10 ages for other LGM moraines, it seems ice retreat was punctuated by minor glacial readvances and still-stands. These may be associated with decadal-scale climate variations, such as the PDO or early ENSO-like systems.

There are relatively little sedimentological exposures in the area other than those on the shores of Lake Heron. The sediment at this location demonstrates the nature of glacial and paraglacial sedimentation during the later stages of ice retreat. They show that ice fronts oscillated across several hundred metres before retreating into Lake Heron proper.

Vegetation change at Staces Tarn (1200m asl) indicates climate amelioration in the early Holocene. The late glacial vegetation cover of herb and small shrubs was replaced by a low, montane forest about 7,000 yrs B.P, approximately at the time of the regional thermal maxima. From 7,000 and 1,400 yrs B.P, temperatures slowly declined, and grasses slowly moved back onto the site, although the montane forest was still the

dominant vegetation. Fires were frequent in the area extending back at least 6,000 years B.P. The largest fire, about 5,300 yrs B.P, caused major forest disruption. But full recovered occurred within about 500 years. Beech forest appears at the site about 3,300 yrs B.P and becomes the dominant forest cover about 1,400 yrs B.P. Cooler, cloudier winters and disturbance by fire promoted the expansion of beech forest at the expense of the previous low, montane forest. Both the increased frequency of fire events and late Holocene beech spread may be linked to ENSO-related variations in rainfall. The youngest zone is characterised by both a dramatic decline in beech forest and an increase in grasses, possibly representing human activity in the area.

Table of contents

List of Figures

List of tables

1 General Introduction

1.1 Introduction

The Late Pleistocene glacial history of New Zealand is well understood, as pioneering glaciologists (Suggate, Soons, Clayton) focused on the geomorphology and categorising the general pattern of glaciation in valley glaciers. However, the timing of events is not, and efforts to link events both locally and globally are hampered by inadequate data. Although the general pattern of glaciation during the last (Otiran) ice age is now well defined, detailed dating and sedimentological studies are limited. The Lake Heron area is an intermontane basin approximately 30 kms west of Mount Hutt, bound by the Arrowsmith Range to the west and the Palmer and Taylor Ranges to the north and east respectively. Sediments within the basin are derived from a lobe of the Rakaia Glacier flowing through from the upper Rakaia Valley. As the topography slopes back into the Rakaia Valley, and no major drainage occupies the valley, phases of ice retreat left large volumes of dead ice in the system. Upon complete ice removal from the basin, large areas of glacial deposits remained largely undisturbed due to minimal reworking from Holocene rivers. This increased the preservation potential of glacial deposits within the basin makes the area an outstanding prospect for detailed glacial sedimentary work.

1.2 Scope of the investigation

The Lake Heron basin was chosen for investigation because of the excellent preservation of glacial features, which provided the opportunity to construct a very detailed glacial history spanning the Last Glacial Maximum (LGM) through to the late Holocene. The main aims of the study were to:

1. Map and describe the glacial geomorphology in the basin in high detail. Apply new techniques, including Surface Exposure Dating (SED) of moraines and reconstruction of ice profiles, to explore ice thicknesses during the Last Glaciation.

2. Using glacial sediments, develop a reconstruction of the Late Glacial/Deglacial dynamics of the ice front.

3. Investigate climate conditions from the late glacial to present based on changes and changes in pollen assemblages.

1.3 Previous research

The geomorphology of the Lake Heron basin was first noted by pioneering geologist Sir Julius Von Haast in 1866 during his expeditions to the headwaters of the Rakaia River. Subsequent excursions under the instructions of the Canterbury Provincial Chambers resulted in the compilation of Von Haast's 1879 Geological Map of the Canterbury-Westland Province (Von Haast, 1879). During these early excursions, Haast collected many plants, as did Speight et al (1910). These scientists were the first to systematically describe the glacial features of the Lake Heron basin. They briefly described moraines and took a particular interest in the large scale features such a ice-planed slopes, Roches moutonees and truncated spurs. Speight (1934) followed up his early work by investigating glacier movement in the Rakaia Valley, describing the Lake Heron basin as "perhaps the main distributory overflow" (Pg. 478). Speight emphasized the important role that the Ashburton and Cameron Glaciers played during glaciation. Speight documented that moraines in the basin were a recessional feature, and inferred that glacial sediments record periods of glacial advance and retreat.

Burrows and Russell (1975) investigated the upper Rakaia valley and identified several Late Glacial/Holocene advances. Of particular importance was their description of the Lake Stream moraine. This glacial advance terminated at the northern tip of the Lake Heron basin. The advance is often associated with the Younger Dryas Chron, a topic of much debate to researchers studying the timing and forcing of inter-hemispheric glaciations. Burrows and Russell also retrieved sediment cores from both Quagmire Tarn and Windy Tarn on Prospect Hill, located at the far northern end of the basin, and their studies of post-glacial vegetation change and the regional fire history have added a great deal to Canterbury glacial climate reconstructions. Burrows et al (1990) using lichonmetric dating to revise the chronology proposed by Burrows and Russell (1975).

Burrows et al (1993) studied the vegetation changes in the Arrowsmith Range. A suite of radiocarbon dates accompanied the paper, which highlighted the sporadic and localised nature of late Holocene fire events in the area. Rodbell (1986) investigated soils-time relationships in the Arrowsmith Range and attempted to develop soil chronofunctions to enable distinction between Holocene and pre-Holocene moraines. His work showed close correlations between Holocene soils and underlying deposits. However, loess redistribution hindered correlations for pre-Holocene deposits.

It was not until Mabin (1980) carried out systematic description and categorisation of glacial deposits in the Rangitata and Ashburton valleys that a chronology was developed for the area. Mabin defined five advances spanning three glaciations and proposed correlations with other South Island east coast glacial systems. He also assigned formal names to the glacial deposits in the Lake Heron basin. From oldest to youngest, the advances are the Pyramid, Dogs Hill, Trinity, Emily and Lake Heron. Mabin (1980) placed Pyramid deposits into the Waimaungan Glaciation and Dogs Hill Deposits into the Waimean Glaciation. Any younger glacial deposits were placed in the Otiran Glaciation. Oliver and Keene (1990) remapped the geology of the Lake Clearwater area and the southern portion of the Lake Heron basin at 1:50 000 scale. From this work they redefined the glacial chronology, renaming late Emily moraines as the Johnston Stream Formation and ascribing the Trinity Formation to deposits in the Lake Clearwater basin.

1.4 Methodology

1. Geomorphological map of Lake Heron basin: mapping was done using aerial photograph interpretation and followed up with ground reconnaissance. Elevations and geographic positions were positioned with a handheld GPS unit. A geomorphological map was drawn using Arcmap, a GIS based mapping program.

2. Surface Exposure Dating (SED): the ages of glacial advances were constrained by dating an *in situ*-produced cosmogenic radionuclide (^{10}Be) in moraine boulders. This procedure indicates the length of time a freshly eroded boulder has been exposed to cosmic rays. Chemical extraction of ^{10}Be isotopes from quartz was undertaken in the

Cosmogenic Preparation Laboratory of the Department of Geological Sciences, University of Canterbury (UoC), and the quartz sample was analysed using the ANTARES accelerator at ANSTO in Sydney.

3. Ice profile reconstructions: Elevations of glacial ice were calculated out using the GLACPRO programme (Locke, 2007). This GLACPRO model uses iterative approach to the modeling of ice masses, based on the theory that ice behaves in a mechanically predictable fashion. It plots the up-ice elevation gain from a terminal moraine.

4. Sedimentology: detailed two-dimensional logs and summary profiles were drawn following systems outlined in Eyles *et al* (1983) and Evans (2004). Clast roundness data were obtained by collecting 50 samples from a designated area and measuring the A, B and C axis. The roundness of the clast was also estimated and any striations or faceted faces were noted. Clast and fabric data were presented using the Stereonet programme.

5. Micropalaeontology: lake sediments will be collected using a hand-operated D-section corer and described according to the Troels-Smith system (1955). Age control of the sediment core was provided by way of luminescence and AMS radiocarbon dating. Pollen slides were prepared following the methods outlined in Hofmann (1986). Counting and identification of pollen grains was carried out using a comparison microscope. Chironomid remains were processed following the method outlined in Walker (2001) and were transferred to a counting tray for examination under a dissection microscope. Head capsules of chironomidae larvae were identified with the aid of a key and figures from Woodward (2006). Charcoal abundance and volume were calculated using the technique described by Clark (1982). They were presented as the volume of charcoal per unit volume of sediment (VR). Results were presented using the PSIMPOLL programme (Bennett, 2002).

2 Setting

2.1 Introduction

The Lake Heron basin is an intermontane basin filled by Quaternary glacial deposits and bounded by glacially sculptured hills composed of Torlesse Supergroup. The greywacke sandstones and siltstones (Oliver and Keene, 1990) of the Torlesse basement are unconformably overlain by Tertiary cover sequences. Only small remnants remain today, usually in fault-angle depressions which developed following uplift and erosion associated with the Kaikoura Orogeny (Oliver, 1977). Late Pleistocene glacial activity filled the basin floor with sediment and deposited moraines on both the basin floor and along the hillsides.

2.2 Geology

2.2.1 Tectonic setting and basin development

The Torlesse terrane is an extremely thick succession of sediments that was deposited during the Triassic Epoch into an elongated oceanic trough situated along the southeast coast of Antarctica. Sediment was supplied from an eroding landscape, with uplift and terrane emplacement driven by subduction of the Phoenix Plate. The Torlesse terrane is divided into the Rakaia subterrane and the younger Pahau subterrane. It was deformed and accreted into a proto-New Zealand during Jurassic times in an event known as the Rangitata Orogeny, forming a mountainous landscape (Bishop et al, 1985).

With the cessation of subduction, plate motion reversed and a zone of rifting occurred within the back-arc region of the Antarctic plate. A major unconformity separating basement rocks from younger 'cover' sequences occurs within fault-bounded marine and non-marine basins (Laird, 2004). In the Canterbury region, extensional tectonism produced fault-angled depressions that in some areas accumulated more than four kilometers of sediment. A transgressive sequence followed, beginning with terrestrial sediments deposited unconformably on the basement Torlesse Supergroup. These

passed into shallow marine sands and glauconitic sediments, culminating in widespread calcareous muds and micritic ooze.

The sea reached its maximum inland extent during the Oligocene; however, the onset of the Kaikoura Orogeny slowly uplifted the land. The change in tectonic setting from extension to oblique collision during the early Pleistocene along the newly-formed plate boundary marks the beginning of the present plate boundary tectonics. From Miocene times to the Quaternary, the Canterbury region experienced major compressional deformation, culminating in the main phase of the Kaikoura Orogeny.

At present, the New Zealand micro-continent straddles the Australia-Pacific plate boundary zone. The relative motion of these plates has defined upper Cenozoic evolution and defined the present shape of the emergent New Zealand landmass. In the South Island, the major features are the Alpine Fault and the Marlborough Fault Zone. These have been recognised as a transform linking obliquely convergent subduction zones of opposite polarity; the Kermadec-Hikurangi trench in the northeast and the Puysegar trench to the southwest (Norris et al, 1990). The Alpine Fault forms a linear feature that trends northeast for 420km along the west side of the South Island (Berryman et al, 1992). Offshore studies indicate that it may extend for a further 200km off the southwest tip of Fiordland (Delteil et al, 1996). Landforms within the northern portion of the Canterbury region reflect the southward transition from oblique subduction to oblique continental collision, with tectonic deformation progressively diminishing to the southeast (Pettinga et al, 2001). Structures in mid Canterbury, such as the Lake Heron basin, trend in a northerly direction in response to continent-continent collision.

Pettinga et al (2001) sub-divided the Canterbury region into eight domains according to structural styles of deformation. The Lake Heron basin occurs within a zone of reverse and back thrusting. Pettinga et al (2001) described this zone as the "'feather-edge' margin of the Southern Alps double-sided wedge style of thrust deformation". Little has been done in terms of systematically mapping active faults in South Canterbury. The most recent relevant to this study is the 1:50,000 geological map produced by Oliver and Keene (1990), who mapped several faults within the Lake Heron basin. The presence of faults indicates the ongoing influence of tectonic activity in the basin.

2.2.2 Bedrock geology of the Lake Heron basin

'Basement' rocks within the Canterbury region are considered to be those that are older than the Cretaceous period. Within the Lake Heron basin, basement rocks consist of the Triassic to Jurassic Torlesse Supergroup. The Mount Somers Group of volcanics is a significant feature of mid Canterbury, and is located to the southeast of the study area. The group consists of a suite of calc-alkaline terrestrial volcanics of mid Cretaceous age erupted onto Torlesse rocks over a period of several million years (Oliver, 1977). In the study area, the Barrosa Andesite Formation occurs on the southeast portion of Clent Hills. Within the Lake Heron basin, Torlesse rocks are subdivided into the Taylor Group, which forms all of the adjacent ranges, and the Clent Hills Group, which is found only on the northern portion of Clent Hills. The thick sandstones and interbedded siltstones of the Taylor Group also form the bedrock ridges of Isolated Hill, Ricky Spur, Longman Range and Mt Sugarloaf (Oliver and Keene, 1990). A finer grained equivalent containing many conglomeratic beds form the middle portion of Clent Hills. The Middle to Upper Jurassic sandstone and siltstones of the Clent Hills Group occur on the northwestern portion of Clent Hills, along the northern margin of the Stour River, and in the floor of the basin (Oliver and Keene, 1990).

Several small Tertiary inliers outcrop within the study area, usually in fault-angle depressions (Oliver, 1990). In the northern part of the Lake Heron basin there are late Eocene to early Miocene marine sediments which are overlain by a friable sandstone. These occur in outcrops in Turkey Gully (Field and Brown, 1986) and up the Smite River (Mason, 1948). A similar sequence of Tertiary strata occurs in two outcrops in the northern branch of the Swin River (Field and Brown, 1986; Fowke, 1974), with the addition of a mudstone unit within the limestone. The most complete sequence of Tertiary rocks occurs on the northwest of Clent Hills, and was noted by Haast (1877). At Haast Stream, the same sequence of marine sediments occurs, but here, late Cretaceous clays and sands underlie it. The Tertiary sequence is of mainly shallow water marine sediments deposited onto a surface of low relief composed of either Torlesse greywacke or Mt Somers Volcanic 'basement'(Field and Brown, 1986). The lack of Tertiary rock preservation can be attributed to post-Oligocene tectonism,

including the Kaikoura Orogeny (Oliver, 1977), and the near vertical dip of beds at Haast Stream is indicative of this.

2.3 Physiography

The Lake Heron basin is 30 km long in a north-south direction and is typically between 7 and 10 km wide, although it narrows considerably north of Lake Heron (Fig. 1.1). Its floor is approximately 700 m above sea level; 1200m below the summits of the bounding mountain ranges. The highest peak is Mount Arrowsmith in the Arrowsmith Ranges, which rises to 2781m asl. Several glaciers stem from this peak, two of which have previously advanced into the Lake Heron basin. The Cameron Glacier is currently in retreat (Chinn, 1996), but during large glaciations it flowed 16 km before coalescing with the lobe of the Rakaia Glacier flowing down-valley from the north. The Cameron River has constructed a large alluvial fan into the northeast corner of Lake Heron, whilst on the opposite side of the basin the Swin River has done the same. The south branch of the Ashburton River also originates from Mt Arrowsmith and is separated to the south of the Cameron Valley by the Wild Mans Brother Range (Figure 2-1).

The Lake Heron basin is capped at its northern end by Shaggy Hill, while at the southern end it is continuous with the east-west trending Lake Clearwater basin. Several glacial lakes occur within the basin, the largest being Lake Heron, from which Lake Stream flows (Figure 2-1). As drainage lines are poorly developed south of Lake Heron, many swamps and small lakes occur. Gentleman Smith Stream transects the southern portion of the basin with contributions from the Clent Hills, Johnston and Jacobs Streams. Gentleman Smith Stream drains into the Maori Lakes, which feeds the south branch of the Ashburton River (Figure 2-1). In the southeastern corner of the basin, Lake Emily and Manuka Lake feed into the Stour River, which sweeps around the east of Clent Hills before discharging into the Ashburton River (Figure 2-1).

Lake Heron itself is an important feature within the basin. It resides within a glaciated depression impounded behind moraines and discharges into the upper Rakaia River to the north (Figure 2-1).

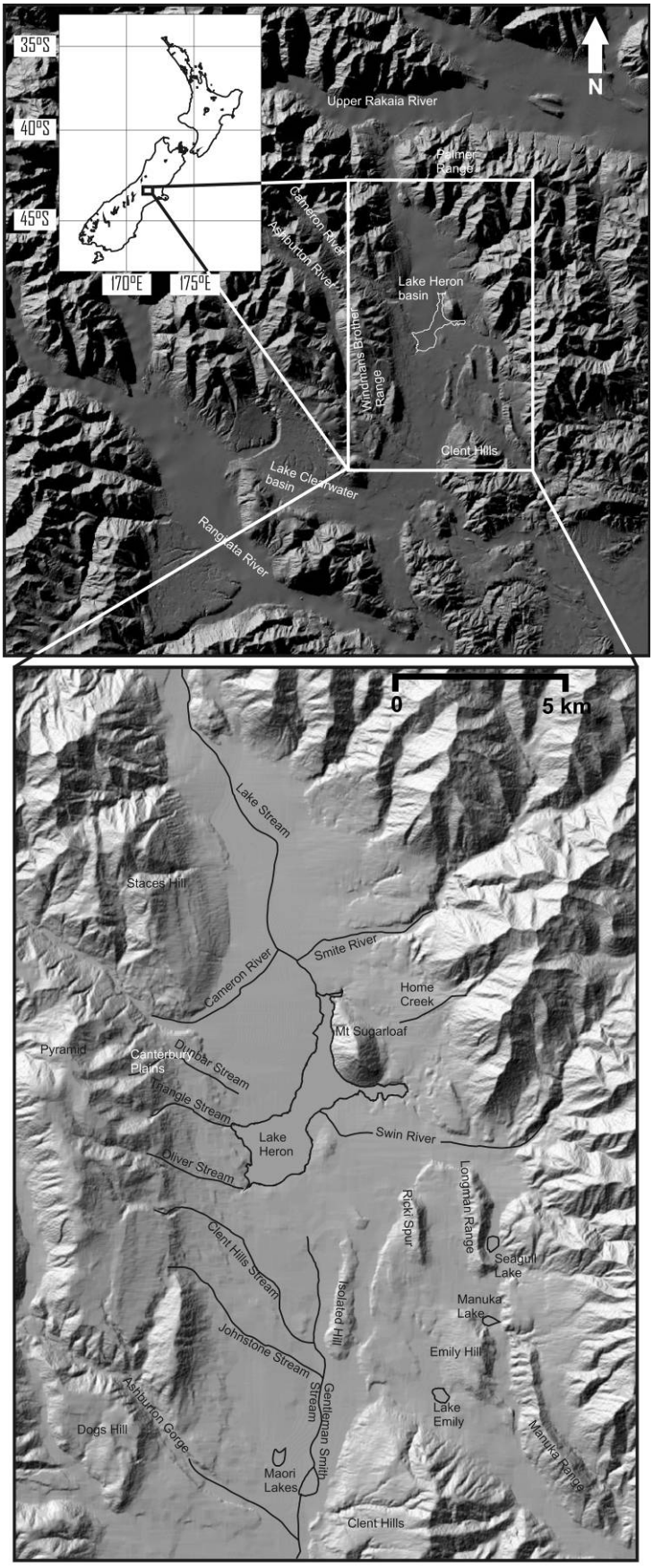

Figure 2-1 Location of Lake Heron basin.

2.4 Climate

A complex climate exists in New Zealand, ranging from subtropical in the far north to cool temperate climates in the far south, with alpine conditions in the mountainous areas. The Southern Alps of the South Island form a natural barrier against the prevailing westerly winds, separating the island into different climate regions whereby average rainfall is enhanced on the upwind side and a rain shadow effect is experienced on the downwind side (Griffiths and McSaveney, 1983; Henderson and Thompson, 1999). This orographic effect produces high river flows on the Canterbury Plains, which often occur in conjunction with high temperatures and low humidity. The mean annual rainfall at Upper Lake Heron Station from 1969 to 1981 was 1047mm with the mean monthly rainfall varying from 46mm in February to 119mm in August (Bowden, 1983). Mean monthly temperatures at the Lake Coleridge Climatological Station in the Rakaia valley range between 3.5°C (July) and 15.3°C (January).

2.5 Vegetation

2.5.1 Introduction

Glaciations, climatic variation and fire, both prior to and during human occupation, have greatly modified the vegetation cover in the basin from one of widespread podocarp and beech cover to a treeless landscape. The Lake Heron basin occurs within a 125km stretch of land on the eastern side of the South Island that is devoid of beech forest and known as the “Canterbury beech gap”. Fossil evidence suggests that this beech gap existed even before the Last Glacial Maximum (LGM) (McGlone, 1988). The current lack of beech forest is attributed to the obliteration of vegetation in the glaciated central Southern Alps during the last (Otiran) glaciation (Burrows, 1965). The remaining isolated beech stands are thought to be derived from pockets that survived the last glaciation (Molloy and Cox, 1972).

Moar (1971) defined five pollen zones in the post-glacial development of vegetation in the Southern Alps.

1. Grassland-shrubland;
2. Shrubland;
3. Podocarpus forest;
4. Nothofagus forest
5. Deforestation- only recognised in Canterbury.

The first phase represents the end of the last glaciation, approximately 14,000 years ago (Suggate, 1965) although it is likely that grass and shrubland already existed in inland Canterbury at this time (see Figure 2-2). Shrubs and tall tussock grassland readily replaced these assemblages. The expansion of podocarp forest occurred about 10,000 years ago, although not necessarily synchronously (Moar, 1971). In the northern South Island, bog pine (*Halocarpus bidwillii*) and celery pine (*Phyllocladus alpinus*) began to replace the shrubland after 12,000 yrs B.P (McGlone et al, 1988). The late-glacial period ended about 10,000 years ago at a time when annual temperatures were similar those of the present day. Beech (*Nothofagus*) expansion on the eastern South Island is poorly defined and is suggested to have occurred somewhere between about 5,000 and 8,000 years ago (Lintott and Burrows, 1973). Deforestation in Canterbury, attributed to Polynesian fires, is recorded in pollen diagrams and evidenced in widespread forest charcoals. Radiocarbon dates suggest deforestation occurred between 500 years and 600 years ago (Molloy, 1977).

2.5.2 Forest

Mountain beech (*Nothofagus solandri var. cliffortiodes*) is the dominant forest type in the Upper Rakaia valley. The Lake Heron basin is devoid of forest, the exception being an isolated remnant of mountain beech forest which occurs near Bush Creek and is the only occurrence of *N. menziesii* in the Rakaia Catchment. Beech forest understory is typically floristically poor, usually limited to a ground cover of divaricating shrubs (*Coprosma*) in wetter areas or ground ferns in drier areas. The study area occurs within the Canterbury ‘beech gap’.

There is no Podocarp forest in the study area, but a few scattered remnants of *Podocarpus hallii* and *Griselinia littoralis* forest occur nearby in the headwaters of the

Wilberforce, Mathias, Rakaia, Lawrence, Clyde and Havelock rivers. The understory of the Podocarp forest is a diverse variety of evergreen shrubs and lianes, including *Libocedrus* and *Metrosideros*. *Weinmania racemosa* is rare. Where beech forest adjoins podocarp forest, mixed podocarp-beech forest occurs (Bowden, 1983).

Molloy and Cox (1972) place the minimum date for the establishment of mountain beech in the Rakaia Catchment at about 5,000 yrs B.P. Forest development in Canterbury was at its maximum between 3,000 and 5,000 years ago (Molloy, 1969), post-dating by several thousand years a putative period of maximum warmth and effective rainfall known as the post-glacial climatic optimum. Since then the area of indigenous forest has shrunk. Bowden (1983) associate this with the deteriorating climate and the inability of the forest to cope with the complete range of climate factors. Wood and charcoal deposits are evidence of former widespread beech and podocarp forests over much of the South Island (Molloy *et al*, 1963). The extent and distribution of subfossil remains and present day stands in the Rakaia catchment suggest that this is also the case there.

2.5.3 Subalpine scrub

Subalpine scrub is best developed in areas of high rainfall such as the Westland mountains and is less extensive on the drier flanks east of the Main Divide (Burrows, 1990). In Canterbury, the most extensive areas of subalpine scrub occur within the "beech gap" and comprise a variety of communities including *Dracophyllum, Coprosma, Oleria, Senecio* and *Hebe*. These commonly occur with *Phyllocladus alpinus* and *Podocarpus nivalis*.

2.5.4 Alpine and subalpine grassland

Alpine and subalpine grasslands occur above the forest and subalpine scrub, of which the dominant cover is snowgrass (*Chionochloa*) (Bowden, 1983).

2.5.5 Current vegetation cover

The present vegetation cover within the Lake Heron basin is tall tussock grassland, dominated by *Chionochloa sp. cf. rigida*, and is estimated to comprise more than 80% of the total vegetation cover of the area (Burrows, 1993). Adventive grasses (*Anthoxanthum odoratum, Agrostis capillaris*) coexist with it on the valley-floor. Snow tussock grassland is extensively developed on hill summits and ridges (Bowden, 1983). Short tussock grassland is dominated by *Festuca novae-zelandiae* and occurs on dry valley flats. Red tussock grassland occurs in the north of basin along the edges of Lake Stream along with various sedges and rushes. This reflects the poor drainage in this part of the basin.

Few native trees occur in the study area, other than isolated stands of *N. menziesii* (silver beech). Burrows (1993) identified *Hoheria lyallii* in the Ashburton and Cameron valleys and *Sophora mycrophylla* near the mouth of the Cameron Valley. He also noted abundant shrub communities in tributary valleys, composed mainly of matagouri, *Olearia virgata, Coprosma spp., Aristotelia fruticosa, Corokia cotoneaster, Hymenanthera alpine. Kunzea ericoides* and *Leptospermum scoparium* are present near where the Cameron River enters the Lake Heron basin (Burrows, 1993).

2.6 Human occupation

Several Maori occupation sites have been identified within the Rakaia Catchment (Douglas *et al*, 1979; McIntyre, 2007). These settlements used the Whitcombe and Browning Passes to gain access to the West Coast. Fires, believed to be both accidental and deliberate, have caused extensive modification of the vegetation, and this has been attributed Maori movements. The loss of vegetation in parts of the country is thought to

have triggered a phase of slope instability. By the time of European colonisation, substantial areas in the Rakaia catchment had been modified.

The Canterbury Association was established in 1848 to guide the development of Banks Peninsula and of the plains area between the Waipara and Ashburton Rivers. After a slow start due to high land prices, by 1852 applications had been made for most of the hill country, with development south of the Rakaia River delayed because of the problem the river posed to transport and communications. At the time of occupation, tussock and matagouri (*Discaria toumatou*), interspersed with wild spaniard (*Astelia ssp.*), predominated in the upper Ashburton region. The farmers' practice was to regularly burn the tussock and scrubland to encourage young growth to be palatable to stock. The first 5 to 10 years of European burning initiated a major phase of slope instability, of which the scars remain visible today.

2.7 New Zealand Glaciation

Evidence of the earliest New Zealand glaciations is fragmentary. The earliest glacial sediments are of Late Pliocene age and a hiatus of about 1.5 million years occurs before glaciations are inferred from uplifted marine terraces and marine sediment cores. On land, there is good evidence for glaciations spanning the last 0.35 m years and there is age constraint in several glaciated valley systems for the last (Otiran) glaciation.

This section is not intended as a complete review of New Zealand glaciations, but rather to be a summary of the timing of those events in South Island east coast valley systems which have relevance to the study. The section highlights the complexity of New Zealand glaciation, especially during the last glaciation.

2.7.1 Late Pliocene to Late Pleistocene

Glaciations occurred at various times in mountainous areas in New Zealand during the Quaternary Epoch (the last 2.6 million years). Early Quaternary glaciation in the North Island are recorded in the marine stratigraphy as uplifted marine basins. These include

the Wanganui, Wairarapa and Hawkes Bay basins (Figure 2-2), and suggest glacially affected sea levels.

On land, the first glacial deposits are of late Pliocene to Early Pleistocene age. Glacial sediments and outwash of the Old Man Group occur on the West Coast of South Island and in Nelson (Figure 2-2); the Moutere Gravel is interpreted as outwash of the same group (Colhoun and Shulmeister, 2007). A later series of glacial deposits unconformably overlie the Moutere Gravels and is attributed to the Porika Glaciation, approximately 1.9 million years ago. Sediments of this glaciation are extremely patchy in distribution and it is therefore unlikely that it represents a single glaciation.

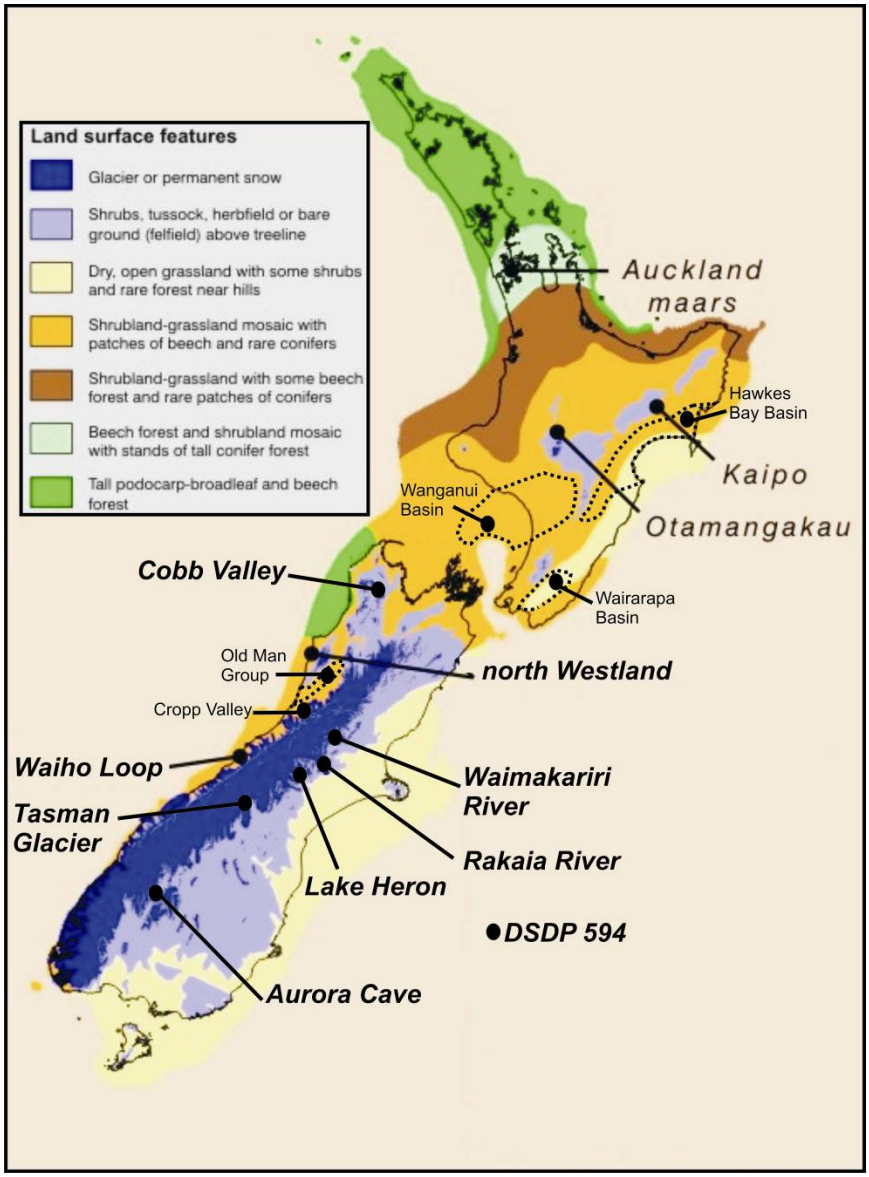

Figure 2-2 Glacier limits and vegetation zones at the Last Glacial Maximum (c. 22,000 cal yrs B.P) and other locations mentioned in the text. Modified from Alloway et al, (2007).

From the middle Quaternary, nine period of South Island glaciation are inferred from a marine sediment core located 250km east of the South Island (Figure 2-2). The sediments from DSDP 594 span Oxygen Isotope Stage 18 – 2 (Nelson et al, 1983; Carter and Gammon, 2004), of which the last ~350 ka is identified onshore (Suggate, 1990) The standard middle Quaternary sequence for South Island correlation are flights of uplifted marine terraces in Westland. As there are few reliable ages beyond ~20 ka ago, the marine terraces correlate with an interglacial high sea level (Suggate, 1990, 2004). Four Quaternary glaciations are recognized in the South Island; the Nemonan (OIS 10), the Waimaungan (OIS 8), the Waimean (OIS 6) and the Late Quaternary Otiran Glaciation (OIS 2 and 4). During the middle Quaternary, glaciers spread several kilometers onto the plains (Soons and Gullentops, 1973).

2.7.2 The Last (Otiran) Glaciation

Based on moraine distributions, the Otiran glaciations were much less extensive than the middle Quaternary glaciations, although the only published dates of terrestrial Waimean glaciation on the east coast of the South Island are glacifluvial gravels in Aurora Cave in Otago (Figure 2-2) (Williams, 1996). Cooke (1988) analysed DSDP 594 and suggested that MIS 5 "exhibits no extreme glacial conditions seen in Stages 2, 4 and 6". However, buried MIS 4 outwash gravels in Westland imply these glacial advances were overrun by subsequent larger glacial advances (Preusser *et al*, 2005). The Aurora Caves also show significant ice advances during MIS 4, recorded in high-level fill approximately 65,000 cal yrs B.P (Williams, 1996). Other OIS 4 deposits include buried sediments in the Rakaia Valley (Figure 2-2) (Shulmeister *et al*, unpub data). Smaller OIS 3 ice advances occur at several sites in the South Island. At Aurora Cave, two advances occurred about 46,000-48,000 and about 41,000-40,000 yrs B.P (Williams, 1996), while similar aged advances occurred in north Westland (Figure 2-2) between 49,000 – 44,000 cal yrs B.P and c. 34,000 – 28,000 yrs B.P (Suggate and Almond, 2005).

2.7.3 The Last Glacial Cold Period

The major advances of the Last Glacial Cold Period (LGCP) are poorly dated and although considered broadly synchronous, the precise timing of events varies according to local environmental factors (Pillans, 1991). The most common technique used to date glacial deposits and landforms has been radiocarbon dating. This may be unreliable due to contamination by younger material, which occurs especially in areas of high precipitation such as the West Coast. The direct dating of glacigenic deposits using luminescence or surface-exposure dating methods is becoming more common, although the methodologies are still being refined (Alloway et al, 2007). The commonly held idea is that there have been two phases of glacier advance. The first was underway by 22,000 cal yrs B.P in Westland and lasted until 18,000 cal yrs B.P, and the second occurred between 16,000 and 14,000 cal yrs B.P (Fitzsimons, 1997).

At Hokitika in Westland, the maximum ice advance is radiocarbon dated to 24,500–21,500 C14 yrs B.P, followed by a smaller advance at 20,500–19,000 C14 yrs B.P (Suggate and Almond, 2005). At Lyndon Stream in the Rakaia Valley, radiocarbon dated organic material suggests two ice advances, one before 24,500 C14 yrs B.P and one after 22,500 C14 yrs B.P (Soons, 1963). Surface exposure ages indicate the largest advance in the Rakaia is the Tui Creek advance at 23,000–21,000 cal yrs B.P (Shulmeister *et al*, 2007). Ice remained in the valley until ~13,000 cal yrs B.P, at which time it rapidly retreated up-valley (Shulmeister *et al,* 2007). In the Waimakariri Valley (Figure 2-2), weathering rind ages (Ricker et al, 1992) suggest the Blackwater advances were the largest advance of the LGM. The Poulter advance was the final advance of the LGCP in the Waimakariri Valley, with retreat prior to c. 17,000 cal yr B.P (Gage, 1958). In Nelson and Marlborough, advances dated between 23,000 cal yrs B.P and 22,000 cal yrs B.P are representative of the LGM (Colhoun and Shulmeister, 2007). Younger advances succeeded these. The St. Arnaud advance in the Nelson Lakes area has been dated as being younger than 17,800 cal yrs B.P (Suggate, 1990) and in the Cobb Valley in northwest Nelson (Figure 2-2), substantial retreat occurred after 19,000 cal yrs B.P (Shulmeister et al, 2005).

2.7.4 The Post Glacial period

The beginning of the present Aranuian interglacial is characterised by a period of sustained retreat (Fitzsimons, 1997) and began approximately 14,000 cal yrs B.P (Suggate, 1961). The position of the last glacial-interglacial boundary has been debated, as commentators discuss the definition of a glacial versus an interglacial. Younger ages have been proposed, such as 13,000 – 12,500 cal yrs B.P (Mabin, 1983) and 10,000 cal yrs B.P (Burrows, 1974). What is unquestioned is that a climate reversal occurred in the early Aranuian (Alloway *et al,* 2007) and that significant ice lingered in glaciated South Island valleys.

The timing and causes of this late glacial readvance have been the focus of considerable research, as the existence of an advance may be coeval with the Younger Dryas Chron (12,900 – 11,600 cal years B.P) or with the Antarctic Cold Reversal (14,500 – 12,900 cal years B.P). In the upper Rakaia valley, the Lake Stream advance occurred at about 12,000 C14 yrs B.P, terminating at the northern end of the Lake Heron basin (Burrows and Russell, 1990). Of particular importance to the debate is the readvance of the Franz Josef Glacier in Westland that constructed the Waiho Loop Moraine several kilometers beyond the mountain front (Figure 2-2). Radiocarbon ages suggest that the moraine was deposited slightly after 11,050 ± 14 yrs B.P (Denton and Hendy, 1994), indicating an advance either immediately before or early in the Younger Dryas Chron (YDC). This has been used as evidence of Northern Hemisphere climate forcing. In contrast, Barrows *et al* (2008) ^{1}°Be dated the moraine at ~10,480 cal yrs B.P, which postdates the YDC. These arguments however may be moot as the Waiho Loop moraine's unique lithological characteristics suggest landslide debris make up a large portion of the sediments (Santa *et al*, unpub). This suggests that a landslide onto the glacier in its upper reaches may have caused the late glacial surge, and therefore no such climate association exists.

The late glacial Misery Moraines at the head of the Waimakariri Valley may be evidence of the YDC (Ivy-Ochs et al, 1999). However, recent recalculations by Barrows *et al* (2008) of the ^{1}°Be ages to 13,420 ± 630 cal yrs B.P suggest ice retreated from the Lake Misery moraines at the end of the Antarctic Cold Reversal. This would

have been about 1,800 years before the conclusion of the YDC and ~3,000 years before the Waiho Loop moraine was abandoned by ice (Barrows *et al*, 2008). There is no evidence of a glacial readvance in the Cobb Valley in northwest Nelson, where no moraines were deposited after 15,500 cal yrs B.P (Shulmeister *et al*, 2005). In the Rakaia valley, a continuous sequence of LGM moraines occurs from about 23,000 cal yrs B.P to 13,000 cal yrs B.P, with no significant late glacial readvance (Shulmeister *et al,* unpub data).

While glaciers generally retreated from their late glacial positions between 12,000-9,000 cal yrs B.P (Gellatly at al, 1988), there is evidence of glacial readvances in the early Holocene. These advances are often poorly dated and ages are often conflicting. The Jagged Stream ice advance in the upper Rakaia valley advanced to within 5 km of the Lake Stream advance. It is radiocarbon dated to be older than 9,520 ± 95 C14 yrs B.P (Burrows, 1975), and is suggested to have occurred between 11,900 and 10,000 cal yrs B.P (Fitzsimons, 1997). A similar aged advance occurs at Cropp River on the West Coast (Figure 2-2), where wood at the base of compacted diamicton has been dated to 10,250 ± 150 C14 yrs B.P. Basher and McSaveney (1989) reconciled this date with the sedimentology and geomorphology of the area and suggested an ice advance occurred between 11,000-10,000 cal yrs B.P.

The Birch Hill moraines, 18 km down valley from the Tasman Glacier (Figure 2-2), have been much debated as conflicting ages have been published (Porter, 1975; Burrows, 1980). The general consensus is that they are older than 8,000 cal yrs B.P, and possibly much older (Porter, 1975; Burrows and Gellatly, 1982). The earliest McGrath advance in the Waimakariri valley have been weathering-rind dated to be about 9,700 ± 900 years B.P, followed by another at 5,900 ± 650 years B.P (Ricker et al, 1992). The youngest set of moraines in Westland occurs at the Franz Josef glacier and date to about 5,000 cal yrs B.P (Sara, 1979). This is roughly coeval with a 4,500 cal yrs B.P age for the Mein Knob advance in the upper Rakaia valley (Burrows, 1975).

3 Glacial Geomorphology and Chronology

3.1 Introduction

The shape of the Lake Heron basin is the result of its geological structure, with the mountainous borders and valley floor dependent on a history of faulting and differential uplift. The Kaikoura Orogeny in the Early Pleistocene (Gage, 1977) determined the basic drainage pattern in the Southern Alps. Stream patterns are influenced by tectonic factors as they utilise the easily erodible belts of strata and fault-crushed rock (Gage, 1977) and move in response to differential uplift. Glaciations have furthered the modifications. The present landforms are the result of erosional and depositional agents that have occurred during the ongoing tectonic movements. The biggest single process that has modified the tectonic landscape is glaciation.

3.2 Methodology

3.2.1 Geomorphic mapping

The geomorphology of the study area was initially mapped from aerial photographs held at the map library at the University of Canterbury. They included the 3731 and 3730 runs from 1964, which were taken at 25,000 ft, the S73 series from 1974 taken at 18500 ft and the 1982 SN 8039 runs taken at 30000 ft. A base map was created which identified areas requiring further attention. This was followed up by ground reconnaissance. Field work was conducted throughout 2007. Elevations and geographic positions were taken with a handheld Garmin e-trex GPS unit. The maps were produced using Arcmap, a GIS based mapping programme. Grid references refer to Department of Lands and Survey Information 1:50,000 topographical map sheets J35 (Arrowsmith) and J36 (Mount Harper / Mahaanui).

3.2.2 Cosmogenic sampling technique

Surface Exposure Dating (SED) counts *in situ*-produced cosmogenic radionuclide (^{10}Be) from moraine boulders, using quartz minerals. The length of time that a freshly eroded boulder has been exposed to cosmic rays is thus able to be calculated. At least 1-3 m of rock must be eroded from a pre-exposed surface. The technique is based on the assumption that glacial plucking and abrasion are highly effective at exposing new surfaces.

Sampling for exposure dating concentrated on glacial erratic boulders associated with moraines at key locations. Boulders were selected according their geomorphic setting and size; they needed to be at least 1.5 m in diameter (Figure 3-1). Boulders that may have been compromised by shielding from the sun's rays, or that may have been previously buried were avoided. Boulders that may have been disturbed subsequent to deposition from a glacier were also avoided, as any disturbance may have exposed a new surface to incoming cosmic rays, resetting the "cosmic clock". Collecting the samples involved chiselling off at least 1.5 kg from the top 4 cm in the center of the boulder (Figure 3-1). All the SED samples were from Torlesse greywacke boulders and sample collection often targeted quartz veins (see Appendix C: SED and C14 data).

Putkonen and Swanson (2003) suggested one to four boulders from small (<20 m high), young (<100,000 year old) moraines. Seven erratic boulders from three separate moraines were sampled for cosmogenic exposure-age dating (map 1). Surface samples were extracted from two erratic boulders from a lateral moraine on Emily Hill (751 m), three from a moraine adjacent to Johnstone Stream (700 m) and two from a moraine near Staces Hill (1210m) (map 1).

Figure 3-1 Erratic boulder on Emily Hill sampled for cosmogenic dating (Mother for scale).

Chemical extraction of ^{10}Be isotopes from quartz was undertaken in the Cosmogenic preparation Laboratory of the Department of Geological Sciences (UoC), supervised by Lab Manager Rob Spiers. Samples were initially crushed and sieved to between 212-500 μm, and then cleaned using phosphoric acid until all that remained was a minimum 30-50 g of pure quartz. The quartz sample was analysed using the ANTARES accelerator at ANSTO in Sydney. Rother (2006) provides a full description of the background of cosmogenic dating and isotope measurement. A production rate of $5.1 \pm 0.3\ a^{-1}$ for ^{10}Be (Stone et al, 2000) was applied to calculate the age of the boulder.

In terms of interpreting the age of a particular moraine, studies have shown that erosion of the moraine surface and consequent exhumation of fresh boulders results in sets of boulders from the same moraine yielding a lower age limits than the "true" age of the moraine (Putkonen and Swanson, 2003; Applegate *et al,* 2008). Putkonen and Swanson (2003) suggested that the oldest obtained boulder age represents ≥90% of the moraine age, while Applegate et al (2008) suggested the age of the moraine lies somewhere close

to the oldest age. Therefore, the oldest sample probably best represents the age of the moraine and will be used in discussion in this study unless otherwise stated.

3.2.3 Ice profile reconstruction

Elevations of glacial advances were reconstructed using GLACPRO (Figure 3-10) (Locke, 1996, 2007). The GLACPRO model is an iterative approach to the modeling of ice masses, based on the theory that ice behaves in a mechanically predictable fashion (Schilling and Hollin, 1981). GLACPRO is a simple, transparent, spreadsheet modeling programme that utilizes geomorphologic indicators of paleoglacier extent, in conjunction with known factors governing ice behaviour, to reconstruct glacier morphology and ice surface contours. The model calculates ice surface elevations along the glacier up-ice from the end moraine. Locke (1995) suggests that the model is generally accurate within mountain ranges, especially where the effective basal shear strength of the former glacier is able to be reliably estimated.

Data were entered into the GLACPRO excel spreadsheet in order to predict glacier elevations. Parameters of the GLACPRO model are map scale, up-ice distance (the distance along a centerline profile from a moraine), step length (the distance along a centerline profile between the location of data for the current step and the previous iteration), bedrock elevation (in this case the lowest point in the basin floor), and moraine crest elevation along a centerline path (Appendix A: GLACPRO data).

The steps involved in GLACPRO ice reconstruction are as follows:

1. Determine the extent of the glacier using terminal and lateral moraines, kame terraces and trimlines. Breached divides assist in constraining minimum elevations.

2. Determine basin floor elevations at constant intervals up-valley from the end moraines. For the Lake Heron reconstructions, a 1km interval was used.

3. Basal shear strength is calculated at each step of the model. Effective basal shear strength is a measure of the distributed force over an area at the base of a glacier that acts parallel to the basal surface (Benn and Evans, 1998). The basal shear strength was initially set at one bar based on glacier mechanical theory. However, effective basal shear strength in the Lake Heron basin dataset was usually adjusted until the "former ice surface" fitted the known parameters as indicated by former moraine heights. This occasionally resulted in basal shear strengths inconsistent with glacial theory. Basal shear strengths for the model varied between 0.1 and 0.8, but were usually about 0.15 to 2.0 for advances terminating in the basin. Basal shear strengths for large advances that extended beyond the confines of the basin varied between 0.3 and 0.8, but were usually about 0.4.

4. The appropriate shape factor is then included into the calculation. The shape factor is the ratio between the "hydraulic radius" (defined as the cross-sectional area of the glacier divided by the wetted perimeter (the length of the glacier/ground interface) and the centerline ice thickness. It varies from 1.0 for an infinitely wide glacier (an ice sheet) to as low as 0.6 or so for a glacier in a deep, narrow gorge. A shape factor of 0.8 was used for most of the ice reconstructions in this study.

3.3 Rivers and streams

The main river in the study area is the South Branch of the Ashburton (called the Ashburton River for purposes of this study). The Ashburton River is the largest fluvial system in the basin and drains the Ashburton Glacier at the southern end of the Arrowsmith Range. After making its way though a small gorge just north of Dogs Hill, the river opens out into a wide, gravel choked bed, which it occupies during times of flood. The river is braided as it passes through the south end of the Lake Heron basin and receives a contribution from the Maori Lakes (Map 1).

The Stour River occurs in the eastern part of the basin between the Mt Somers Range and Clent Hills. Smaller systems that feed into Maori Lakes include Gentleman Smith, Jacobs, Clent Hill and Johnston Stream. These meandering streams drain farmland from the area south of Lake Heron (Map 1).

Streams in the northern part of the basin have their origins in the hillsides and tributary valleys and most feed into Lake Heron (Map 1). The lake currently drains to the north via Lake Stream into the Rakaia River. The gently sloping topography means that Lake Stream passes through a swampy area, while in other places it is greatly restricted by large alluvial fans. During glaciations, the Cameron Glacier extended into the Lake Heron basin, coalescing with the main lobe of ice. Meltwater from the Cameron glacier presently feeds into Lake Stream (Map 1).

3.4 Lakes

Lakes are present in the study area and the majority have glacial origins. Lake Heron, at 6.6km long and 3.1km wide, is the largest and lies in a glaciated depression in the centre of the basin. It has a catchment of 115km², of which the lake covers 6.84km². It is 679m asl. The lake's only outlet occurs at the northern end through Lake Stream, which feeds into the Rakaia River. It has a maximum depth of 37m at the southern end (Bowden, 1983), associated with overdeepening at the front of a glacier. Due to the invasion of alluvial fans along the margins, much of the lake is shallow, with 60% being less than 5m deep (Bowden, 1983).

Lake Heron is dammed at the southern end by glacial deposits. Lake benches exist between 700m and 737m asl, cut into the glacial deposits around the southern shores of the lake. These benches suggest that the lake was once much larger. More benches occur further up-valley. Also, a former lake outlet at the southern end of the lake (J35/629440), with an elevation of 697m, indicates that the lake surface was previously higher and that the lake drained to the south.

Lake Emily's (J36/668380) origin is similar to that of Lake Heron in that it is dammed behind a moraine complex. The lake is approximately 450m wide and 400m long. Emily Hill forms the margin to the east and a swampy area of subdued topography occurs to the north. Lake benches around the lake suggest that previously it occupied a larger area.

In the south end of the study area, the Maori Lakes (J36/620359) abut the rear of a glacial moraine. The lakes have formed in a poorly drained area and it is likely that the lakes are of post-glacial origin and have accumulated in a depression. Manuka Lake and Seagull Lake occur in the east of the basin and are both dammed on each sides by hills. Their presence is essentially due to post-glacial fan building.

Two large kettle holes occur in the moraine to the south of the Cameron River fan. They occupy hollows due to the melting of dead ice that had been buried by gravels from the Cameron Valley. The largest, at 300m long, is aligned parallel to the direction of ice flow and lies on a relatively flat surface (J36/595473).

Another kettle hole, 150m in diameter, occurs to the north of the Cameron River and is located within hummocky ground moraine with several small lateral moraines located immediately to the north, from which it receives runoff. It is unknown as to whether the kettle hole is bedrock-cored, but as the surrounding area is mantled in glacial deposits it probably originated from the melting out of buried ice. Smaller kettle holes, up to 100 m wide, occur in moraine at the south end of Lake Heron (J35/629440) and within the recessional moraines to the south of the Longman Range (J36/670415). They also have originated from the melting out of buried ice. Here, the kettle holes are regenerated by runoff and drain into Lake Emily.

A tarn (named Staces Tarn for this study) occurs on the ridgeline (J36/582517) 250 m below the summit of Staces Hill. It occurs in bedrock, dammed along its eastern margin by moraine and is filled with fine-grained lake muds. It presently has no outlet, and formed following the retreat of a small lobe of ice that pushed over the ridge from the

adjacent valley. Staces Tarn is described in chapter 5, a micropaleontogical study into past vegetation.

3.5 Faults

The most conspicuous fault trace in the study area is the Lake Heron Fault (Map 1), which skirts around the base of the Wild Mans Brother Range from Dunbar Stream (J35/593481), near the mouth of the Cameron Valley, to the Spider Lakes (J36/582317) in the Clearwater Catchment (Oliver and Keene, 1990). Its likely continuation is a fault trace through the Balmacaan saddle. The reverse dip-slip nature of the fault has displaced outwash surfaces along its length between 4 m and 30 m, depending on the relative age of the deposit. Moraines near the mouth of the Ashburton River have been displaced between 20 m and 30 m, however, younger river terraces on the riverbed show displacements between 2 m and 5 m.

Oliver and Keene (1990) also map multiple faults south of Maori Lakes that trend in a north-north east orientation. Displacement on these reverse faults is up to 5 m in the degraded moraines south of the Ashburton River and only a few meters in the younger river terrace adjacent to the current river channel. The east-west trending Barrosa Fault cuts Clent Hills. It is identified as a deep gully in the west-facing hillside and has a reverse sense of movement.

3.6 Mass movement

3.6.1 Alluvial fans

In this study, the relationship between glacial deposits and alluvial fans suggest that the fans are largely a post-glacial feature. The Cameron River fan (Figure 3-5) occurs below the height of kame terraces and former lake benches along the western margins of Lake

Heron. Its fluvial outwash surface is traceable to the Cameron Glacier, 8 km up-valley. This suggests that rapid fan growth occurred following ice retreat. During glaciations, outwash from the Cameron glacier was forced to exit the Cameron valley jammed between the Lake Heron ice lobe and the western hillsides. This provided an abundance of sediment, which was deposited as numerous kame terraces (Map 1). This is also apparent in alluvial fans derived from the Swin and Smite Rivers and from Home Creek to the east of Lake Heron (Map 1). Small recessional moraines and horizontal benches near the base of the distal reaches of alluvial fans suggest that material from theses systems was deposited against a receding glacier and that their current position is owing to the fans having incised to a new base level.

3.6.2 Colluvial fans

The process of freeze and thaw was more active in glacial times in the Lake Heron basin and produced rock debris, which moved gradually downhill. Following the retreat of ice, subaerial processes of denudation worked upon the freshly exposed bedrock faces on mountainsides (Map 1). A large slope deposit occurs on the east-facing hillside below Trig A (J36/589401). The slope has a gradient of 28.5º. The upper portion of the hillside is covered in a thin veneer of weathered material with an increasing thickness further down the slope. Several v-shaped gullies, 2-10m deep, occur on the hillside and angular debris collects near the base. Where gradient decreases at the base of the hillside, the debris has spread out onto glacial deposits, suggesting that the fans are of post-glacial origin. A similar relationship occurs between colluvium and glacial deposits in the depression between Ricki Spur and the Longman Range. At this location, small fans have built out over recessional moraines, which suggest that the slope movement occurred following glacial retreat.

3.6.3 Landslide

A large, approximately 3 km² triangular-shaped hummocky area on the north bank of the Cameron River mouth is probably a landslide (Davies T 2008 pers. comm., 14 Mar). Small scale rotational slumps are also recognised. Within the hummocky area of the landslide are two pronounced ridges, similar to a lateral moraine, which are sub-parallel to the adjacent Staces Hill ridgeline (Map 1). A large portion of the hillside is composed of sub-horizontal benches comprised of angular greywacke boulders. The ridges are moving slowing down slope (Figure 3-2). Slope failure may have occurred in the immediate post-glacial period, due to the removal of ice support provided by the Cameron Glacier. However, it cannot be discounted that a seismic relationship existed (Davies T 2008 pers. comm., 14 Mar).

Figure 3-2 Rotational slumping along the top surface of a landslide below Staces Hill.

3.7 Glacial deposits

3.7.1 Dump moraines

Dump moraines are continuous concentric mounds that extend from the bordering hillsides into the center of the basin. Distinctions are able to be made between a terminal moraine, deposited at the ice front, a lateral moraine, deposited between the ice margin and the valley side. Dump moraines are usually between 10m and 40m high and are up to 100m wide. Sediment within the moraine is derived primarily from supraglacial debris (Benn and Evans, 1998), although recent studies of New Zealand moraines suggest a large proportion of moraines are reworked proglacial sediments (Hyatt *et al*, 2007). The size of the moraine is related to supraglacial debris volume and to the length of the standstill period (Benn and Evans, 1998).

At the south end of Lake Heron lies an arcuate belt of three moraines that are well preserved (Map 1). They are up to 15m high and extend south from the mouth of the Cameron River around the shores of the lake, although the eastern portion has been removed by the Swin River alluvial fan. The moraines occur within a 1km stretch of each other, separated either by meltwater channels or by hummocky moraine. Large boulders, up to 2m high, often occur on the moraine crest and these were targeted for SED sampling.

One kilometer north of Johnstone Stream, there is a large moraine complex comprised primarily of dump moraines. The crest is draped by about six push moraines (Map 1). The moraine complex is 300m wide, and up to 20m high above its outwash surface and links into lateral moraines to the northwest. The moraine complex implies the deposition of large amounts of glacial debris at a relatively stable ice-front.

A moraine complex on the north bank of the Ashburton River has a severely pitted surface and has had large portions removed and reworked by the outwash and meltwater

of subsequent glacial advances. Although their original form has been compromised, at least four lateral moraines associated with the complex occur along the valley side to the west. These lateral moraines are up to 100m high and up to 1km long (Map 1).

3.7.2 Push moraines

In the Lake Heron basin, push moraines (Benn and Evans, 1998) range up to 5m high and are long, winding, broadly arcuate humps that traverse the basin floor, mimicking the morphology of the glacier snout. The size of the moraine may relate to the length of time that ice was stable in that position and also to the degree of subsequent degradation (Figure 3-4). Push moraines usually occur within an outwash surface or atop a moraine complex and accurately drape topography with little loss of form. Boulders are not apparent on the crest. In the area between the Longman Range and Ricki Spur, approximately 20 recessional moraines record oscillations at the ice front during the northward migration of ice. These moraines are slightly larger, up to 3m high, and are often separated by meltwater channels. The immediate area is swampy and poorly drained.

In some places, small, streamlined humps occur ice-proximal relative to the push moraine, and trend down valley for several meters, terminating at the base of a push moraine. In Map 1, they are labelled as fluting. More obvious fluting occurs in overrun sediments north of Lake Emily. The fluting is similar to streamlined sediment that has been described in the adjacent Clearwater basin (Evans, 2008) and to “streamlined deposits” in the lower Rakaia river (Hyatt *et al*, 2007). Benn and Evans (1998) note the presence of fluting within push moraines at the southern end of Lake Pukaki, New Zealand. Benn and Evans suggest push moraines record minor, often annual, glacial readvances during overall ice retreat, and their mode of formation is illustrated in Figure 3-4 Suggested mode of push moraine formation; a combination of subglacial deformation and ice marginal squeezing (modified from Evans and Benn, 1998)..

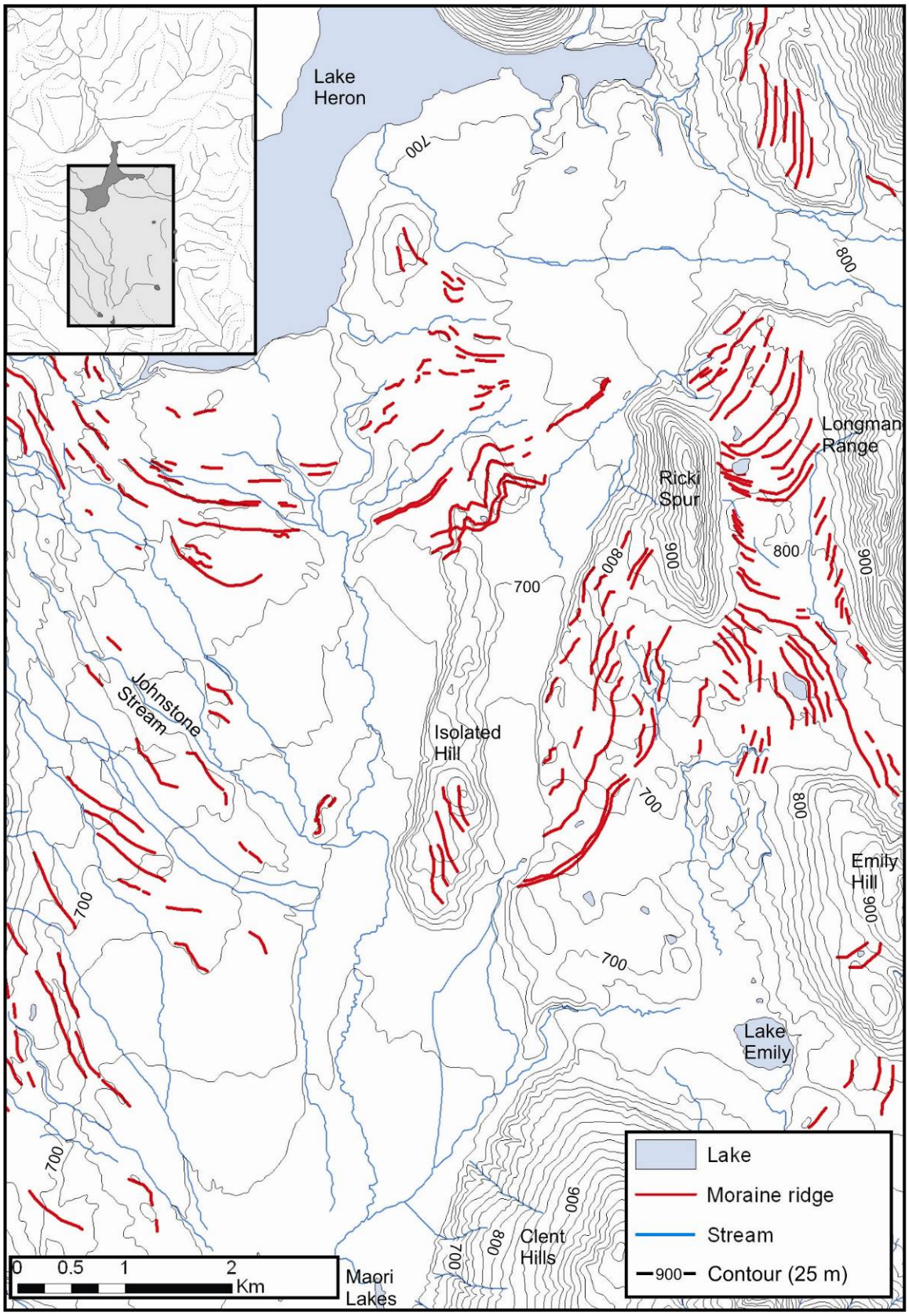

Figure 3-3 Push moraine ridges in the Lake Heron basin.

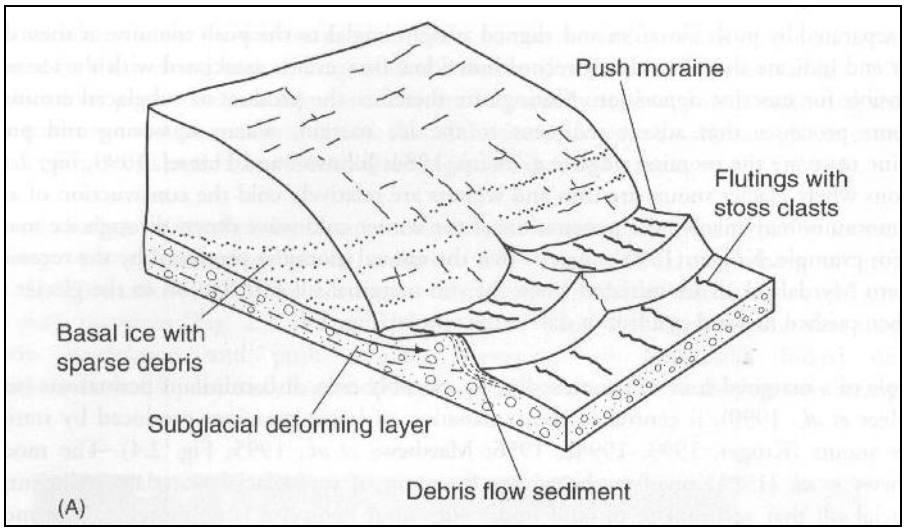

Figure 3-4 Suggested mode of push moraine formation; a combination of subglacial deformation and ice marginal squeezing (modified from Evans and Benn, 1998).

3.7.3 Hummocky moraine

The term "hummocky moraine" (Benn and Evans, 1998) is used in this chapter to described terrain that appears in an assortment of shapes and sizes but that has the characteristically hummocky and pitted surface expression that is often incised by meltwater channels. It is purely a descriptive term. It is preferred over another term, "dead-ice moraine", as the latter has implications for the state of ice during the formation of the moraine. Mabin (1980) used the term "ablation moraine". However, this also has strong implications for the origin of the sediments. Occurrences of hummocky moraine in the study area are similar in height to the area's terminal moraines. They occur as large sediment mounds, up to 2km wide, located between or up-ice of terminal moraines (Map 1). The hummocky surface is the result of various processes, including post-depositional fluvial action and buried ice melting out, which explains its the pitted appearance. Large boulders are often scattered over the surface.

The largest deposit of hummocky moraine occurs at the southern margin of Lake Heron (J35/629440). It covers an area 2km wide, 1km long and at its highest point 721m asl. A terminal moraine loop encompasses most of the moraine while a drainage channel

borders the eastern edge. The surface of the moraine contains many kettles holes. Braids apparent in the western portion indicate post depositional fluvial reworking. The eastern portion of the area is relatively flat and grades slightly to the south. Several meltwater channels drain the moraine and feed into Gentleman Smith Stream. A former lake outlet borders the eastern margin.

3.8 Glaciofluvial features

3.8.1 Kame Terraces

Kame terraces are described by Evans and Benn (1998) as "gently sloping depositional terraces perched on valley sides, which are deposited by meltwater streams flowing between glacier margins and the adjacent valley wall". Kame terraces are primarily composed of sand and gravel, as they are constructed from the deposits of meltwater streams flowing along the ice margin, incorporating supraglacial sediments along with debris from the adjacent valley wall.

Kame terraces are a striking feature in the Lake Heron basin, especially on the western hill slopes between the Cameron and Ashburton Rivers (Figure 3-5). Von Haast (1879) was unsure of their origin, originally suggesting that they were marine benches. However, after further examination with a spirit level he concluded that they "had a slight fall", and were therefore "the banks of ancient river channels…of glacial or subaerial origin" (Von Haast, 1879: 372).

In the Lake Heron basin, kame terraces occur as near-horizontal benches, being typically 15m high and 10m wide, whilst dipping at gentle angles, usually between 3 and 10º, in a down-valley direction. As they are constructed by fluvial processes at the margin of the glacier, they indicate the minimum height of the ice at that time. The surface form of a kame terrace is similar to that of an outwash surface in that it is usually flat and

sometimes contains large erratic boulders. Often the surface is pitted to the point that broader surfaces contain kettles holes, underlining their close association with the glacier.

The preservation of a kame terrace is associated with glacial retreat (Sissons, 1958). An advancing glacier will remove or cover deposits left by preceding advances within the extent of the advance. The deposits that remain are those belonging to recession from that advance. Thus, kame terraces mark the stepwise retreat of ice back through the basin.

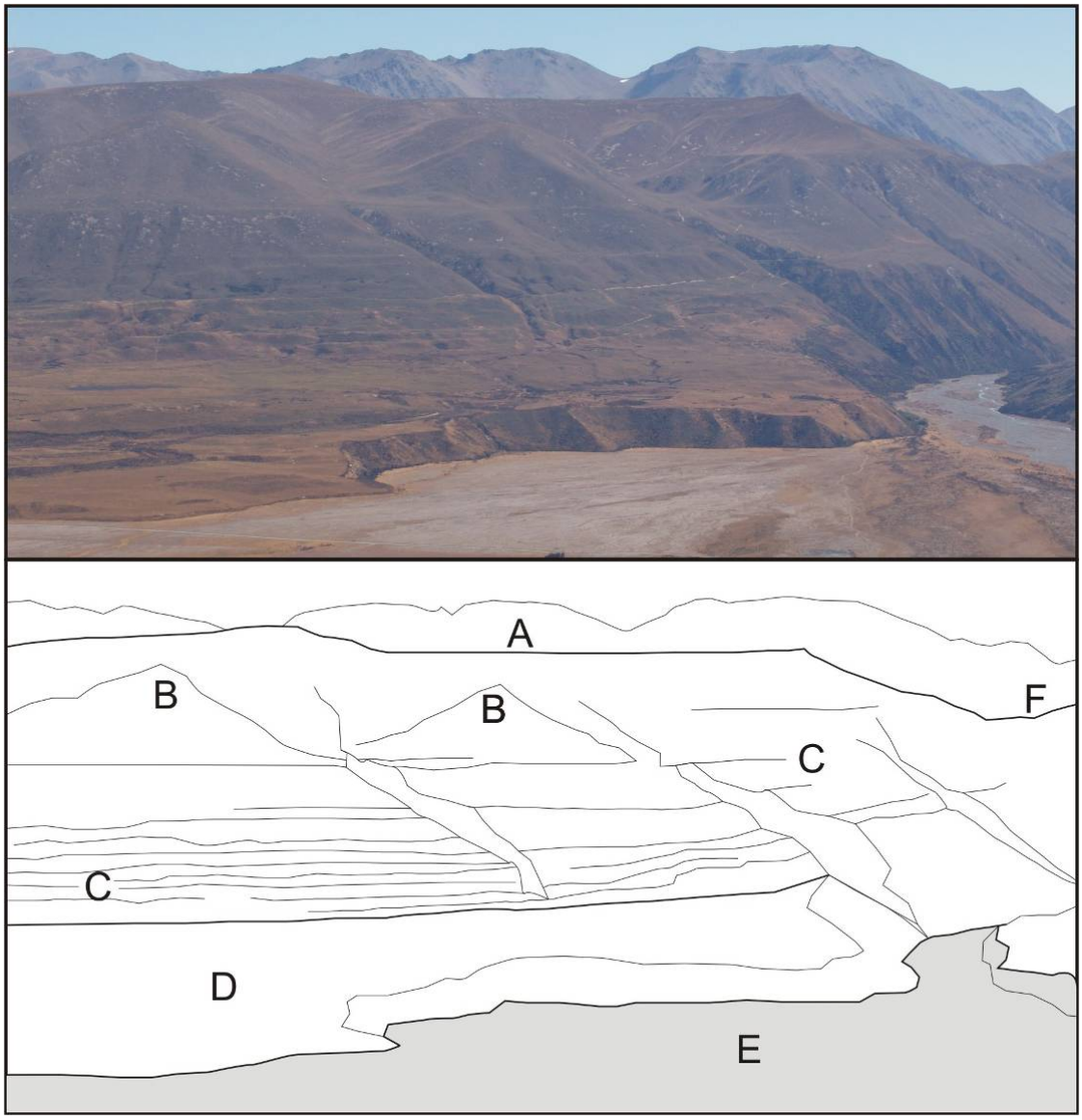

Figure 3-5 Southwest view at glacial features below Pyramid. Ice flowed from right to left. A) Glacially cut surface B) Truncated spurs C) Kame terraces D) moraine deposits E) Cameron River alluvial fan F) transfluence col with adjacent Ashburton Glacier.

3.8.2 Outwash surfaces

Outwash surfaces in the study area are identifiable as flat surfaces that dip away gradually from a point of origin, which is usually a moraine. The surfaces often have a sinuous, braided topography that radiates from a point or points of origin. The largest outwash surface occurs south of Johnston Stream (Map 1), and covers approximately 7km². The surface decreases in elevation from 720m asl near the head of Johnston Stream to 630m asl at Maori Lakes and is traversed by several small streams. Outwash surfaces decrease in age at lower elevations and in an up-ice direction.

3.8.3 Lake benches and lake deposits

Lake benches occur around the margins of both Lake Heron and Lake Emily. Lake benches are identified as broad, flat surfaces usually between 5m and 40m wide and predominantly constructed into glacial deposits.

At Lake Emily, a lake bench has formed into the ice-proximal side of a moraine complex. The area occupied by the lake (see 3.12.6) when it was larger now has a flat and subdued topography. A former outflow channel is incised through the terminal moraine and issues into the Stour River valley. This was abandoned as the lake expanded and a new lower outflow channel was established around the northern end of Clent Hills.

Around the current margins of Lake Heron, the highest set of lake benches occurs at 737m asl and the lowest at 700m asl. Steep scarps up to 2m high mark the inner and outer margins of the benches, and these represent the abandonment of the land surface by the lake. Former delta fans at the ends of meltwater channels on the south-western margin of the lake are further evidence of the existence a larger lake in the past (see 3.12.6).

3.8.4 Meltwater channels

Glacial meltwater is sourced from a variety of locations, including melting ice, snowmelt, rainfall, dew runoff from ice-free slopes, and the release of englacially stored water (Benn and Evans, 1998). It passes through either supraglacial, englacial or subglacial pathways, exerting an important influence on glacial behaviour and geomorphological processes. In the Lake Heron Basin, meltwater drainage systems have produced both depositional and erosional features. Large amounts of meltwater are transported laterally between the ice and the valley wall, producing flights of kame terraces as seen on the east-facing slopes below Pyramid (Map 1). On the basin floor, drainage channels have incised distinct arcs in the outwash surfaces.

Along the western margin of the basin between the southern end of Lake Heron and Johnston Stream, meltwater channels occur as arcuate belts. The location and direction of the channels is controlled by existing depositional structures, such as moraines. The meltwater channels issue onto outwash surfaces but are often encased on both sides by a moraine. Encasing a channel between moraines occurs during the stabilisation of a new terminal position following glacial retreat.

In the same way that a kame terrace is constructed at a lower elevation than the preceding advance, a meltwater channel formed in the basin floor also flows at a slightly lower elevation. A situation arises in which the new channel either erodes the preceding latero-frontal moraine or flows behind the preceding moraine. In the Lake Heron basin, meltwater channels delineate frontal ice positions even if a terminal moraine is not preserved.

3.8.5 High surfaces

Broad, flat areas with terraces often mantled by highly weathered greywacke boulders occur at elevations above approximately 900m on Pyramid (J35/559492). The surface is

often hummocky, although not pitted, and deep gullies have incised the peripheral extents. The degraded and eroded high-level benches are interpreted as former glacial moraine and as outwash deposits.

3.9 Erosional features

3.9.1 Ice sculptured phenomena

The erosive power of the Late Pleistocene glaciers has had the overall effect of steepening the slopes of mountainsides by straightening the pre-glacial river courses, rounding off sharp bends, and cutting back corners and the ends of spurs. Ice migration through the Lake Heron basin has smoothed the valley walls, such that, without the addition of sediment fill, the basin would resemble a broad 'U' shaped valley. Truncated spurs are prominent features in the upper parts of the basin at high elevations on the sides of mountains and are useful in recognising the height that former glaciers achieved (Figure 3-5).

On the surface of Isolated Hill are several bedrock ridges, up to 5m wide and 40m long. They occur at the south end of the hill and trend south for most of their length before. In aerial photographs, these ridges appear similar to the recessional moraines between Ricki Spur and the Longman Range. However, on inspection of the site it was found that they were in fact sculptured bedrock lineations, and that the orientation of the bedding may have played a part in their final form. This means that the ridges are the product of ice overrunning the hill.

Trimlines are best seen at high elevations on the north side of Clent Hills. Changes in vegetation-cover highlight the lines, which gradually slope down-valley between 2º and 10º gradient. Trimlines mark the minimum elevation of the surface of a glacier, and the sharpness of the boundary depends on the effectiveness of glacial erosion.

3.9.2 Roches Moutonees

Evans and Benn (1998) describe roche moutonees as asymmetric bedrock bumps or hills with abraded stoss faces and quarried lee faces. Roches moutonees range in size from 1m to several kilometers in length and span the largest spatial scale of all glacial landforms (Lewis, 1947; Bennett and Glasser, 1996). Roche moutonees larger than 1km are termed flyggbergs (Rudberg, 1988).

Mt Sugarloaf is a flyggberg to the northeast of Lake Heron and is composed of indurated greywacke and argillites of the Torlesse Supergroup (Warren, 1967). It is 2.8kms long, 1.4km wide and rises to 1238m asl, or 550 m above the floor of the basin (Figure 3-6). Its long axis has a north-south orientation of 160º, parallel to the strike of the basin.

The lower elevations of Mt Sugarloaf are covered by colluvium and vegetation, while the northern end is draped by sediment. A sediment outcrop exposed on the northeast corner by a vehicle access road shows deformed fluvial sediments, probably overrun by a subsequent glacial advance, resting on bedrock. The exposure comprises deformed gravel and matrix supported diamicton unconformably underlying well-sorted, cross-bedded sands. The sands, including several rip-up clasts, occur within a small channel, which suggests a fluvial origin, although a lake-beach origin is possible. The deposit has been subjected to compaction, which is illustrated by the presence of deformation, thrust faults and hydro fractures. The outcrop is capped by a thin colluvium layer and by loess. The northern, up-ice end of Mt Sugarloaf has had sediment plastered against it by an advancing glacier.

Several moraine ridges occur along the northern flank of Mt Sugarloaf. Four are apparent on the surface of the deposits that drape the hill and these can be traced into lateral moraine and kame deposits. Three ridges occur at greater elevations along the north ridge. These ridges are up to 3m high and 20m wide. A small outcrop of well cemented glacial till, containing 5cm rounded clasts, occurs in the up-ice face of the second highest moraine ridge.

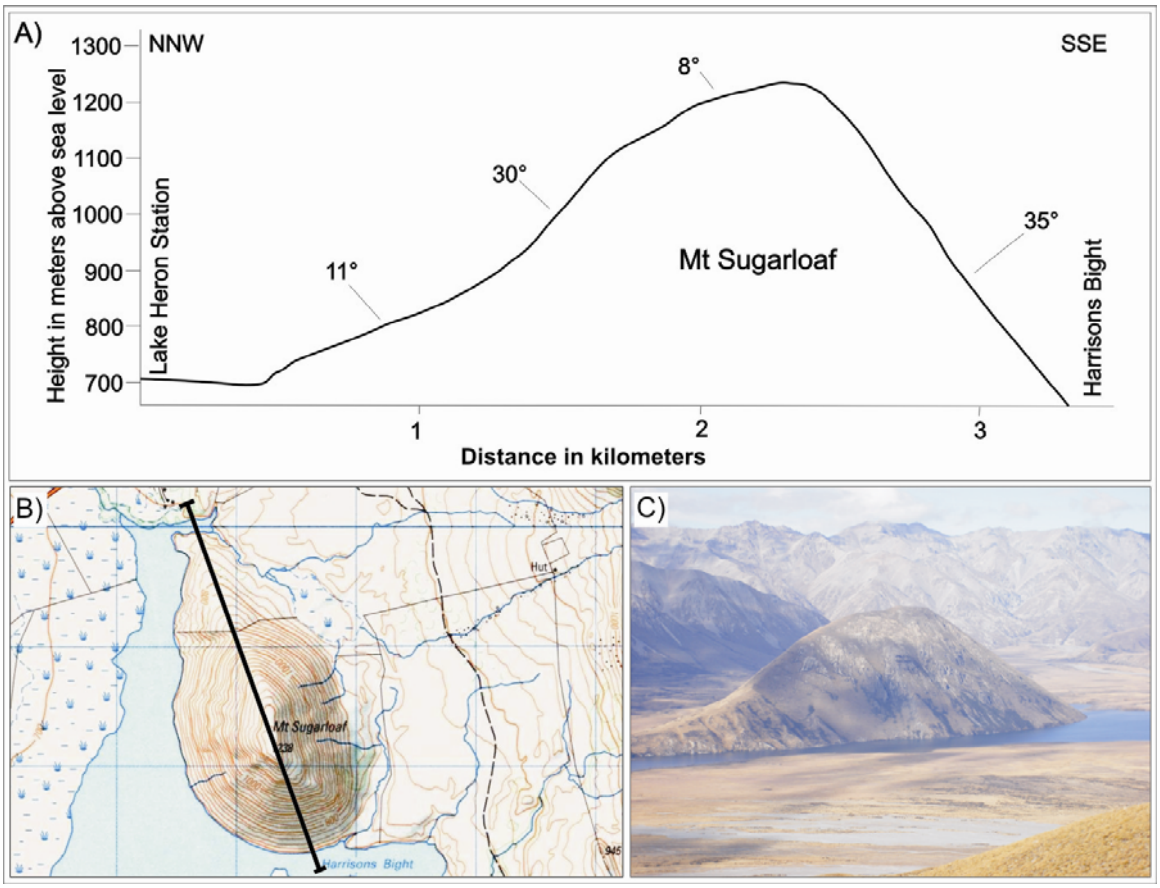

Figure 3-6 The form of Mt Sugarloaf. A) Cross-profile of Mt Sugarloaf showing slope gradients (vertical exaggeration 2:1). B) Black line indication location of cross-profile on 1:50 000 topographic map of Mt Sugarloaf (NZMS 260 J35). C) View looking SE at Mt Sugarloaf. Ice flowed from left to right.

3.9.3 Rock drumlins/bedrock perturbations

Rock drumlins are described by Benn and Evans (1998) as elongate, smoothed bedrock humps which lack the quarried lee faces characteristic of roche moutonees. Rock drumlins are asymmetrical in profile, with steeper stoss faces and a gradually tapering lee side and are generally smaller than roche moutonees (Benn and Evans, 1998).

In the basin south of Lake Heron, several distinctively elongate bedrock landforms occur, such as Isolated Hill, Ricki Spur and Longman Range. These are aligned sub-parallel to Mt Sugarloaf's orientation and are composed of the same lithology.

The Longman Range is an elongated bedrock spur with a north-south orientation located near the eastern margin in the central portion of the basin. Alluvial fans stemming from the Swin River and Finger Stream flow beside the eastern and northern slopes. A group of recessional moraines and their associated outwash form the surfaces adjacent to the west and south. The Longman Range is 3.2km long, 900m wide and reaches an elevation of 1054m asl, or approximately 250m above the floor of surrounding planar surfaces (Figure 3-7). The hillsides of the range are steeply dipping and although some sections of the ridgeline are flat, the ridgeline is mostly jagged and undulating. The range is composed of sandstones and siltstones of the Torlesse Supergroup (Oliver and Keene, 1990). The exposed bedrock of the Longman Range has been glacially rounded and smoothed.

Ricki Spur is 2.1km long, 700m wide and raises to a maximum height of 1014m asl or approximately 200m above adjacent planar surfaces (Figure 3-7). The surfaces of Ricki Spur have been glacially sculptured. The northern face climbs steeply to the summit at an angle of 28º; the ridgeline slopes gently at only 3º to the south for approximately 1km. The southern-most face dips steeply at an angle of 22 º.

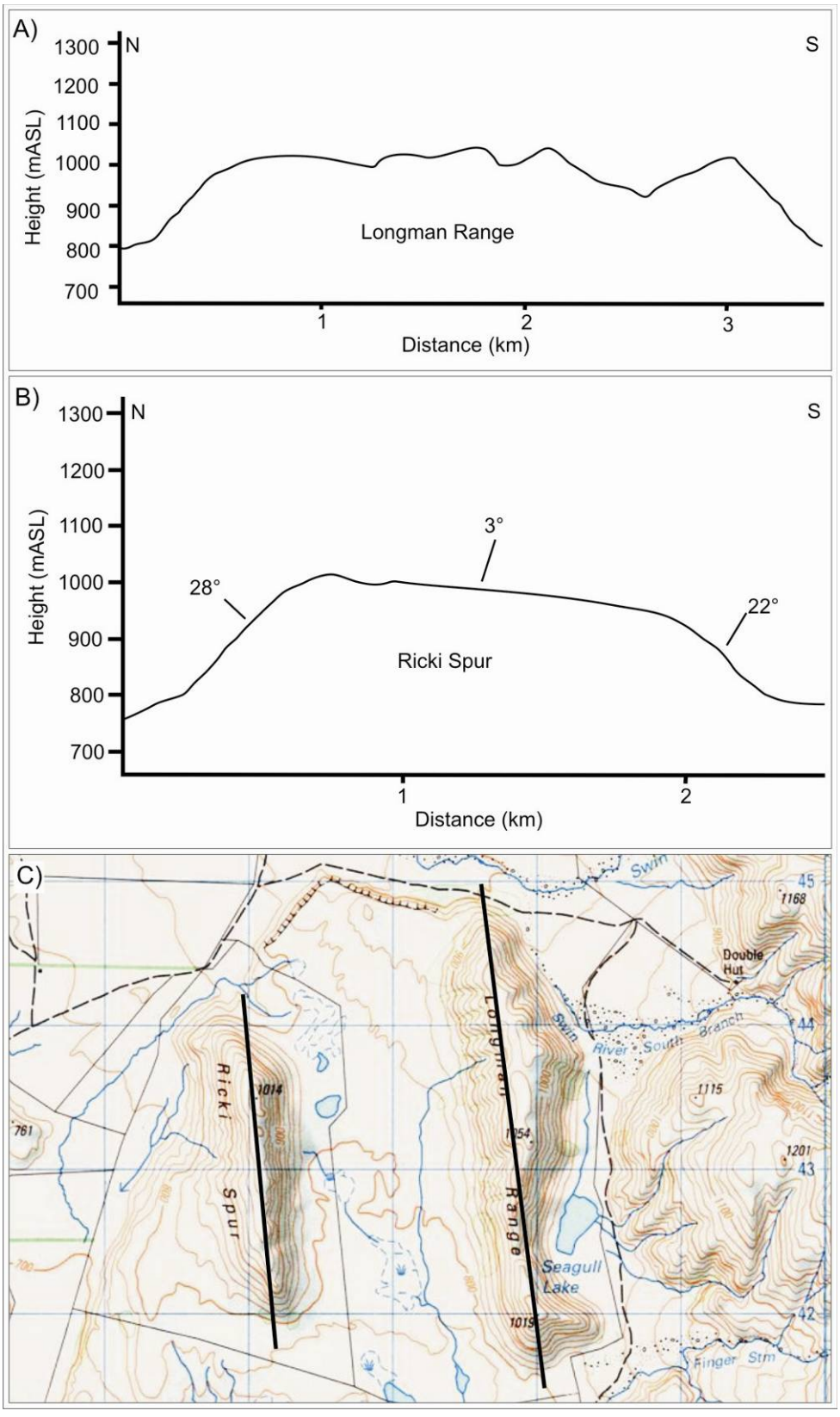

Figure 3-7 Paired cross-profiles of A) Longman Range and B) Ricki Spur (vertical exaggeration 2:1). C) Black lines indicate locations of cross-profiles on 1:50 000 topographic map (NZMS 260 J35).

3.10 Style of deglaciation

The geomorphological map (Map 1) provides evidence that the largest glaciations were of much greater extent than subsequent glaciations. The geomorphology suggests at least two stages of glaciation; the first preserved on the degraded surfaces above 1200m elevation that extended out onto the plains, and a second confined to within the basin. After the first glacial period, tectonic uplift and down-cutting by rivers built the current basin floor, which was filled during the last glacial advances. Deposits in the basin floor are well preserved, whereas those on the high surfaces are weathered and severely degraded, supporting assumptions at least two separate glaciations.

There are at least 70 push moraines in the basin over a distance of about 10km between the Ashburton River and Lake Heron. Three dump moraines also occur within this distance; on the north bank of the Ashburton, adjacent to Johnstone Stream and south of Lake Heron. While moraines are usually used as markers for ice positions, meltwater channels, kame terraces and trimlines can also serve this similar purpose. Mabin (1980) counted 28 kame terraces on the western hillside below Pyramid, all preserving ice elevations. Streams, including Johnstone Stream, appear arcuate when viewed from above, and often occupy former ice-front meltwater-channels. These also delineate former ice positions. These moraines suggest that recession from extended glacial positions was punctuated by at least 70 minor readvances and three still stands.

A contrast occurs between moraine deposits on either side of the valley. Three suites of latero-terminal moraines occur in the west of the basin; on the north bank of the Ashburton River, adjacent to Johnston Stream and at the south end of Lake Heron. At least twenty moraines ridges are identified in the topographically raised eastern side of the basin (Figure 3-3). These moraines are no more than 10m high and usually less than 5m. The exception to the rule in the eastern side is the moraine complex south of Lake Emily, comprising four moraine ridges. It appears as though the ice-front behaved differently in the eastern and western parts of the basin. Mabin (1980) recognised this and suggested that the ice front fluctuated for longer in the east than it did in the west, and

that ice-source was responsible for the contrasts. Lake Heron ice was derived primarily from the main divide, 56 km away. However, the Cameron Glacier, sourced 29 km to the northwest, was less favourably situated with respect to the main snow-bearing winds. Thus, small fluctuations in regional snowline may have had a greater effect on the Cameron Glacier than the Rakaia Glacier. Because of this, ice in the western part of the basin was unable to maintain an advance position, and fluctuated often. Therefore, prominent end-moraines were unable to develop.

Large areas of hummocky ground terrain were deposited during ice recession. Combined with evidence of former moraine-dammed lakes, it appears that phases of ice retreat were characterised by downwasting and subsequent proglacial lake development. Furthermore, retreat from terminal positions was often rapid, as the newly-vacated area between the ice front and the moraine was not subsequently filled with glacial sediment. The presence of lateral/kames terraces are evidence of the large amounts of material transported at lateral margins. However, lake growth was either sufficiently rapid that sediment input was unable to fill the lake, or lateral meltwater remained trapped by moraine in lateral positions during initial development.

Ice marginal moraines and delta fronts at higher elevations are evidence that alluvial fan growth from the Swin River and Home Creek was coeval with the development of glacial Lake Heron (see 3.12.6). While the alluvial fans undoubtedly existed during glacial times, their current form relates to both the very last phases of glaciation in the basin and predominantly the post-glacial period. Soons (1994) suggested fan growth may have lasted a maximum of 4,000 years. Similar coeval development in the Waimakariri River catchment indicates rapid post-glacial fan growth and has been suggested to reflect high levels of precipitation (Gage, 1958; Soons, 1996).

3.11 Glacial chronology

Formal naming of glacial deposits is ascribed to Mabin (1980), who defined five advances spanning three glaciations and postulated possible correlations with other South Island east coast glacial systems. From oldest to youngest, the advances are the Pyramid, Dogs Hill, Trinity, Emily and Lake Heron (Table 3-1). Deposits of the Pyramid and Dogs Hill advances occur as flat-lying benches at high elevations. During these advances, the Lake Heron distributory lobe coalesced with ice from the Lake Clearwater catchment, forming a piedmont lobe that extended through the foothills onto the Canterbury Plains. The Pyramid and Dogs Hill advances are inferred to be separated by an interglacial period, based on the degree of weathering on Pyramid deposits. Another interglacial is presumed to separate the Dogs Hill advance from the Trinity, Emily and Lake Heron advances, which Mabin placed in the Otiran and separated by interstadials. Moraines and outwash of these advances are preserved within the basin (Figure 3-8).

More recently, Oliver and Keene (1990) mapped the geology of the Lake Clearwater area and the southern portion of the Lake Heron basin at 1:50 000 scale. They redefined the glacial chronology, renaming the late Emily moraines as the Johnston Stream Formation.

Table 3-1 Pre-existing glacial chronology of the Lake Heron basin

GLACIATION	MABIN (1984)	OLIVER AND KEENE (1990)	SUGGESTED AGE
Late Otiran	Lake Heron advance	Lake Heron Formation	17 – 14 ka (Oliver and Keene, 1990)
	Emily advance	Johnstone Stream Formation	> 22 800 ± 800 yr (Oliver and Keene, 1990)
Early Otiran	Trinity advance	Emily Formation	59 - 71 ka
Waimean	Dogs Hill advance	Dogs Hill Formation	128 – 186 ka
Waimaungan	Pyramid advance	Pyramid Formation	246 – 303 ka

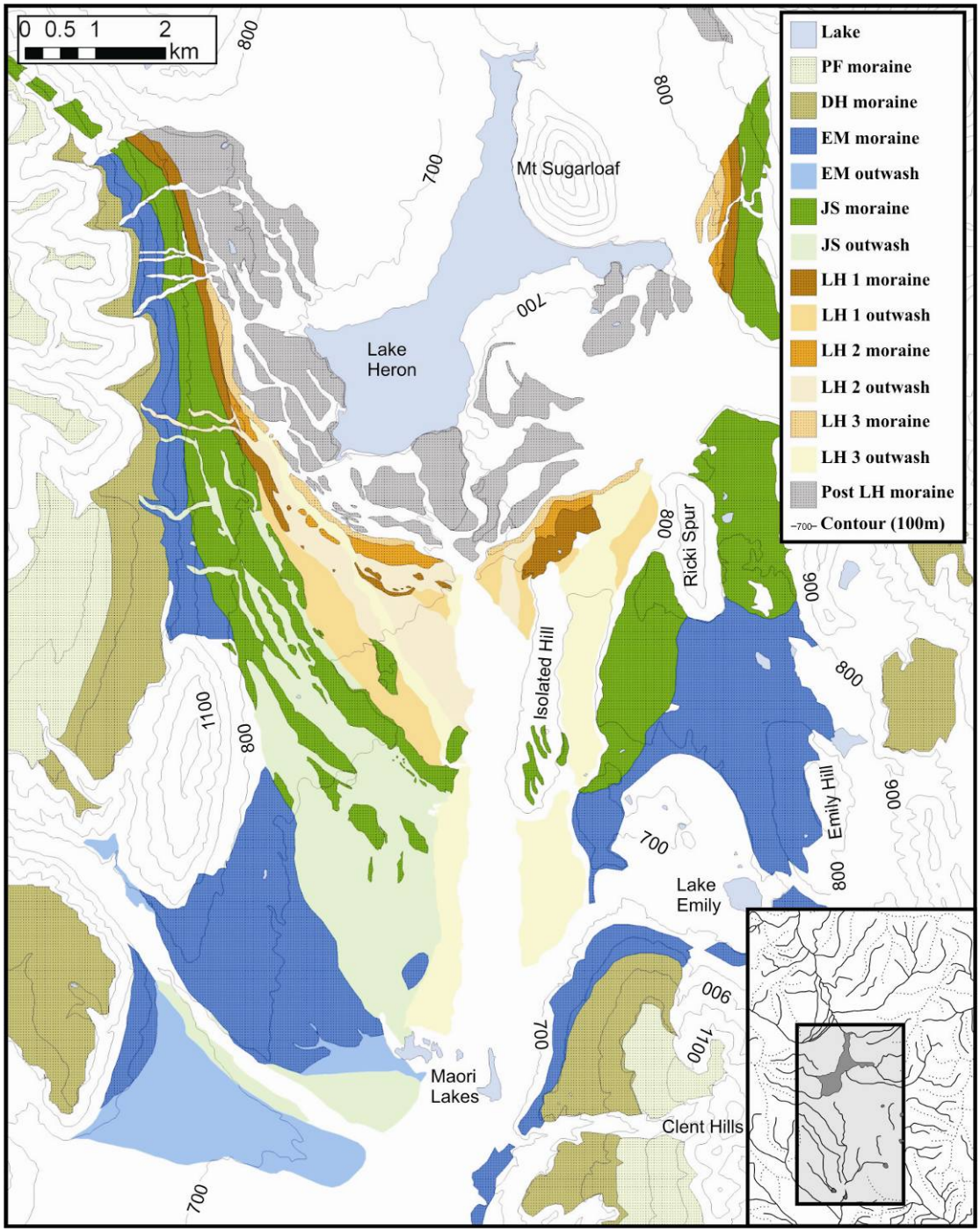

Figure 3-8 Glacial deposits in the Lake Heron basin. PF = Pyramid Formation, DH = Dogs Hill Formation, EM = Emily Formation, JS = Johnstone Stream Formation, LH 1 = Lake Heron 1 , LH 2 = Lake Heron 2, LH 3 = Lake Heron 3.

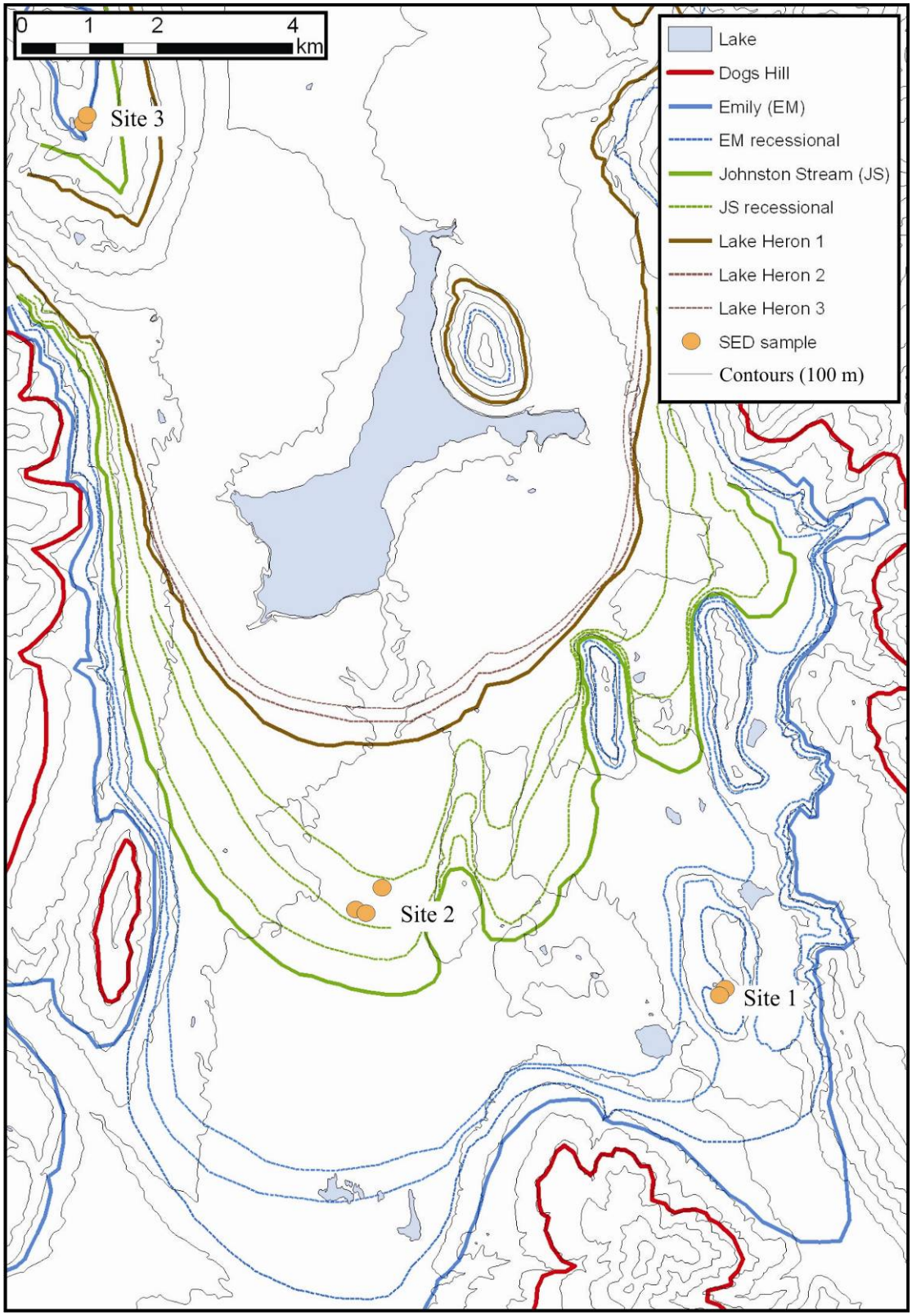

Figure 3-9 Extent of Late Pleistocene glacial advances in the Lake Heron basin. The locations of SED samples are also placed on the map.

Ice profile (Figure 3-10) transects in this study begin in the Ashburton Gorge between Trinity Hill and the Clent Hills and track along the lowest point of the basin, moving north into the Rakaia Valley. Ground elevations follow the bed of the Ashburton River, Gentleman Smith Stream, across Lake Heron and Lake Stream to the Rakaia River. Ice profiles for the Otiran advances were constrained at the terminus by well-defined terminal positions. The lower ~6km of the Johnstone Stream and Lake Heron profiles were further constrained by the extensive kame terraces and lateral moraines below Pyramid. The Pyramid and Dogs Hill Formations were less well constrained. Dogs Hill moraine occurs south of Pyramid and on the Clent Hills, but often occurs as only broad, flat areas buried by loess. Pyramid Formation deposits are degraded and buried by loess; thus the Pyramid ice profile was constructed using values derived from maximum elevation discernable from deposits.

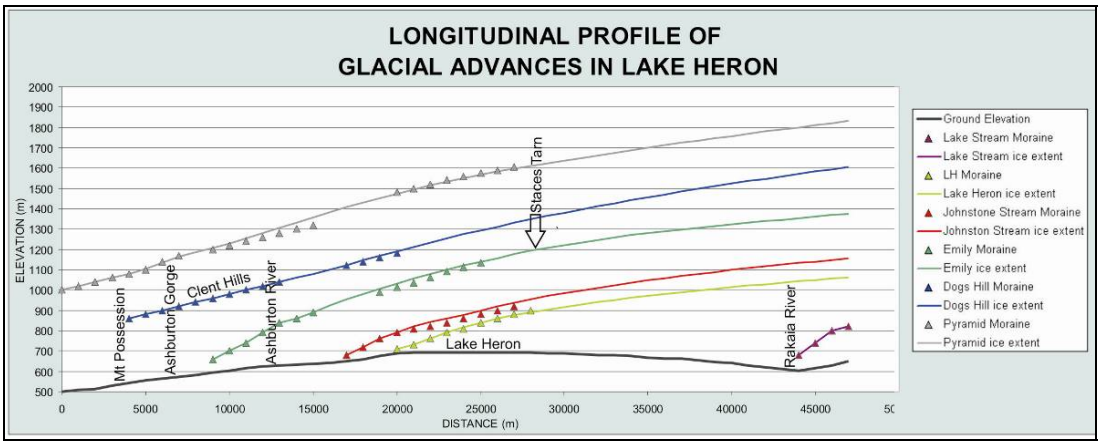

Figure 3-10 Longitudinal glacier ice profiles in the Lake Heron basin.

3.12 Glacial Formations

3.12.1 Pyramid Formation

The Pyramid Formation (PF), from Pyramid (Trig V, J35/559492) occurs as rounded hilltops and planar benches at high elevations in the western ranges of the basin (Figure 3-10). Pyramid ice reached elevations up to 1,800m asl in the northern part of the basin, 1,500m asl in the southern part. Middle Hill (J35: 574548), which has an elevation of 1624m, is rounded due to being overrun by Pyramid ice. Bedrock

perturbations in the center of the basin have been sculptured into stoss and lee forms by the great thickness of ice during this advance. Mt Sugarloaf (J35: 643482), at 1238m asl and 550 m above the floor of the basin, had ice overtopping it during this advance. The degraded and eroded high-level benches attributed to this advance are glacifluvial outwash surfaces mantled by weathered greywacke boulders. Streams have caused deep incision of Pyramid surfaces (Figure 3-8).

During this advance, ice from the Lake Heron basin coalesced with ice from the Clearwater catchment and passed through valleys onto the Canterbury Plains, forming a piedmont glacier east of the foothills at least 5km beyond the study area (Figure 3-9) (Oliver and Keene, 1990).

Age constraint on the Pyramid Advance is limited. A radiocarbon ages from a Pyramid surface in the lower Ashburton valley provides a minimum age of 40,900 C14 yrs B.P (NZ 1684; Harvey, 1974). Oliver and Keene (1990) suggest a correlation with the Waimaungan Glaciation of Suggate (1965).

3.12.2 Dogs Hill Formation

Deposits of the Dogs Hill (DH) advance occur at elevations between 900m and 1300m along the western ranges (Figure 3-11). DH lateral moraines occur below the Pyramid surface and are typically hummocky, extensively eroded and covered by several meters of loess. They can be distinguished from Pyramid surfaces by lower elevations and better preserved surface form (Figure 3-8).

At full ice extent, DH ice overtopped Mt Sugarloaf, received additional ice from the Cameron and Ashburton catchments, and coalesced with ice from the Clearwater catchment (Figure 3-9). A lobe pushed down the Stour Valley, but fluvial erosion has removed any record of its extent. The lobe was deflected by Trinity Hill into the Trinity Valley and the Ashburton Gorge, and extended several kilometers towards the Canterbury Plains.

Although no age constraint exist, the Dogs Hill Formation is correlated with the Woodlands Formation deposits of the Canterbury Plains and has been placed in the Waimean Glaciation (Oliver and Keene, 1990).

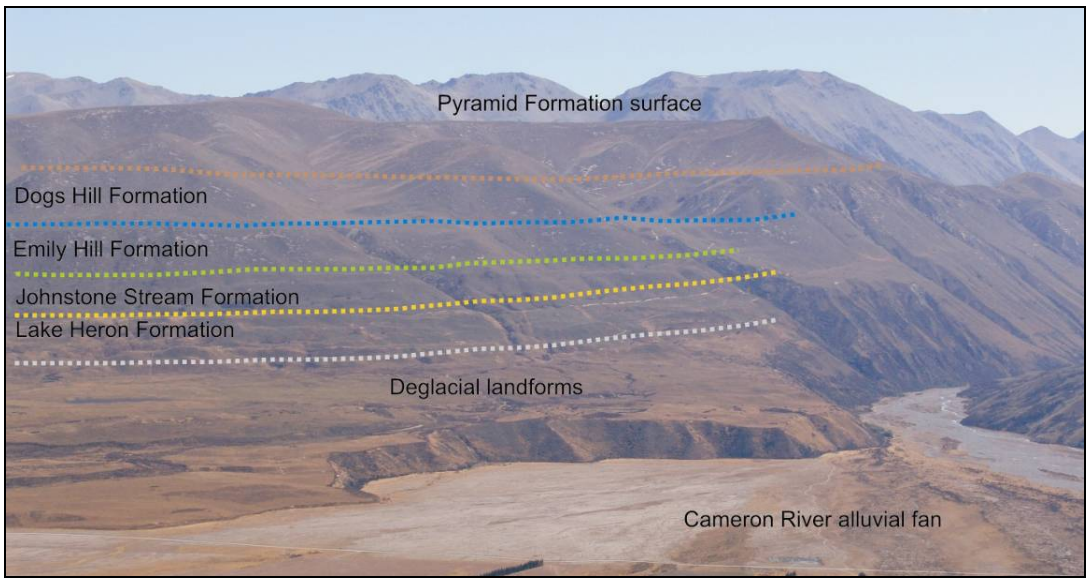

Figure 3-11 View looking west at glacial deposits on the Wild Mans Brother Range near the mouth of the Cameron Valley.

3.12.3 Emily Formation

Emily Formation (EM) occurs on the hillsides on both sides of the basin below the Dogs Hill Formation (Figure 3-8). It occurs at lower elevations and deposits are well preserved compared to the older advances (Figure 3-10). At full extent during the Emily advance, Lake Heron ice joined with the Clearwater ice lobe near Paddle Hill Creek. Outwash terraces (Figure 3-12) records the retreat of the Clearwater ice lobe. A discontinuous moraine complex and at least seventeen push moraines between Emily Hill and the Longman Range comprise the Emily Formation.

Emily advances were initially mapped by Mabin (1980) as the Trinity advance and was renamed the Emily Formation by Oliver and Keene (1990). The latter terminology is used as Trinity Formation now used solely to refer to glacial deposits in the Lake Clearwater area. The oldest EM deposits occur on the eastern flank of Dogs Hill as three lateral moraines, marking the elevation of Lake Heron ice as it coalesced with Clearwater ice lobe. The coalesced ice lobe advanced as far as Potato

Stream, approximately 1 km east of Hakatere Station, and south into the Trinity Valley (Figure 3-9) (Oliver and Keene, 1990).

Retreat of the two ice lobes was not synchronous. The Clearwater lobe retreated earlier than the Lake Heron lobe, as indicated by glacifluvial outwash that accumulated against the Lake Heron ice front. This formed a large moraine complex on the north bank of the Ashburton River. Figure 3-12 shows the direction of Paddle Creek outwash during retreat of the Clearwater ice lobe. The highest terrace surfaces issuing from Paddle Hill Creek slope northwards, while younger degradational terraces preserve the successive pullback of the Clearwater lobe.

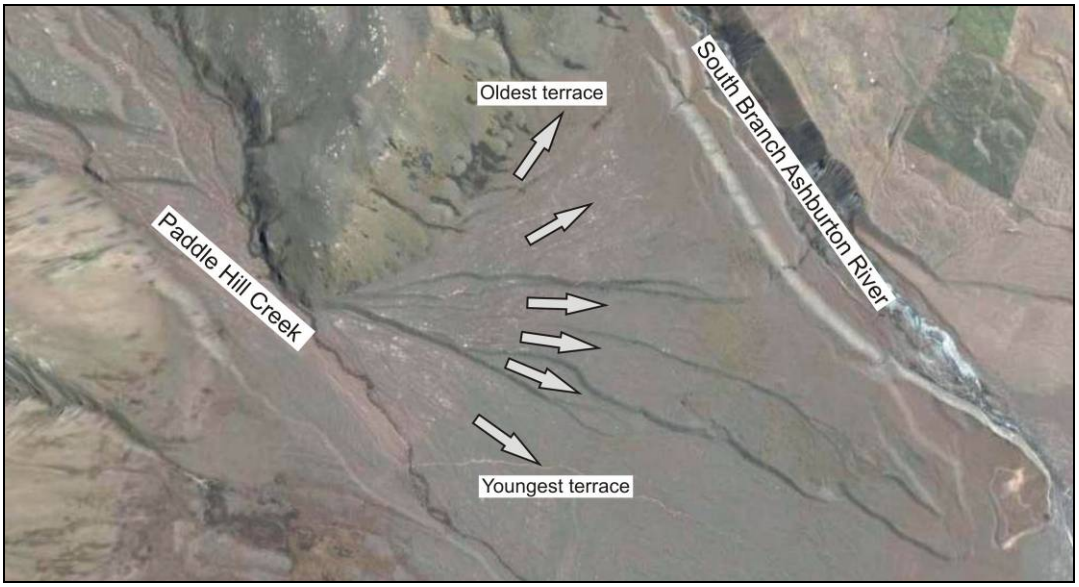

Figure 3-12 Aerial view of the south end of Lake Heron basin. Arrows indicate the dip direction of outwash surfaces between Paddle Hill Creek and the Ashburton River. (Google image, 2007).

During this glacial advances, ice from the Lake Heron lobe was pushing up the Ashburton valley, recorded in lateral moraines on the south of the Wild Mans Brother Range, but it did not coalesce with the Ashburton Glacier. EM moraine occurs on the north and west flanks of Clent Hills between 640m and 800m elevation. Large (10m high) moraines along the west of Clent Hills have a subdued and hummocky topography. In the east of the basin, EM ice would have advanced into the Stour Valley, but subsequent fluvial reworking has removed any glacial deposits that may have been left there (Figure 3-9).

On the north bank of the Ashburton River, a younger EM advance constructed three latero-terminal moraines, occurring between 760m and 900m elevations (Figure 3-14). On the surface of the moraine complex are three moraine ridges, ranging in height from 15m to 40m and with lengths up to 3kms long. The surface of the complex is degraded and pitted surface, probably from both buried ice melting out and fluvial erosion from the early recession of the Clearwater lobe. Kame terraces associated with this advance are preserved on hill slopes on the west of the basin below Pyramid. The kame terraces exit from the mouth of the Cameron Valley at 1140m and descend to the south to approximately 1000m asl. The Cameron Glacier coalesced with the Lake Heron lobe during this time.

Figure 3-13 shows two lateral moraines and a moraine-dammed tarn in a small saddle on Emily Hill. Sitting on the moraines are several large erratic boulders, some more than 2m high. These moraines wrap around the north and south flanks of Emily Hill. The bedrock knobs of Ricki Spur, the Longman Range and Emily Hill were not overtopped by ice during this advance.

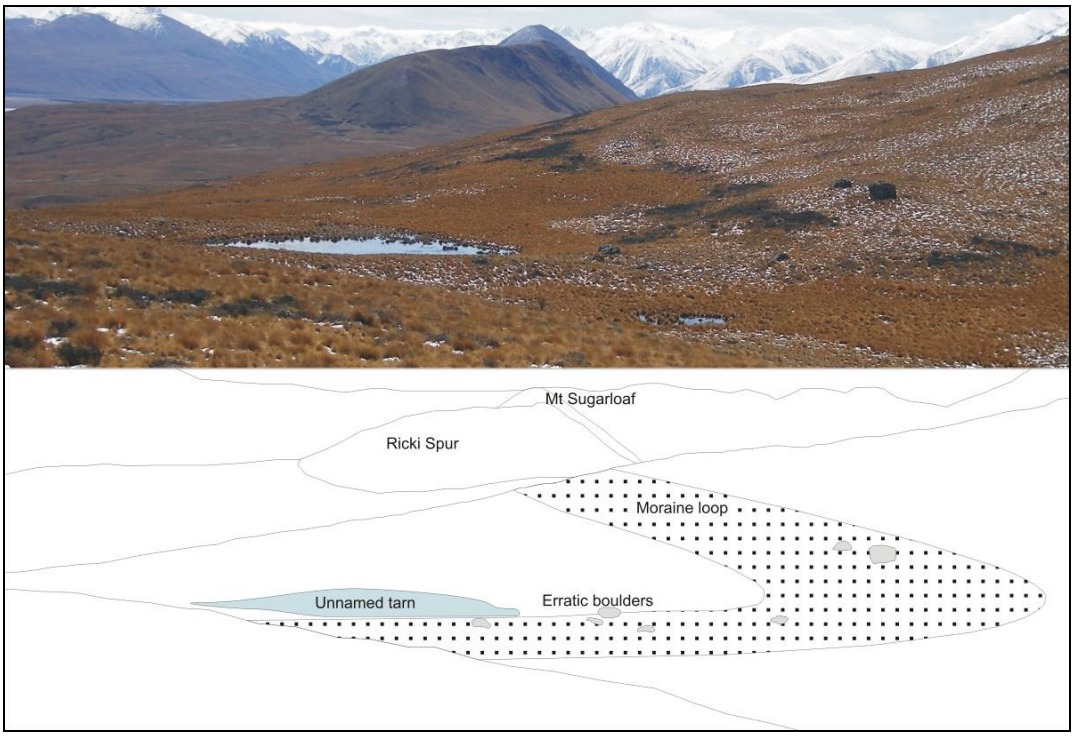

Figure 3-13 View north of erratic boulders on the crest of Emily moraine on Emily Hill. These boulders were sampled for cosmogenic dating.

Further retreat of the Lake Heron ice lobe is recorded in two lateral moraines between 720m and 800 m, up-ice of the earlier moraines (Figure 3-14). They are up to 20m high and up to 100m wide. A prominent ridge almost 1 km long occurs in a belt of pitted moraine. On the eastern side of the basin, ice wrapped around the north end of Clent Hills and constructed a terminal moraine south of Lake Emily (J36: 675377). Three prominent ridges are preserved on the surface of the complex and are up to 8m high and 100m in length. Lake Emily formed as the ice retreated from the moraine.

During the early stages of retreat, Lake Emily discharged into the Stour River valley through a channel in the moraine complex. Degradational terraces record drops in lake levels. With continuing ice retreat, the lake enlarged and a new outlet formed that drained into the centre of the basin. The height of the lake during this conversion was 690m, as is the height of the stranded outlet channel through the moraines. Lake Emily, at 685m, is the remnant of the proglacial lake and is surrounded by a rolling, swampy landscape. Ice of this advance pushed into the valley between Emily Hill and the Manuka Range (Figure 3-9).

Minor readvances during further retreat built push moraines on both sides of the basin. Six push moraines, separated by outwash surfaces, occur within the two kms north of the Ashburton River. The outwash surfaces discharge into the region now occupied by Maori Lakes (J36: 355625). At the same time, ice pushed near to Manuka Lake and Lake Emily in the east of the basin. Seventeen moraine ridges associated with retreat from the Emily advance occur between Emily Hill and the Longman Range. Meltwater in this area would have fed into a larger Lake Emily.

EM is considered contemporaneous with deposits of the Trinity Advance in the Clearwater basin. Outwash from this advance is traceable into the Canterbury Plains where it has been correlated with the Windwhistle Formation. Mabin (1980) and Oliver and Keene (1990) suggest an early Otiran age for the formation.

Figure 3-14 Emily Hill latero-terminal moraines on the north bank of the Ashburton River.

3.12.4 Johnstone Stream Formation

The Johnstone Stream Formation (JS) occur adjacent to both banks of Johnstone Stream and on the elevation surface between Isolated Hill, Ricki Spur and the Longman Range (Figure 3-8). JS kame terraces occur at lower elevations on the hillsides than the kame terraces of the Emily Formation. Mabin (1980) originally mapped the moraines as the late Emily advances, which Oliver and Keene (1990) renamed as the Johnstone Stream Formation. The latter naming system has been adhered in this study as it allows for an improvement in the detail of descriptions of moraines. The Cameron Glacier merged with the Lake Heron ice lobe at high elevations during the Johnston Stream advance and proglacial drainage concentrated in the center of the basin, issuing onto the plains via the Ashburton Gorge.

In the floor of the basin, JS deposits (J35: 610400) occur 3kms north of the Emily terminal moraine deposits as a belt of degraded latero-terminal moraines. The moraine belt is up to 10m higher than its outwash surface and has three prominent ridges along its crest. The moraines extend for 4kms from the base of the Wild Mans Brother Range to near Isolated Hill. Kame terraces associated with the moraines occur below those of the Emily advance and extend out of the mouth of the Cameron Valley. During this period, JS ice draped most of Isolated Hill (Figure 3-9). Further east, the largest JS advance is preserved as a moraine couplet, which extends in a northeast direction to the base of Ricki Spur. It also pushed all the way down the valley

between Ricki Spur and the Longman Range. JS meltwater from this part of the basin fed into Lake Emily.

Meltwater from the latter stages of the JS advance have incised through the ealier moraine and formed a new surface 2m lower. These moraines are 15m higher than their outwash surfaces and have two prominent ridges along their crest. Kame terraces associated with the moraines occur below those of the previous advance. Five push moraines between Ricki Spur and the Longman Range were construction during JS retreat.

Subsequent to further retreat, a readvance deposited a latero-terminal moraine 0.5 km north of Johnstone Stream (Figure 3-15). A 500 m wide meltwater channel that fronts the moraine belt has eroded, and removed, earlier JS deposits. Johnstone Stream is utilizing this channel before issuing into Gentleman Smith Stream. Nine more push moraines occur between Ricki Spur and the Longman Range that correlate with this period.

Figure 3-15 Terminal moraine of the Johnstone Stream Formation. The fence line marks a moraine ridge.

The final stage of the JS formation is a large moraine deposit near the old Mt Arrowsmith homestead. The moraine is a continuance of lateral moraines and kame terraces. During this time, ice draped only the northern tip of Isolated Hill. Four push moraines that occur at the northern end of Ricki Spur (Figure 3-16), and the lateral moraines that occur on the north bank of the Swin River alluvial fan, were deposited at this time.

According to Oliver and Keene (1990), the Johnstone Stream Formation is correlated with the Hakatere Formation in the Lake Clearwater basin and with the Bayfield-I advance in the Rakaia valley and is suggested to be older than 22 800 ± 800 C14 yrs B.P (uncalibrated), within the Otiran Glaciation (Soons and Burrows, 1978). ^{10}Be dated moraines near the Lake Heron Road opposite Isolated Hill (map 1) yielded an average age of 23.5 ka.

Figure 3-16 View east of Johnston Stream recessional moraines (dashed lines) at the north end of the valley between Ricki Spur and the Longman Range.

3.12.5 Lake Heron Formation

The Lake Heron Formation comprises three moraine belts at the south end of Lake Heron, 2.5km north of the Johnston Stream Formation. The moraines form arcuate belts approximately 6.5 km long, extending from hill slopes in the west of the basin to the northern tip of Ricki Spur (Figure 3-8). Lake Heron moraine deposits occur up-ice of the Johnston Stream Formation (Figure 3-10), and river terraces and kame terraces occur at lower elevations. Lake Heron kame terraces extend into the Cameron Valley at low elevations, suggesting that the Cameron Glacier contributed ice to the main lobe (Figure 3-9). Lake Heron outwash issued down the center of the basin, eroding the ice-proximal side of the Johnston Stream Formation moraine. The outwash surface is currently occupied by Gentleman Smith Stream (Figure 3-8).

Lake Heron 1

Remnant lateral and terminal moraines of the Lake Heron 1 (LH 1) advance occur 2.5km north of the Johnston Stream Formation. The LH 1 moraine is up to 10m high and 15m wide. West of Gentleman Smith Stream, a 1 km long segment of moraine is 15m high and 20m wide (Figure 3-17). Several outwash surfaces are associated with the LH 1 advance. The largest portion of outwash extends from the front of lateral moraines in the western basin floor and is 4km long and 600m wide. Lake Heron 1 moraine drapes the northern end of Isolated Hill. This portion of moraine is 1.5km long, 350m wide and 5 m high, and has three 5m high moraine ridges.

Figure 3-17 View looking north along the crest of the Lake Heron 1 moraine.

Lake Heron 2

Lake Heron 2 (LH 2) moraine abuts against the back of the previous moraine in the area at the northern end of Isolated Hill. At this location, it is 1km long, 150m wide and has a single 5m high moraine ridge on its crest. To the west of Gentleman Smith Stream, LH 2 moraine is separated from the previous moraine by a meltwater channel. The meltwater channel has eroded LH 1 moraine and formed an outwash surface that extends for 3km towards the south end of Isolated Hill, 3m lower than Lake Heron 1 outwash. A 1200m long, 100m wide and 10m high portion of LH 2 moraine is crossed by the Lake Heron Road. The area immediately behind the moraine is hummocky and pitted, interpreted as ablation moraine. Several kettle holes occur here. Several segments of LH 2 moraine occur west of Lake Heron Road, none greater than 350m long or 100m wide (Figure 3-18).

Figure 3-18 View looking east at remnant Lake Heron 2 moraine. Lake Heron to the left of centre.

Lake Heron 3

To the west of the Lake Heron Road, Lake Heron 3 (LH 3) terminal moraine is up to 10m high and 100m wide with a single moraine ridge and is separated from LH 2 by a 100m wide meltwater channel incised 5m below the LH 2 outwash surface. In the area at the north end of Isolated Hill, LH 3 moraine is 2km long and 80m wide and abuts against the back of LH 2. Here, two moraine ridges occur on a hummocky surface. LH 3 outwash surface occurs in the valley between Isolated Hill and Ricki Spur. River braids are still visible on the outwash surface, distinguishing it from higher terraces that are generally devoid of channels (Map 1). Outwash continues through a narrow bedrock gorge at the southern end of Isolated Hill and forms the 2km long, 1km wide outwash surface that Castleridge Station (J36: 643377) is located on.

No age constraints exist for the Lake Heron Advance, which must post-date the Johnstone Stream Formation. Oliver and Keene (1990) considered it as contemporaneous with the Spider Lakes Advance in the Lake Clearwater basin and estimated an age range of 17,000 to 14,000 cal years B.P.

3.12.6 Post-Lake Heron Formation glacial landforms

A substantial period of ice retreat without deposition or preservations of further moraines occurred following deposition of the Lake Heron Formation (Figure 3-8). Initial downwasting of the ice front was succeeded by the development of a proglacial lake, as indicated by lake benches, dammed between the ice margin and the area of hummocky terrane located behind the LH 3 moraine. The lake drained to the south via the channel currently occupied by Gentleman Smith Stream. Degradation terraces occur within LH 3 outwash recording fluctuations in lake levels.

On the lateral margins of the glacier, a complex relationship developed between fluvial channels and sediment deposition whereby excessive amounts of meltwater from the Cameron and Swin Rivers thwarted deposition of further moraines, or removed them following their deposition. As the Cameron Glacier retreated towards its head, meltwater exited the valley to the south and constructed a large kame complex adjacent to the Lake Heron ice lobe. Drainage channels incised the kame surface as meltwater fed into the proglacial lake. The kame surface is hummocky with several kettle holes.

The movements of the Swin River during ice retreat are recorded in recessional moraines and in river terraces in the area between Isolated Hill and Lake Hill. Initially, the Swin River drained behind the LH 3 moraine into the central drainage channel. However, as the ice pulled back, the Swin River constructed terraces and channels at lower elevations as it incised to lowering proglacial-lake levels.

Speight (1934) was the first to propose that Lake Heron was formerly of much greater extent than it is at present. He suggested that it extended about 5 miles further to the

north. Burrows and Russell (1975) describe lake benches near Prospect Hill, the most prominent at 737m, 700m and 689m asl. They suggested that a re advance blocked the north end of the basin, known as the Lake Stream Valley, filled the basin with meltwater and formed a lake, named ‘Greater Lake Heron’ (Figure 3-19). Lake benches around the southern and western margins of Lake Heron at elevations that match those noted by Burrows and Russell suggest the presence of larger lake. However, the lake is more likely to have existed during the retreat phase of the Lake Heron lobe rather than from a readvance. Terraces cut into the former alluvial fans suggest that the fans have made adjustments according to variations in the base level. The best example occurs to the south east of Mt Sugarloaf, where alluvium from Home Creek was diverted to the south by a glacier that existed along the eastern margin of Mt Sugarloaf. The fan fed into a proglacial lake and the terraces formed in the lower portions of the fan as it adjusted to fluctuations in the lake’s elevation.

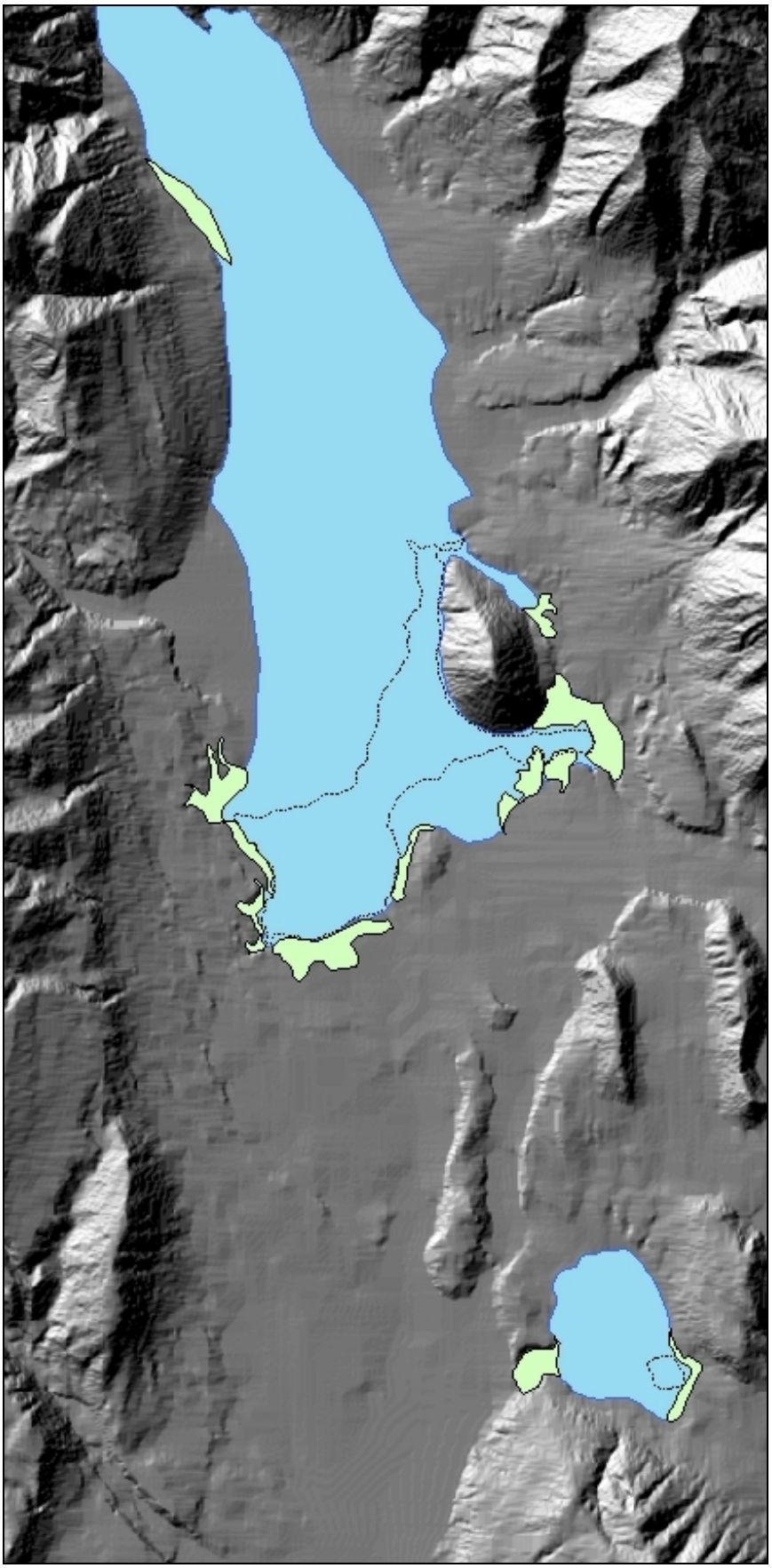

Figure 3-19 Location of lake deposits and extents of former proglacial lakes.

3.13 Re-examination of the glacial chronology

This section is a compilation of age constraints for Late Otiran glacial activity in the Lake Heron basin and neighbouring valleys. Note that SED (^{10}Be) ages are expressed as calendar years but radiocarbon dates are expressed as uncalibrated ages.

3.13.1 Review of local age constraints

In the Lake Heron basin, two SED dates from the lateral moraine at ~860m asl on the Emily Hill ridgeline (Figure 3-14) dated at 23.3 ± 1.6 and 24.6 ± 1.8 ka B.P (Table 3-2). This moraine is associated with the Emily Formation. In the center of the basin, three SED dates from the Johnstone Stream Formation yielded ages of 23.4 ± 1.6, 23.2 ± 1.7 and 20.2 ± 1.5 ka B.P (Table 3-2). A high elevation (~1200m asl) latero-terminal moraine near the summit of Staces Hill, mapped as being within the ice limits of the Emily Formation, was SED dated at 21.7 ± 1.4 and 18.6 ± 1.2 ka B.P (Table 3-2).

In the Lake Clearwater basin, SED dates from Evans (2008) decrease in age through the basin, from 18.3 k to 13.5 ka B.P. The Hakatere moraine, previously correlated with Johnstone Stream Formation (Oliver and Keene, 1990), was dated to 18.3 ka B.P (^{10}Be). The three moraines of the Spider Lakes Advance had an age spread of 1,000 years, the oldest dated to about 16.5 ka B.P and the youngest 15.5 ka B.P (^{10}Be). Younger moraines (Lake Clearwater Formation; Evans, 2008) occur behind the Spider Lakes moraines and are dated between ~15 and 13 ka B.P (^{10}Be).

A well-preserved sequence of terminal moraines occurs in the lower Rakaia valley. Surface exposure ages from Shulmeister *et al* (unpub data) show moraine ages decreasing up-valley during the LGM. The Tui Creek advance, which was previously ascribed to OIS 4 (Soons and Gullentops, 1973), was dated at 21.7 ka B.P (^{10}Be). Soons and Burrows (1978) suggested that the Bayfield 2 advance, recorded by three moraine loops, is older than 22,800 ± 800 C14 B.P, as indicated by radiocarbon dated plant fragments on Bayfield 2 till. However, Shulmeister *et al* (unpub data) dated the

Bayfield 2 and 3 moraines at 16 ka B.P and 12.5 ka B.P respectively (^{10}Be). The formerly undated Acheron advances, occurring up-valley of the Bayfield moraines, were dated 13.7, 12.8 and 13.9 ka B.P respectively (^{10}Be). In the bank of the Acheron River, within the Rakaia catchment, wood imbedded in laminated proglacial sediments has been dated to 11,650 ± 200 C14 B.P (Soons and Gullentops, 1973; Burrows, 1988). The silts were deposited following the ice retreat from the last of the LGM moraines.

The Lake Stream Advance occurs 29km from the Rakaia valley head at the north end of the Lake Heron basin (Figure 3-10). Burrows and Russell (1990) constrained the age of an inorganic silt layer, argued to represent the Lake Stream Advance, in a sediment core from Quagmire Tarn by carbon dating organic silts stratigraphically above and below it. The inorganic silt was interpreted as both slopewash and loess, suggesting glacial conditions. The organic layer below the inorganic sediment was dated at 11,900 ± 200 yr C14 B.P, while the layer above was dated at 10,000 ± 150 yr C14 B.P. From this data, Burrows and Russell suggested that ice had evacuated from Prospect Hill no later than about 13,000 yr BP. A surface exposure age of 12,700 yrs B.P (^{10}Be) on Prospect Hill dates the Lake Stream Advance (Easterbrook, 2003). 18km up-valley from the Lake Stream Advance are the Jagged Stream and the Reischek Drift moraines. Birkeland (1982) suggested, based on rock weathering data, that the Lake Stream, Jagged Stream and Reischek Drift are all of a similar age and were deposited between 8.5 ka and 10 ka B.P.

In the Cameron Valley, a buried soil resting on fluvial gravels and till was dated at 9,520 ± 150 C14 yr B.P (Burrows, 1975), providing a minimum age of deposition for the Wildmans 2 advance.

Table 3-2 Surface Exposure Dates (SED) for samples in the Lake Heron basin.

Sample (sites in Figure 3-9)	10Be/9Be ratio (1E-15)	Mass	9Be carrier mass	10Be Conc. (At/g-Q) (1E 6)	Altitude (meters asl)	Latitude	Prod. scaling	Shielding	Thickness correction	Site Prod. rate	Min. exp. Age (ka)	QuaD Error (ka)
SITE 1												
HER-EH-1-1	525.9	65.33	0.4269	0.230	859	43.50		0.999	2.902	9.89	**23.3**	**1.6**
HER-EH-1-2	232.7	19.14	0.3054	0.248	872	43.50		0.999	2.902	10.14	**24.6**	**1.8**
SITE 2												
RAN-LE-1-1	375.3	45.6	0.355	0.208	665	43.50	1.731	0.999	0.960	8.464	**23.2**	**1.7**
RAN-LE-1-3	503.4	60.5	0.355	0.208	683	43.50	1.731	0.999	0.960	8.464	**23.4**	**1.6**
RAN-LE-1-4	506.5	70.8	0.355	0.179	682	43.50	1.731	0.999	0.960	8.464	**20.2**	**1.5**
SITE 3												
LH-ST-1-1	707.1	63.33	0.4109	0.307	1207	43.50		0.999	2.902	14.21	**21.7**	**1.4**
LH-ST-1-2	592.2	76.60	0.5088	0.263	1200	43.50		0.999	2.902	14.21	**18.6**	**1.2**

10Be/9Be = measured ratio of 10Be from which the amount of 10Be per gram of quartz in calculated.
Mass = amount of pure quartz remaining after pre-treatment then used in the chemical extraction of 10Be.
9Be carrier mass = amount of 9Be added to the samples.
10Be concentration = final calculated amount of 10Be per gram of quartz.
Prod. scaling = adjusts local 10Be production rate to the altitude and latitude.
Shielding = amount of shielding that occurs in the field.
Thickness correction = corrects samples for thickness (in this case 4 cm).
Site production rate = local production rate of 10Be per year per gram of quartz.
Min. exp.e age and QuaD error = minimum age and error (in ka).

NOTE: SED ages from Sites 1 and 3 are from a preliminary age report and geomagnetic correction has not yet been performed. This would make the ages ~5% younger. Also, no erosion rate has been calculated, which would make the ages ~5% older. There fore the ages are not expected to move much in either direction.

3.13.2 Revision of the glacial chronology

In attempting to make correlations between different glacial systems, it needs to be noted that factors other than climate might have influenced the construction, or destruction, of a moraine. Climate change is indisputably the major driver of glaciations, although thee is discussion as to the relative importance of temperature and precipitation in the mid latitudes of the Southern Hemisphere (Anderson and Mackintosh, 2006; Rother and Shulmeister, 2006). Other influential factors include glacier response times (Oerlemans, 1994), relative areas of net accumulation (Porter, 1975), and landslides (Santa *et al*, unpub). The Lake Clearwater and Lake Heron basins, although contiguous at their southern extents, received ice from different glaciers. The Lake Clearwater basin received ice from the Rangitata Glacier while the Lake Heron basin was fed by ice from the upper Rakaia Valley. Therefore, it is likely that the two areas could have acted quite differently, as the ice fronts in the different basins were over 30km from their source during the LGM.

Most glaciated valleys in the South Island have acquired their own specific glacial nomenclature, which has then been tentatively correlated with other glacial systems. In many cases, the lack of age control of moraines resulted in correlation of deposits based on morphology, degree of weathering, loess accumulation and down-valley distance of the moraine. In light of the new dates, it seems some of the earlier correlations require revision.

The revised glacial chronology for the Rakaia River valley, the Lake Heron basin and the Lake Clearwater basin is depicted in Table 3-3. The largest advance of the Last Glaciation Maximum (LGM) in the Lake Heron basin is the Emily Formation, and in the Rakaia valley, it is the Tui Creek advance. Both produced SED ages of around 24 ka B.P. The much-degraded moraines of the Emily Formation were previously thought to have advanced in the early Otiran/OIS 4 (Mabin, 1980; Oliver and Keene, 1990), but the SED ages firmly suggest it is late Otiran/OIS 2 (Table 3-3). The Emily Formation correlates with the Trinity Hill Formation in the Lake Clearwater basin; therefore, the latter is probably also the maximum advance of the LGM (Figure 3-20). The Rangitata glacier ice therefore extended further east than the Rakaia Glacier

advanced through the Lake Heron basin. This is supported by the disproportionate down-valley distances between the Johnstone Stream and Hakatere Formations end moraines.

The Hakatere Formation (18.5 ka B.P), which was previously correlated with the Johnstone Stream Formation (23.4 ka B.P), returned an SED age almost 5,000 years younger. The ages suggest that the Lake Heron ice lobe retreated up the basin earlier than did the ice in the Lake Clearwater basin (Figure 3-20). In the east of the lower part of the Lake Heron basin between Lake Emily and Ricki Spur, a sequence of at least 50 moraine ridges (Figure 3-3) suggests that the front of the glacier fluctuated episodically while in a constant state of retreat. The more pronounced terminal moraine in the west of the Lake Heron basin, from where the Site 2 SED samples were retrieved, represents a glacier still-stand during overall ice-retreat. However, at least ten moraine ridges occur within the Johnstone Stream Formation in the west side of the Lake Heron basin (Figure 3-3), suggesting ice-front oscillations still occurred during this period. In addition, no moraine in the Lake Clearwater basin has presently been dated at 23.4 ka B.P or earlier. This absence of a correlating moraine suggests that the Lake Heron and Lake Clearwater ice lobes acted independently of each other.

The SED dates from the lower Rakaia Valley show that between ~18 ka and ~11 ka B.P, significant morainic deposition occurred approximately every 1,000 years (Shulmeister *et al,* unpub data). A similar series of SED ages occurs in the Lake Clearwater basin. In the Lake Clearwater basin, the earliest moraine dates at ~18 ka B.P, and was followed by at least six moraines that returned ages between 16.5 ka and ~13 ka B.P (Evans, 2008). In the Lake Heron basin, the recessional sequence appears to have begun earlier with the Emily Formation, followed by the Johnstone Stream and Lake Heron Formations. The SED ages suggest a nearly contemporaneous LGM maximum was followed by a recessional sequence punctuated by minor readvances.

The presently undated moraines of the Lake Heron Formation were deposited slightly after the Hakatere moraine in the Lake Clearwater basin (Figure 3-20) and at around the same time as the younger Bayfield moraines in the lower Rakaia valley (Table 3-3). A proglacial lake formed during ice retreat from the Lake Heron 3 moraine,

which impeded the preservation of further end moraines. However, extensive kame terraces and lateral moraines up valley from the Lake Heron 3 moraine imply that further oscillations of the ice front occurred following glacier retreat from Lake Heron 3 (Map 1). The idea that further oscillations occurred is supported by the deposition of moraines that yielded SED ages through into the Late Glacial period. In the Lake Clearwater basin, the Lake Clearwater moraines (Evans, 2008) were deposited between ~15 ka and 13 ka. The Acheron moraines in the lower Rakaia valley (Shulmeister *et al,* unpub data) were deposited between ~14 and 13 ka B.P.

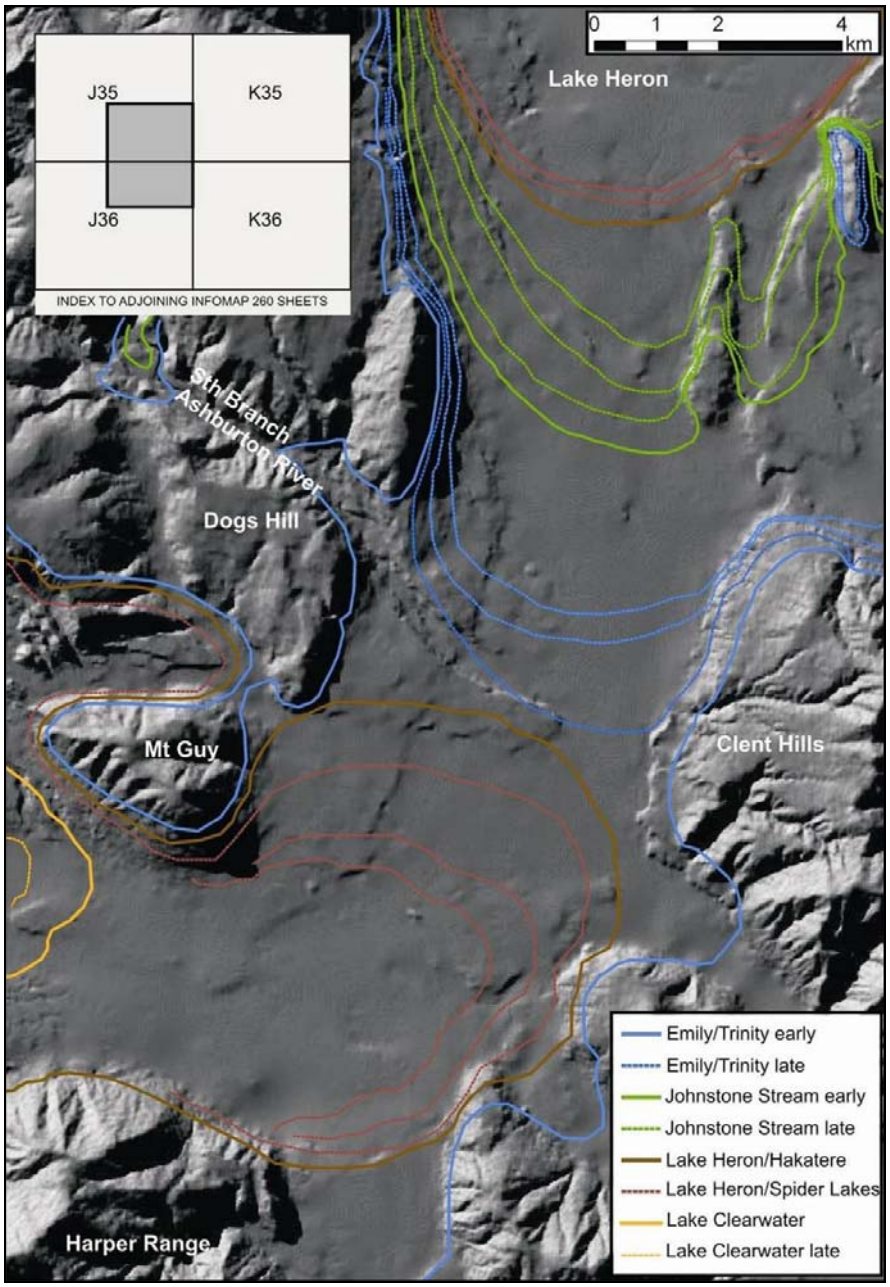

Figure 3-20 Correlation of Late Otiran ice extents in the Lake Heron and Lake Clearwater basins.

Table 3-3 Revised glacial chronology for the Lake Heron, Rakaia and Lake Clearwater area.

CHRONOLOGY				RANGITATA GLACIER	LAKE HERON BASIN	RAKAIA GLACIER	
GLACIATION/ INTERGLACIAL	EVENT STRATIGRAPHY	AGE	OIS	LAKE CLEARWATER		RAKAIA VALLEY	CAMERON VALLEY
							Arrowsmith
	Holocene warm period	6.5				Lyell/Whitcombe	Marquee 2
Aranuian (Int)							Marquee 1
	Holocene warm period					Reischek Drift/ Jagged Stream	Wildmans 2
						Lake Stream	Wildmans 1
				Lake Clearwater		Acheron 3	
	Late glacial climate reversal	11		Spider Lakes 3		Acheron 2	
	Late glacial warm period	13		Spider Lakes 2	Lake Heron 3	Acheron 1	
		14	2	Spider Lakes 1	Lake Heron 2	Bayfield 3	
Otiran (Glac)				Hakatere	Lake Heron 1	Bayfield 2	
		18			Johnstone Stream	Bayfield 1	
		24		Trinity Hill	Emily	Tui Creek	
	Late glacial interglacial		3	No deposits identified			
		59	4				
	Late glacial cold period						
		73					
Kaihinu (Int)			5	No deposits identified			
		128					
Waimean (Glac)			6	Dogs Hill	Dogs Hill	Woodlands	
		188					
Karoro (Int)			7	No deposits identified			
		241					
		291	8	Pyramid	Pyramid	Hororata	
Waimaungan (Glac) Nemona (Glac)		360	9	No deposits identified			

4 Sedimentology

4.1 Introduction

Very few glacial sediment exposures occur in the Lake Heron basin. One major exception is a glacitectonized sequence of proglacial sediments exposed along the southern shoreline of Lake Heron (Figure 4-1). Although recent work in the South Island has shown the value of detailed studies into glacial sediments (Hart, 1996; Mager and Fitzsimons, 2007), sediment studies in the Lake Heron basin have largely focused on non-glacial Tertiary outcrops (Haast, 1879; Speight, 1919; Mason, 1948). The sedimentological information presented in this chapter illustrates the nature of glacier dynamics near the end of the Last Glacial Maximum. The glacial history of Lake Heron has been studied (Mabin, 1980; this study), but the Quaternary sediments of the Lake Heron outcrop described in this chapter have never before been described.

The exposures that are described are located on the southern shoreline of Lake Heron and extends in an east-west direction for over 1 km (J35 615444). The outcrop occurs within the limits of the Lake Heron ice advance (see Figure 3-9) and immediately up-ice of an area of hummocky and subdued topography comprising moraine deposits and kettle holes (Figure 4-1). Drainage channels, river terraces and lake benches at higher elevations suggest that the lake formerly occupied a larger area and that the sediments have been exposed by lowered lake levels.

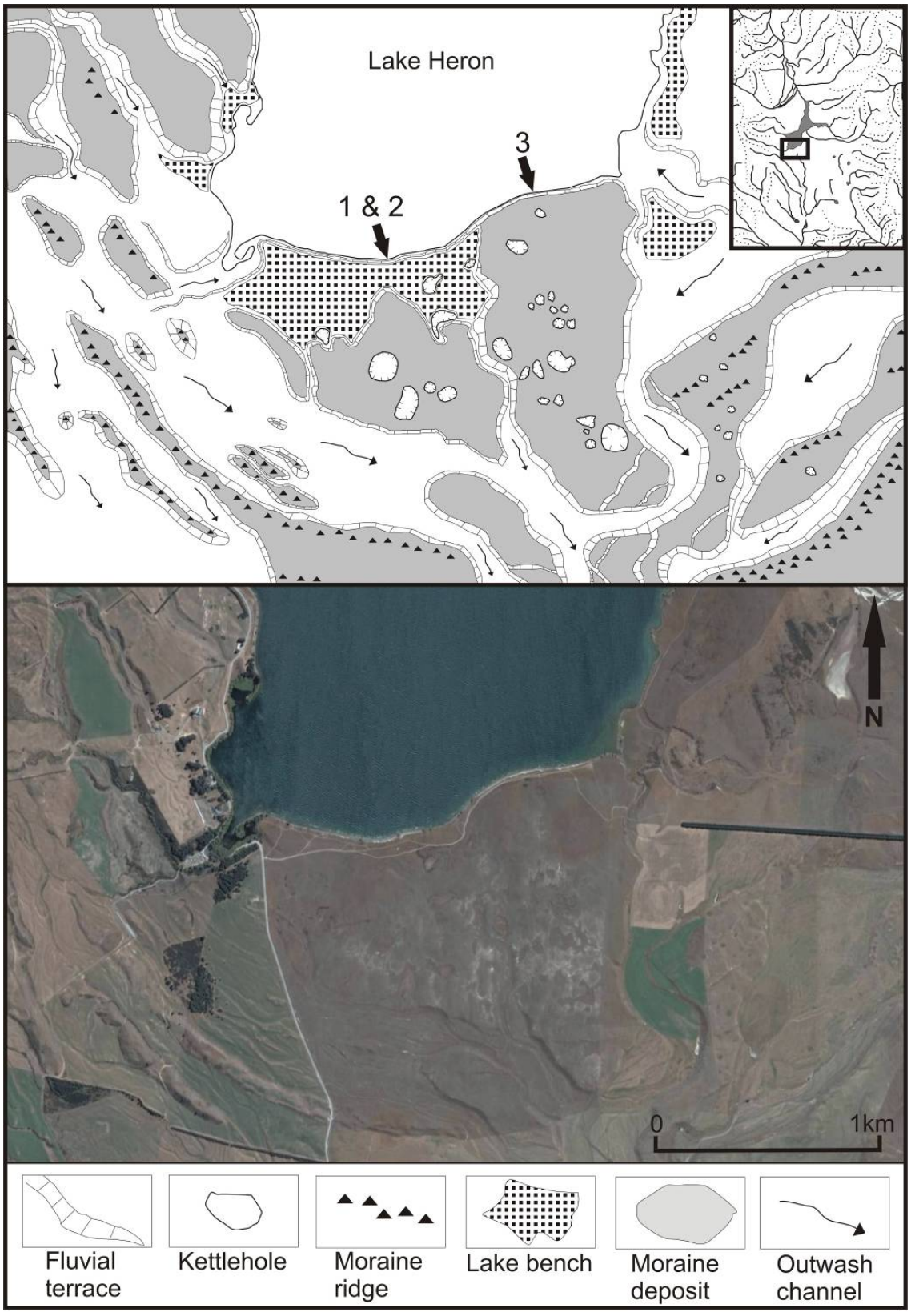

Figure 4-1 Location and geomorphological map of the southern margin of Lake Heron. Numbers 1, 2 and 3 refer to sites in the text. Image from Google Earth (2008).

4.2 Methodology

Aerial photographs were used to map in detail the geomorphology of the major landforms in order to assist in defining the spatial relationships existing between the sediments and the landforms. The best sediment exposures along the lake shoreline were mapped with detailed two-dimensional logs and representative summary profiles. Exposures were logged following systems outlined in Eyles *et al* (1983) and Evans (2004). To evaluate the effects of glacial transport and deposition, clast roundness data was obtained by collecting 50 clast samples within a designated bed, measuring the A, B and C axis and estimating the roundness of the clast and noting any striations or faceted faces.

Benn and Evans (1998) regard clast form as the sum of three characteristics, at different scales, affected by active transport:

(a) Shape is the relative dimension of the long, intermediate and short axes. Clast shape is highly dependent on both process and lithology. Almost all the sampled clasts are derived from the Torlesse Supergroup, a greywacke sandstone and siltstone, with initial shape characteristics probably closely related to preferential plucking along bedding, fracture and fault planes. Ternary diagrams illustrate whether a clast shape is predominantly block, slab or elongate (Figure 4-2; Figure 4-3; Figure 4-4). This data is derived from the relationship between the A, B and C axis.

(b) Roundness is the degree of curvature of clast edges. Roundness is the product of the contrasting effects of fracturing, which creates new sharp edges and faces, and abrasion, which increases edge rounding. Clast roundness, presented in this chapter in histograms (Figure 4-2; Figure 4-3; Figure 4-4), illustrates the dominance of subrounded clasts.

(c) Texture is the character of the clast surface. Common clast features of subglacial process include striations, faceted faces and the development of stoss- and lee-shaped clasts.

Subglacial tills that have been subjected to high cumulative strains will display strong clast fabric (Evans et al, 2006). Slippage between clasts and the surrounding, faster moving, matrix causes elongated clasts to orientate parallel to the main stress direction (Ildefonse and Mancktelow, 1993). Evans *et al* (2006) emphasized that a continuum of fabric strengths exists according to the maturity of the subglacial sediment, more specifically its strain history. However, scepticism exists as to the applicability of the technique in evaluating till genesis and strain signatures (Hooyer and Iverson, 2000; Benn, 2002). While this variability casts doubt on the technique, it most probably reflects "the heterogeneity of subglacial beds and their concomitant responses to glacial shear stress" (Evans *et al,* 2006). Therefore, measurements of the A/B plane dip and orientation avoid the problem of the transverse orientations observed for clast A-axes. A/B planes of clasts tend to rotate parallel to the direction of shear and A/B planes will adopt a flow parallel dip more readily than A-axes, which may align transverse to flow (Evans *et al*, 2007).

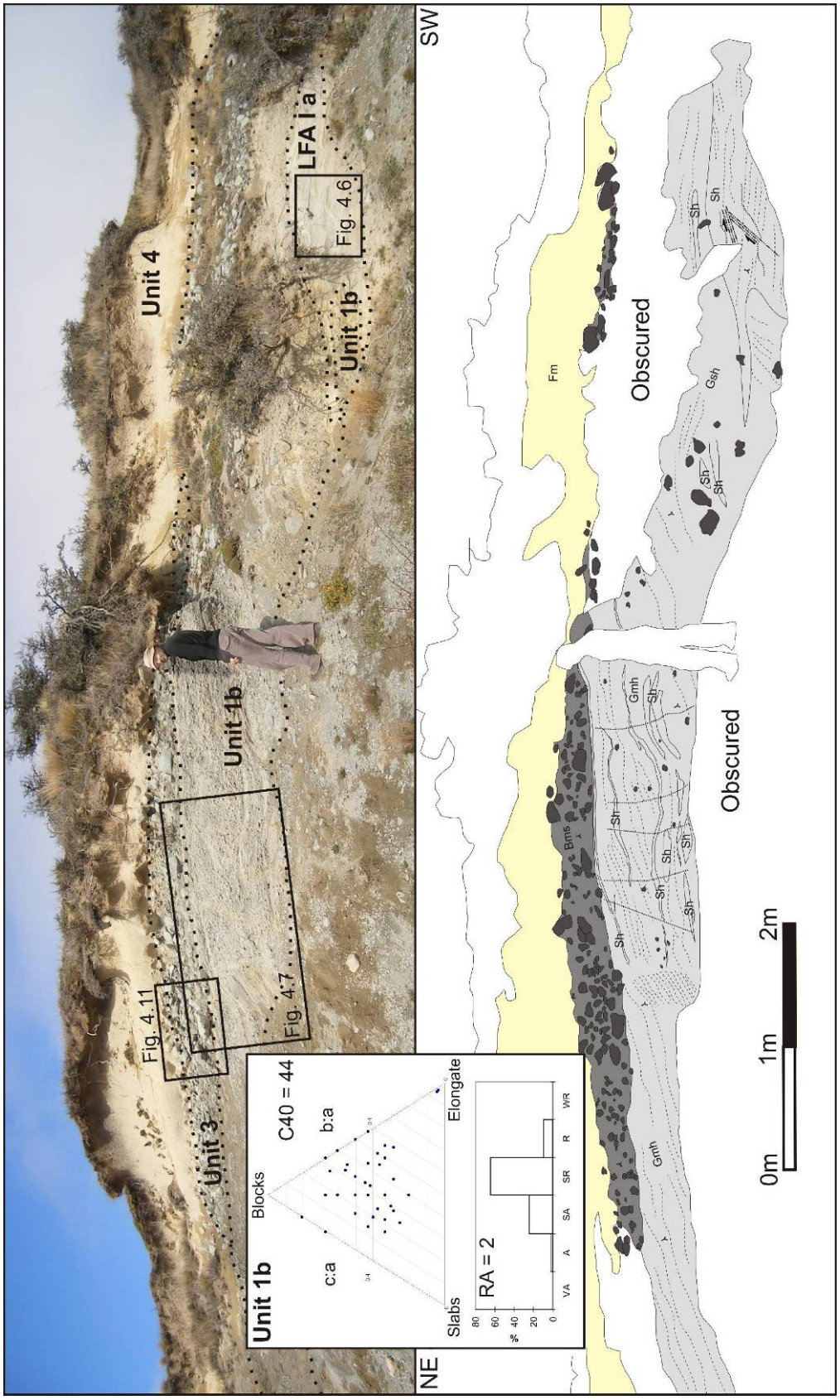

Figure 4-2 Annotated photograph of the westernmost exposure (location 1; E2361650/N5744329) showing main units and location of detailed figures. Clast shape and roundness data for unit 1b. Roundness categories are as follows: VA = very angular; A = angular; SA = sub-angular; SR = sub-rounded; R = rounded; WR = well rounded. C40 is the percentage of clasts with c:a ratios <0.4 and RA is the percentage of clasts in the VA and A categories.

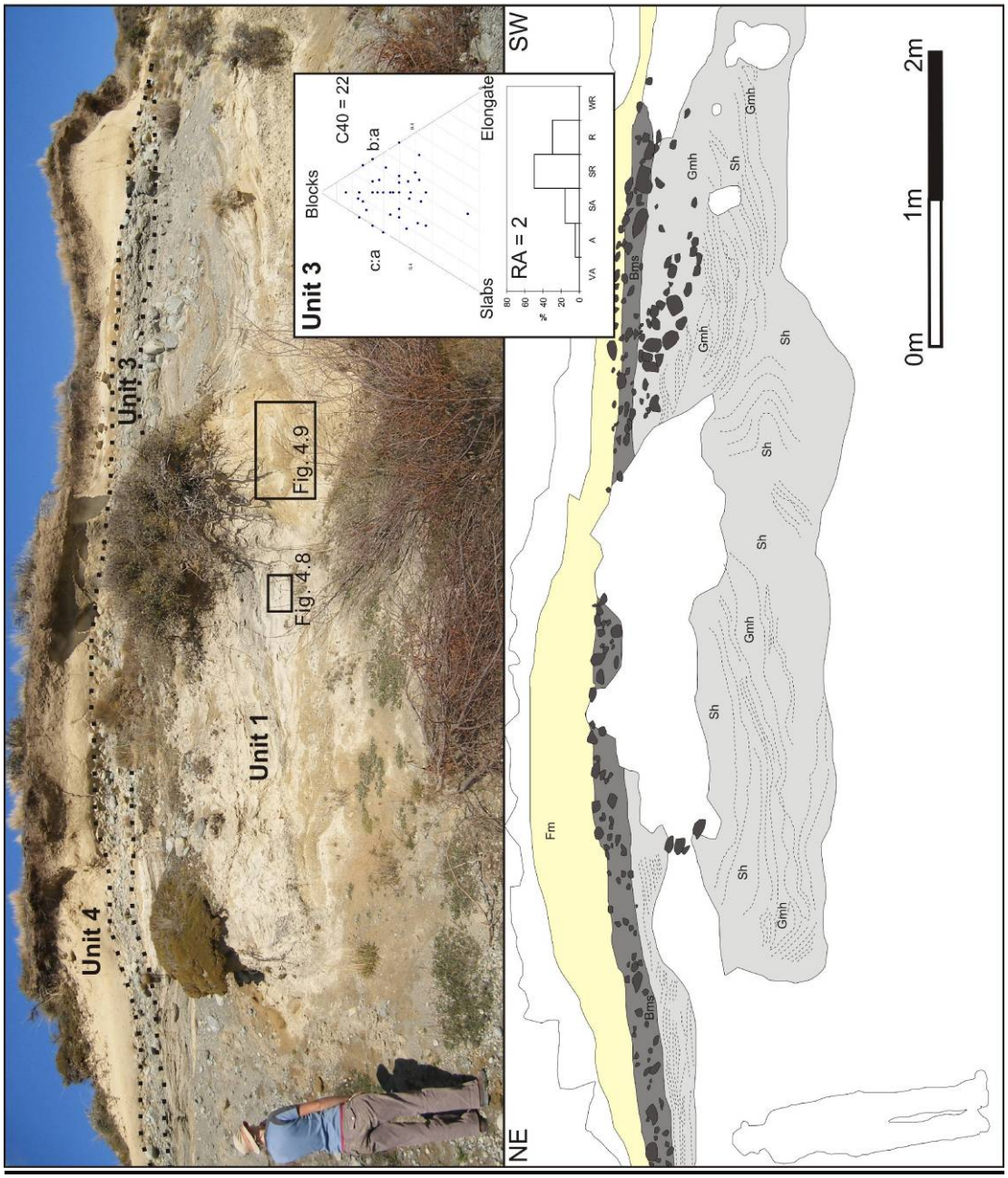

Figure 4-3 Annotated photograph of the central exposure (location 2; 20 m northeast of first outcrop) showing main units and location of detailed figures. Clast shape and roundness data for unit 3 (abbreviations as in Fig. 4.2).

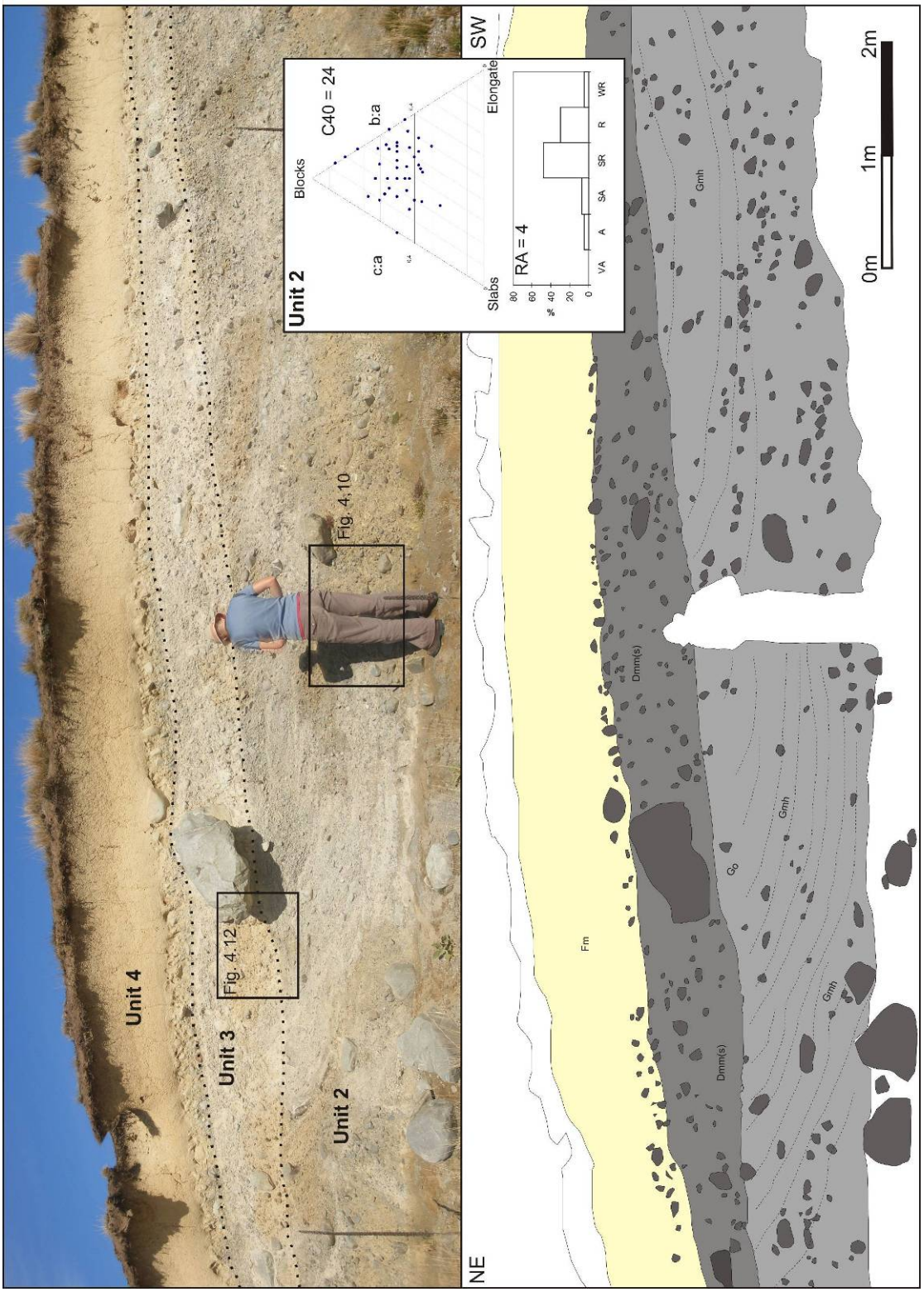

Figure 4-4 Annotated photograph of the easternmost exposure (location 3; E2362324/N5744665; 068/248° strike of face) showing main units and location of detailed figures. Clast shape and roundness data for unit 2 (abbreviations as in Fig. 4.2).

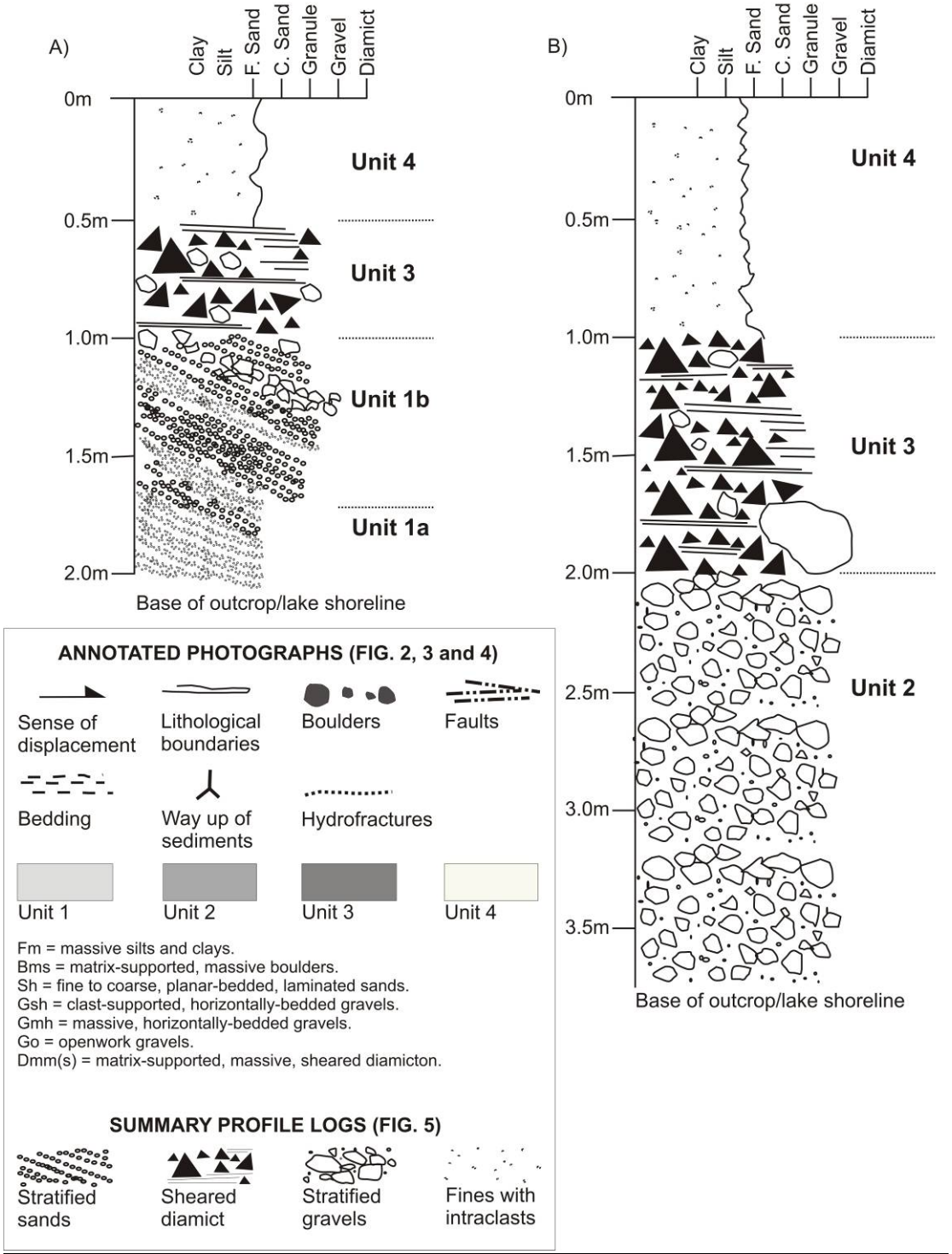

Figure 4-5 Summary profile logs of a) the combined western and central exposures and b) the easternmost exposure. Key to annotated photographs and summary logs.

4.3 Description and interpretation of units

4.3.1 Unit 1: Sands and gravels

Unit 1a: In the westernmost exposure (Figure 4-2), the lowermost sediments consist of interbedded fine to coarse-grained sands (Figure 4-6). It is 1 m thick, although the basal contact is obscured, and is normally graded whilst varying from laminated (1mm thick) to massive. There are occasional small sub-angular pebbles. A variety of deformation structures are present, including steeply dipping and near horizontal fractures and faulting. The unit has either a sheared or an interfingered contact with unit 2 to the east.

Within the unit is a <10cm thick gravel bed near the bottom of the exposure, consisting of moderately sorted granules with some pebbles. The contact between the bed and the sands is sheared and deformed. The bed pinches out to the east.

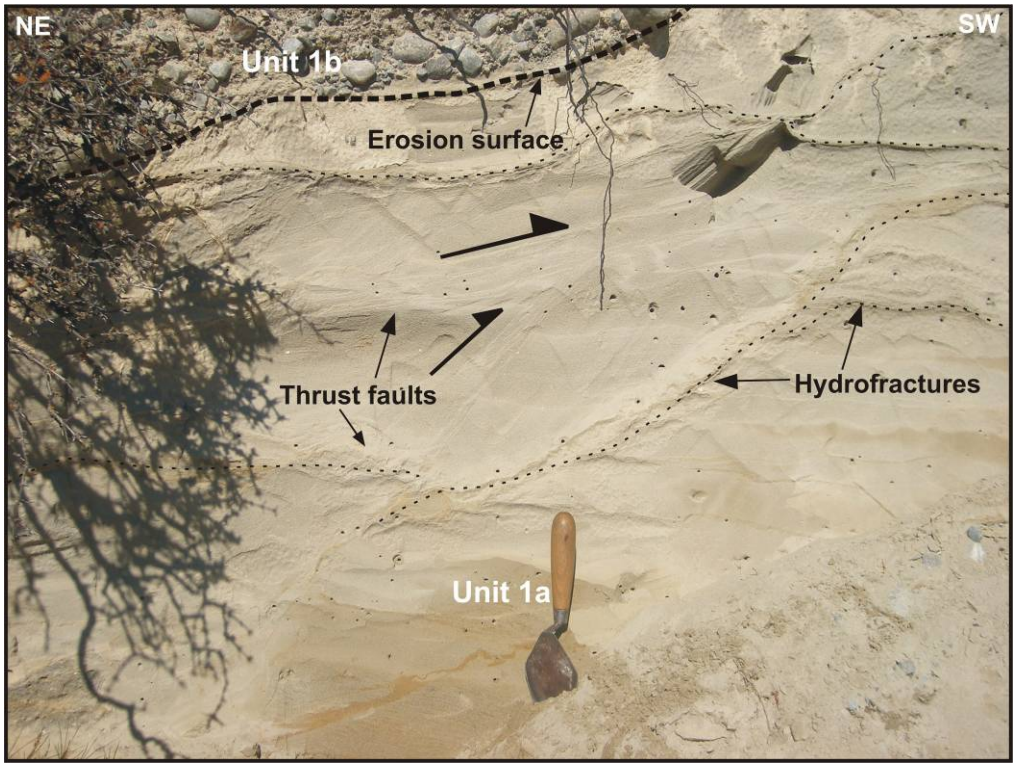

Figure 4-6 Detail of thrusts and flame structures within horizontally bedded unit 1a at western exposure. The structures are truncated by an erosion surfcae at the base of unit Ib.

Unit 1b: consists of clast (and locally matrix) supported gravels with sandy interbeds. The contact between the gravels and the underlying sands is erosive and sharp. Bedding

in the lower part of the unit is sub-horizontal whilst the upper portion dips to the east. Sediment in Unit 1b is poorly to moderately sorted and contains granule interbeds. Clast size varies from pebbles to boulders. In general, the unit coarsens to the east. Beds of unit 1a occur in the western exposure and consist of 1cm to 20cm thick beds of sub-rounded gravels containing interbedded silts and sands (Figure 4-7). The gravels are mainly clast-supported; however, some pockets are matrix-supported with fine sands as matrix. The interbedded sediments vary between laminated to cross-beds of predominantly openwork, fine to coarse-grained pebbles. Clasts within the unit are predominantly sub-round, with a minor sub-angular component and blocky with a small proportion of elongated and slabby clasts (Figure 4-2). Internal structures include hydrofractures and faults with variable displacement (1cm to 1m).

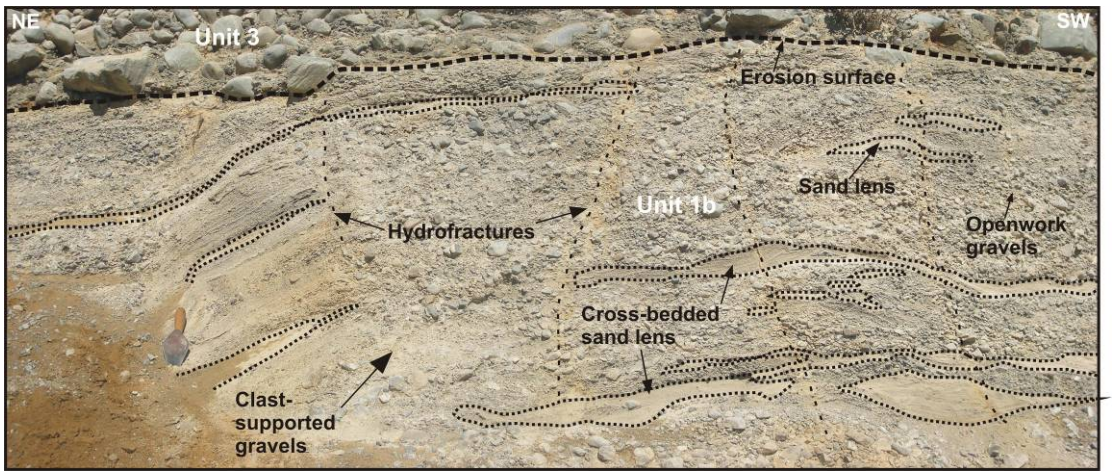

Figure 4-7 Detail of interbedded sand lenses within unit 1b in the western exposure. Note the termination of hydrofractures at the erosion surface at the base of unit II.

In the central exposure (Figure 4-3), 20m along the outcrop, unit 1 is at least 2m thick and is highly deformed. Sediments within the facies consist of moderately sorted pebble to small cobbles and vary from matrix to clast supported. Stratification occurs as both discontinuous (15cm thick) interbeds of both cross-bedded granules and coarse sands and laminated fine sands and silts (<10cm thick). Some fine-grained interbeds are compacted and show planar cross bedding (Figure 4-8).

Figure 4-8 Planar cross beds in unit 1 in the central exposure.

Figure 4-9 Ductile deformation of fine sands within unit 1 in the central exposure.

Ductile deformation (>1m) and small-scale brittle normal faulting occurs predominantly in the finer grained sediments within unit 1. Figure 4-9 shows tight folding of laminated fine sands in the central exposure. Adjacent to the tight fold are convoluted beds of coarse and fine sands. Unit 1 is not present in the easternmost exposure.

The sands and gravels of unit 1 are interpreted as having been deposited in a proglacial environment. The close association between gravels and fine-grained beds suggests either fluctuations in sediment supply or higher discharge and/or velocities into ice-marginal streams and sediment traps. Within a few beds, beds of less deformation overlie the ductile deformation structures. This suggests that unit 1 was predominately subject to syndepositional or immediately post-depositional deformation as the units had not dewatered. Hydrofractures are further evidence of loading above water-saturated sediment. Slump structures are indicative of extensional deformation. Small-scale thrust faults post-date the extensional structures and relate to a later event.

4.3.2 Unit 2: Stratified gravels

The crudely- to well-stratified gravels occur exclusively in the easternmost exposure and consist of pebbles to cobbles in a silt to fine-sand matrix (Figure 4-10). It is poorly to moderately sorted and stratification increases up-section. Some large boulders (<60 cm) occur within the gravels, while the basal portion has more cobbles and boulders than exist in the upper, more stratified pebble and boulder beds. Clasts are sub-round to round and are predominantly blocky (Figure 4-4), with striations present on 12% of clasts. In the eastern exposure, the gravels take a ‘u’-shaped form (Figure 4-4) and minor normal faulting is apparent. The unit varies from clast to matrix supported with a minor openwork component. The unit is at least 2m thick, although the bottom of the unit is not seen.

Unit 2 is interpreted to be proximal glacial outwash. The down-folded section in the eastern exposure is a cross-section through a channel-fill deposit. Flow was directed down-valley at an orientation of approximately 180°. Minor normal faulting is present and is of similar size and extent to that seen in unit 1. It is likely that unit 2 was subject to the same extensional deformation, such as buried ice melt-out.

Figure 4-10 Stratified and clast-supported sediments of unit 2 in the eastern exposure.

4.3.3 Unit 3: Till

Unit 3 occurs along the entire Lake Heron outcrop; however, deformation is more pronounced in the eastern exposure. The unit is laterally continuous and traceable along the length of the outcrop. In the western and central exposures, unit 3 is no more than 60cm thick and consists of poorly sorted, crudely stratified, clast to matrix supported cobble and boulders with some granules and pebbles. In some places, the pebbles have an openwork matrix (Figure 4-11). Clasts are blocky (Figure 4-3) and are predominantly sub-round to round, with roundness increasing up through the unit. Striations were present on 24% of clasts and faceting on 6% of unit 2 clasts.

In the easternmost exposure, unit 3 is identified by the nature of the clasts, which are predominantly pebbles to cobbles, with some large boulders (Figure 4-12). However, at this location unit 3 is massive, fissile, clast to matrix supported and much indurated. Silt and fine sands comprise the matrix. Striations on the top surface of a large boulder range between 1-60º (Figure 4-12), predominantly perpendicular to the strike of the exposure (068/248º), which may be evidence of a subglacial derivation. Stratification occurs within rip-up beds of underlying gravels. A sharp, planar erosion surface occurs at the base of unit 3 (Figure 4-12).

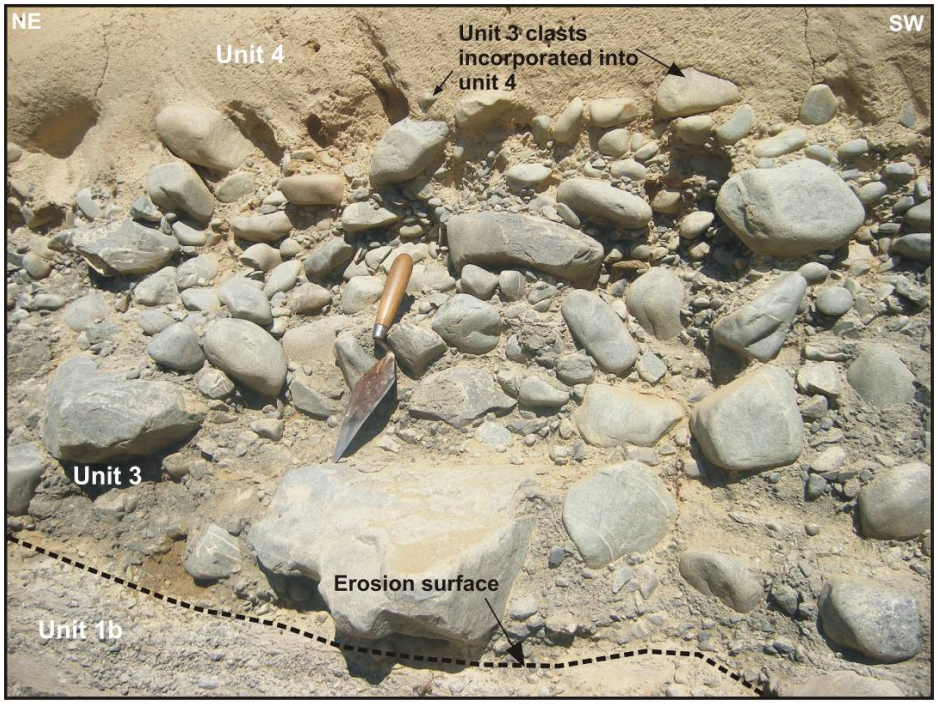

Figure 4-11 Detail of unit 3 showing the sharp erosional contact at the base with and the erosional contact with the overlying loess.

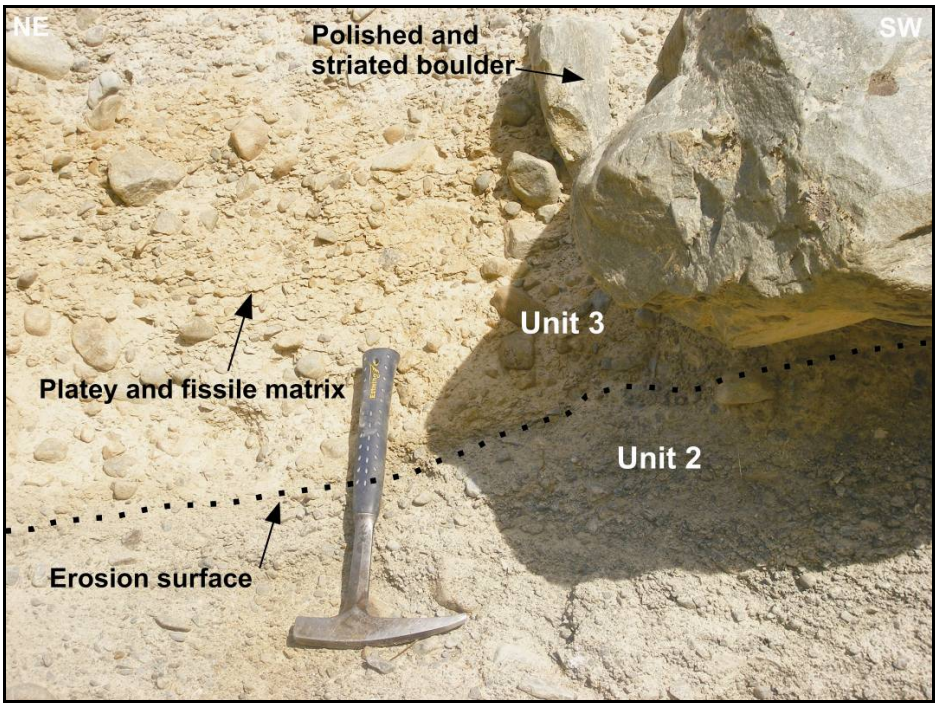

Figure 4-12 Detail of boundary between unit 2 and 3. The erosion surface marks an angular unconformity between the gently dipping gravels and the till.

Although no deformation is seen in the western and central exposures, the fissile nature of the eastern exposure is indicative of subglacial deformation. It is suggested that ice overrode the sediments, developing small shear planes along which the sediment moves.

4.3.4 Unit 4: Loess

Unit 4 consists of silts and fine sands containing very few pebble to granular sized clasts. It is crudely stratified. It forms a gradational boundary with underling units and the lower portion of the facies often contains clasts acquired from below. Unit 4 is present as the uppermost unit along the entire exposure and is no more than 1 m thick. Pebble to granular clasts are a common feature of loess deposits in inland Canterbury, where there are powerful westerly winds. The westerly at times is so strong that sand dunes have formed in the lower Rakaia Valley to the immediate north of the study area (Soons, 1963; Eden and Hammond, 2003).

4.4 Discussion

4.4.1 Clast analysis

Macrofabric data comprising 50 clasts were collected from unit 2 and plotted on Fisher equal-area lower hemisphere projections using the Stereonet programme. Figure 4-13 shows the dominant glacier stress-flow direction. Clasts that were approaching a rod-like shape were selected as they exhibited a definite short, intermediate and long axis. Sphere shaped clasts were not measured since they "have infinite combinations of three mutually perpendicular axes … make very weak fabric, have no preferred directions, and indicate little about emplacement or strain" (Klein et al., 2001).

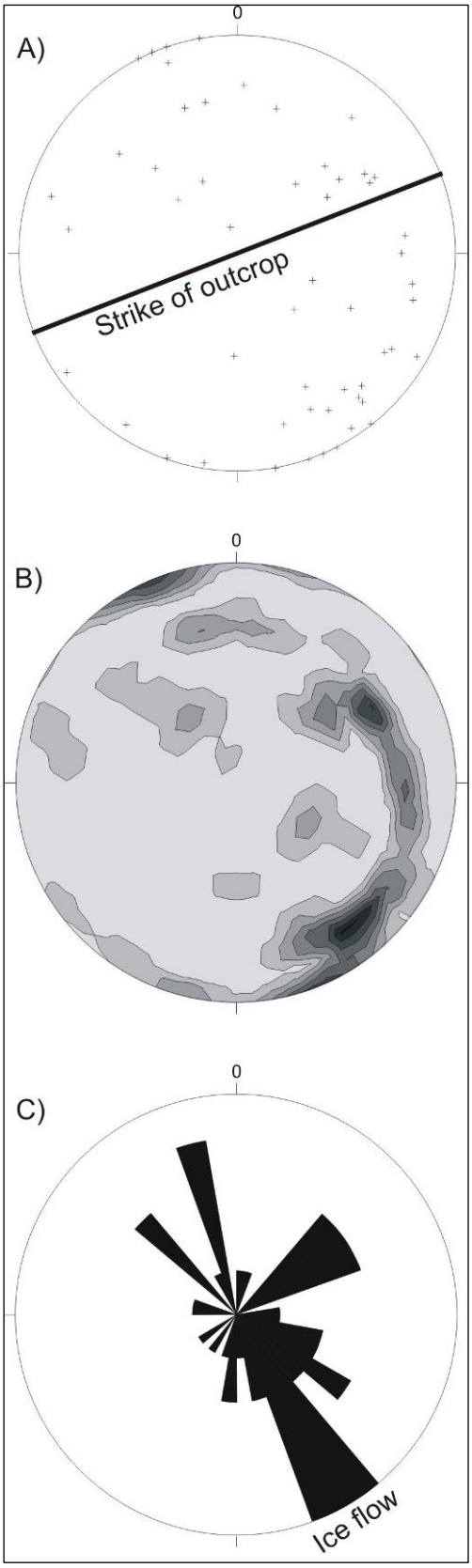

The fissile nature of unit 2 is indicative of subglacial deformation, suggesting that ice has over-ridden the sediments. Small shear planes have developed along which the sediment moves. The fabric data shows two closely related clusters at almost opposite poles, 320° - 350º and 140° – 170° (Figure 4-13B). The clusters represent a transverse fabric in response to the low dip angle. The data suggests a stress direction in the SSE – NNW quadrants, broadly perpendicular to the strike of the exposure (068/248º). Striations on the large boulder imbedded in unit 2 range between 1° and 60º. The stress direction as indicated by unit 2 clast orientations supports the theory of ice moving south through the Lake Heron basin.

Further interpretation of the clast fabric data was carried out using eigenvector analysis. This procedure is a computer-based statistical type analysis, which determines the mean orientation and the scatter of clasts about that mean. The preferred long axis eigenvector (V1) was calculated to be in the direction (139.8 / 10.7), the intermediate eigenvector (V2) was calculated to be in the direction (41.0 / 38.8) and the minimum eigenvector (V3) was

Figure 4-13 Fisher equal-area stereonet plot of unit 2 clast fabrics produced in Stereonet software. A) Equal-area stereographic scatter plot of the clasts (n = 50). The strike of the eastern exposure also indicated. B) Equal-area stereographic contour plot of the clasts (contour increments of 1.00. Maximum density of 7.15 at 145/ 18). C) Rose diagram of clast orientation (largest petal 5.00).

calculated to be in the direction (242.5 / 49.2). Eigenvalues give an indication of fabric strength, such that a strong fabric would have a high value in the direction of preferred long axis orientation (S1) and a small value in the direction of minimum orientation (S3). The calculated eigenvalues for unit 2 indicate a relatively weak fabric, with a value of 0.493 for eigenvalue S1 and a value of 0.143 for eigenvalue S3. Based on the till classification scheme developed by Dowdeswell *et al* (1985), unit 2 is interpreted as a glacigenic sediment flow (Figure 4.14).

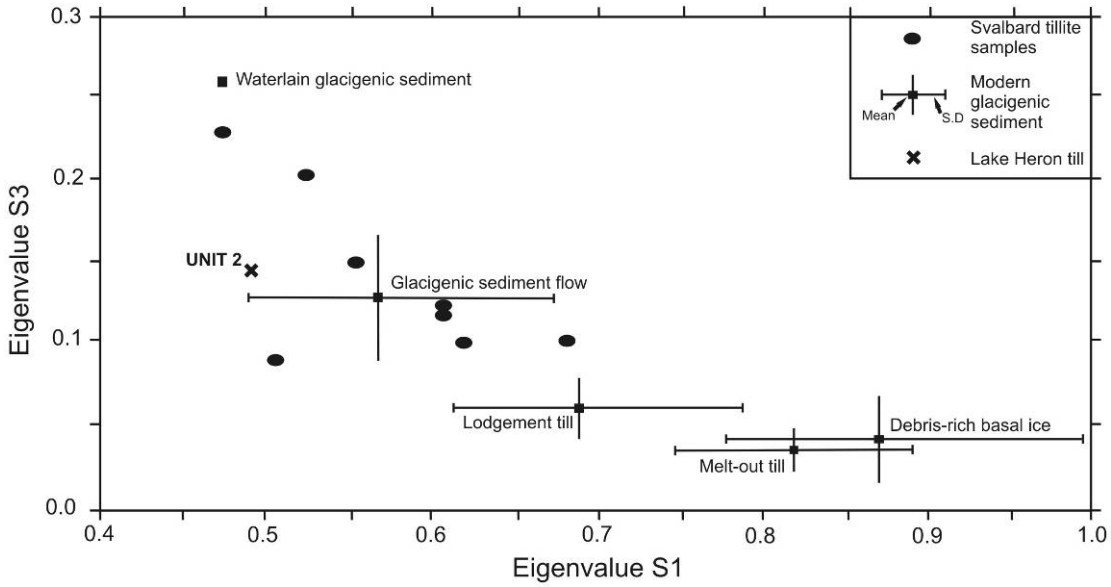

Figure 4-14 Plot of S1 against S3 eigenvalues for unit 2 and fabrics measured in five modern glacial environments and tillites from Svalbard (Dowdeswell *et al*, 1985). The variability of fabric strength in modern environments (data derived from Lawson (1979), Sharp (1982) and Gibbard (1986)) is shown as standard deviation (S.D) and range about the mean eigenvalues. (Modified from Dowdeswell *et al*, 1985).

4.4.2 Depositional reconstruction

Reconstruction of the depositional history of sediments at the Lake Heron southern shoreline is constrained by environmental interpretations of the units, interpretations of local landforms, and inferred glacier-flow direction derived from A/B planes from a subglacial till. The model presented in Figure 4-15 shows a series of longitudinal sections of the ice-marginal environment of the Lake Heron glacier during glacial readvance near the end of the last glaciation.

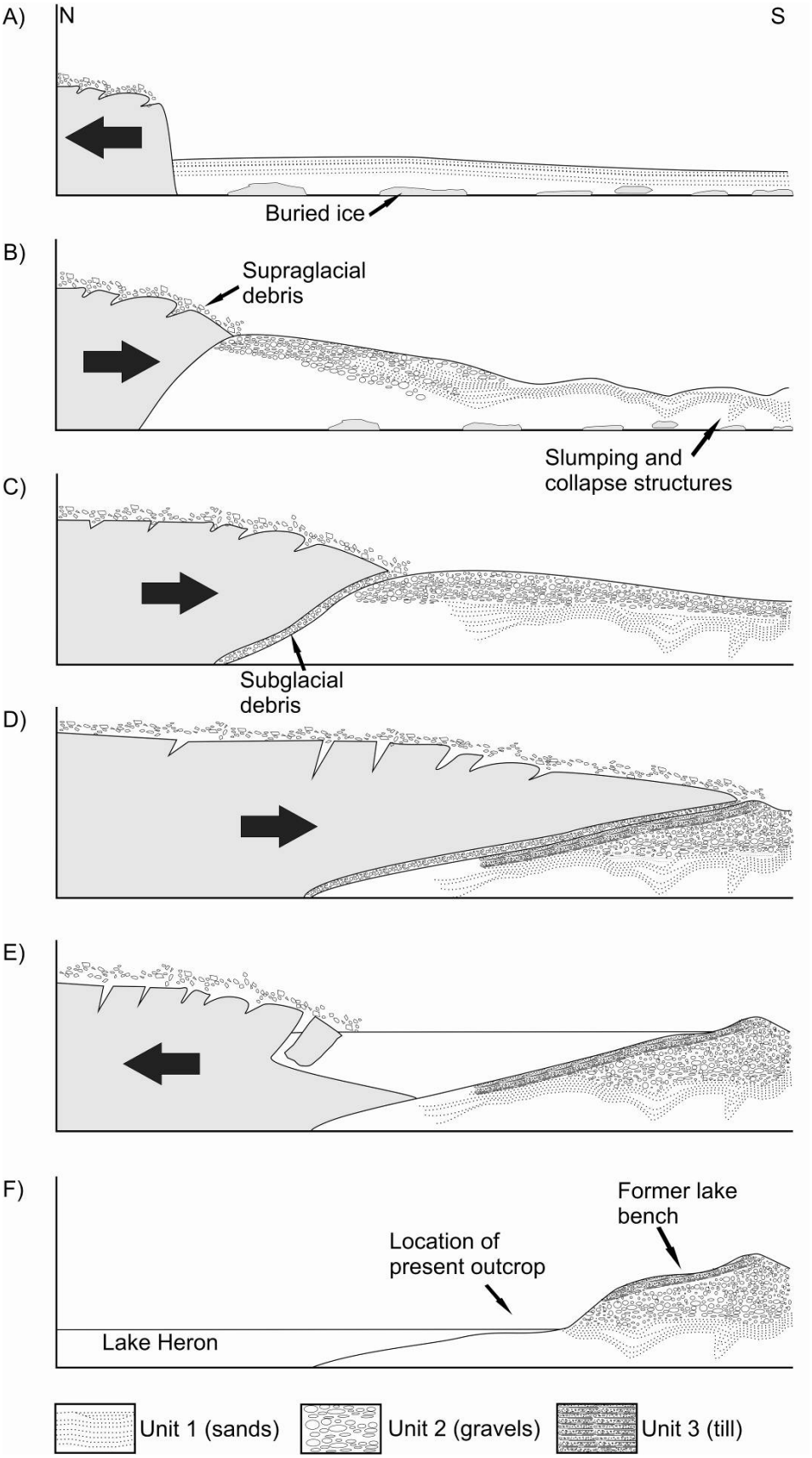

Figure 4-15Conceptual reconstruction of Lake Heron outcrop. A) Antecedent conditions showing proglacial sediment deposited on buried ice following glacier retreat. B) Glacier readvances, depositing more proximal sediments. C) Glacier advances over proglacial sediments depositing subglacial till. D) Small moraine constructed at ice front. E) Glacier retreats and a moraine-dammed lake develops. F) Present situation where lowered lake levels have exposed the outcrop.

The antecedent condition in Figure 4-15A shows the glaciers position prior to the formation of the Lake Heron Formation moraines but during ice retreat. During this phase, sediment was transported from the ice front via predominantly low to moderate energy proglacial streams and was deposited over buried ice. These transport systems fluctuated dramatically in their sediment concentration over short periods of time. As ice adjacent to and under the sediment melted out, the overlying sediment was disturbed and slumped into vacated areas. Extensional deformation is present as collapse-structures and as normal faulting in the sediments seen in unit 1.

The glacier readvanced and deposited more proximal, pro-glacial sediments above the deformed unit 1 sediments (Figure 4-15B). By this stage the buried ice had almost completely melted out, as is suggested by the fact that only minor normal faulting is present in unit 2 sediments.

Next, the glacier advanced over units 1 and 2 (Figure 4-15C). A decollement surface formed between subglacial sediments and the underlying proglacial sediments. This is recorded in the sharp erosion surface at the base of unit 3.

The down-valley extension of ice is marked by a small push moraine which rests on the overridden sediments (Figure 4-15D).

Figure 4-15E shows the glacial retreat from this position and the formation of a pro-glacial lake. The lake then cut benches around its margins and incised drainage channels through the end moraine.

Figure 4-15F shows the present day situation, with the south shoreline outcrop exposed due to incision around the present lake margin. The glacier has retreated entirely from the basin into its valley head and alluvial fans now occur around most of the lakes margin.

4.4.3 Nature of the glacier

While the sediments and geomorphology show a glacial readvance over proglacial sediments, other aspects indicate the advance was relatively short in duration and extent.

The lack of deformation in the till and underlying sediments suggests that the ice either did not advance very far over the sediments and/or was not thick enough to cause major disruption to underlying sediments. Small-scale thrust faults and hydrofractures were present in unit 1, and this supports the ice-overrun model. However, the features are not of the scale of deformation often described in glacitectonized sediments. Evans *et al* (1999) describe extensive deformation in ice over-run glacilacustrine sediments along the shore of Barrier Lake in the Canadian Rocky Mountains. They document large thrust faults (>3m). In contrast, the thrust faults seen in unit 1 are never longer than 50cm and most are less than 30cm.

An estimation of ice thickness during the Lake Heron Formation is shown in Figure 4-16. The model reconstructs ice thicknesses using the elevations of moraines, kame terraces and trimlines as constraints and accounts for other factors including valley width and basal sliding. Figure 4-16 suggests that ice thickness during construction of the Lake Heron Formation was no greater than 100 m above the current Lake Heron shoreline. As the sediments studied represent a readvance subsequent to a phase of retreat from the Lake Heron Formation position, the ice thickness is very unlikely to have achieved a similar thicknesses. Numerous kame terraces up-valley indicate periods of thinner ice.

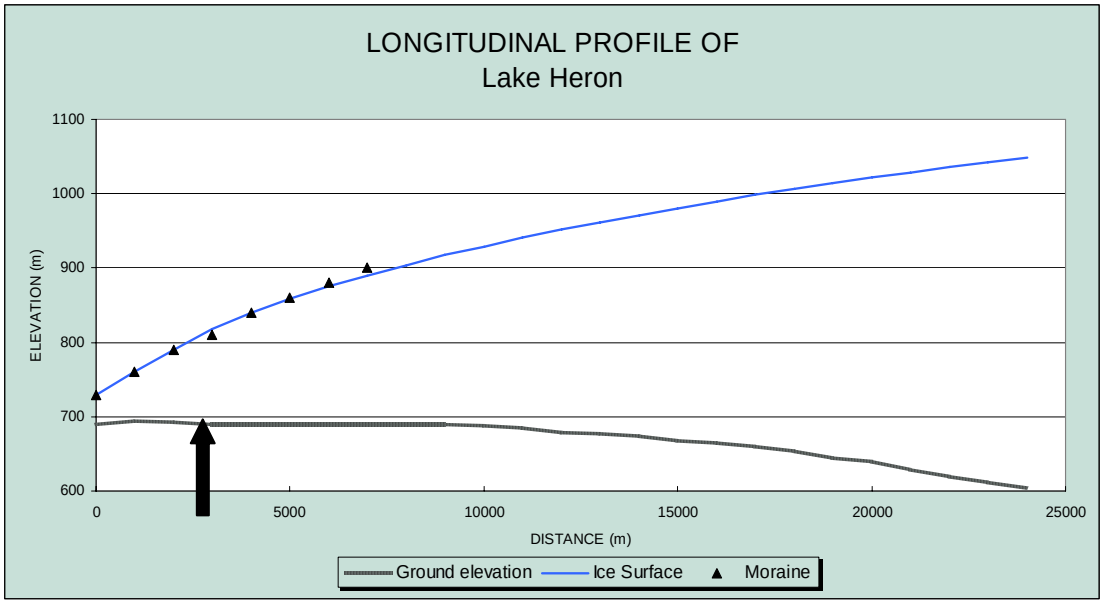

Figure 4-16 Calculation of ice thickness during deposition of Lake Heron terminal moraine using GLACPRO programme. Outcrop location indicated by arrow.

It is hard to assign the compressional deformation directly to a specific advance because the deformation could be associated with any moraine down-valley. The minimal degree of deformation suggests the ice advanced only a few hundred meters down-valley from the outcrop. Between the Lake Heron 3 moraine and the southeast margin of the lake there are at least seven push moraines and the readvance certainly relates to at least one of these moraines (Figure 4-1). In contrast to dump moraines, which are constructed at the margin of a more stable ice front, push moraines are associated with minor, often annual (Benn and Evans, 1998), readvances. This may explain the minor deformation in the sediments.

The age of the readvance is likely to be younger than ~16 ka B.P, the estimated age of for the Lake Heron 3 moraine, but older than ~13 ka years B.P, which is the age for complete evacuation of ice from the Lake Stream Valley (Burrows and Russell, 1990; Easterbrook, 2003). No glaciolacustrine sediments occur in the outcrop, which suggests either that a lake did not form prior to the readvance, or that it was subsequently filled in and/or reworked. Proglacial lake development often precludes rapid glacial retreat (Kirkbride, 1993). The proglacial sediments record an oscillating ice-front rather than rapid deglaciation and therefore may closely postdate the Lake Heron Formation. A proglacial lake formed during subsequent retreat and although lateral moraine/kames

indicate that glacier fluctuations occurred, rapid retreat ensued and the basin was ice-free in about 2,000 years.

4.5 Conclusion

Glacigenic sediments exposed at the southern Lake Heron shoreline record a Late Glacial readvance during an overall glacial retreat. Four units are identified, of which the lower three are of glacial origin. The two lowermost units are composed of sands, gravels and boulders deposited in glacifluvial environments. Unconformably overlying the proglacial sediments is subglacial till. Loess caps the glacial sequence.

Following recession from the Lake Heron 3 end moraine, the melting-out of buried ice disturbed proglacial sediments. The glacier then advanced over the proglacial sediments, producing thrust faults and hydrofractures, and it deposited subglacial sediments above a well-defined erosion surface. The till has a weakly-formed fabric and clasts are oriented in the direction of ice-flow. Compressional deformation is limited, suggesting that the glacier was not very thick and did not advance far down-valley. Small push moraines within the limits of the Lake Heron Formation probably relate to small readvances of this type. A proglacial lake formed during subsequent ice retreat and despite further glacial readvances, no further end moraines were preserved in the basin.

5 Micropaleontology

5.1 Introduction

This chapter presents data on the vegetation history of a tarn located on a ridgeline in the centre of the Lake Heron basin. Changes in the sediments, invertebrate fossils and pollen assemblages are correlated with the glacial history, climatic changes and fire history of the region.

The high elevation of the site makes its a potentially exciting prospect for several reasons.

1. The increased potential of the tarn having survived destruction by recent glacial advances and thus having a long record.
2. The tarn's presence at the modern treeline makes it sensitive to small shifts in climatic.
3. There is a possibility of comparisons with pollen studies at lower elevations within the local area.
4. Chironomidae are usually very common in modern lake settings and they may provide a long record for reconstruction of paleotemperatures;
5. There may be possibility of evaluating post-glacial spread of beech forest into inland Canterbury.

Staces Tarn (NZMS 260 J35/581516) is a shallow (<1m deep) mesotrophic lake situated in a trough on a ridgeline 1.5 km south of Staces Hill (1479 m amsl) at the confluence of the Cameron Valley and Lake Heron basin (Figure 5-1). Staces Tarn is 130 m long, 30 m wide and occurs at 1200 m (amsl). The tarn has no outlet; a moraine impounds the lake along its southwest margin and a delta occurs at the north end, from where the core was recovered.

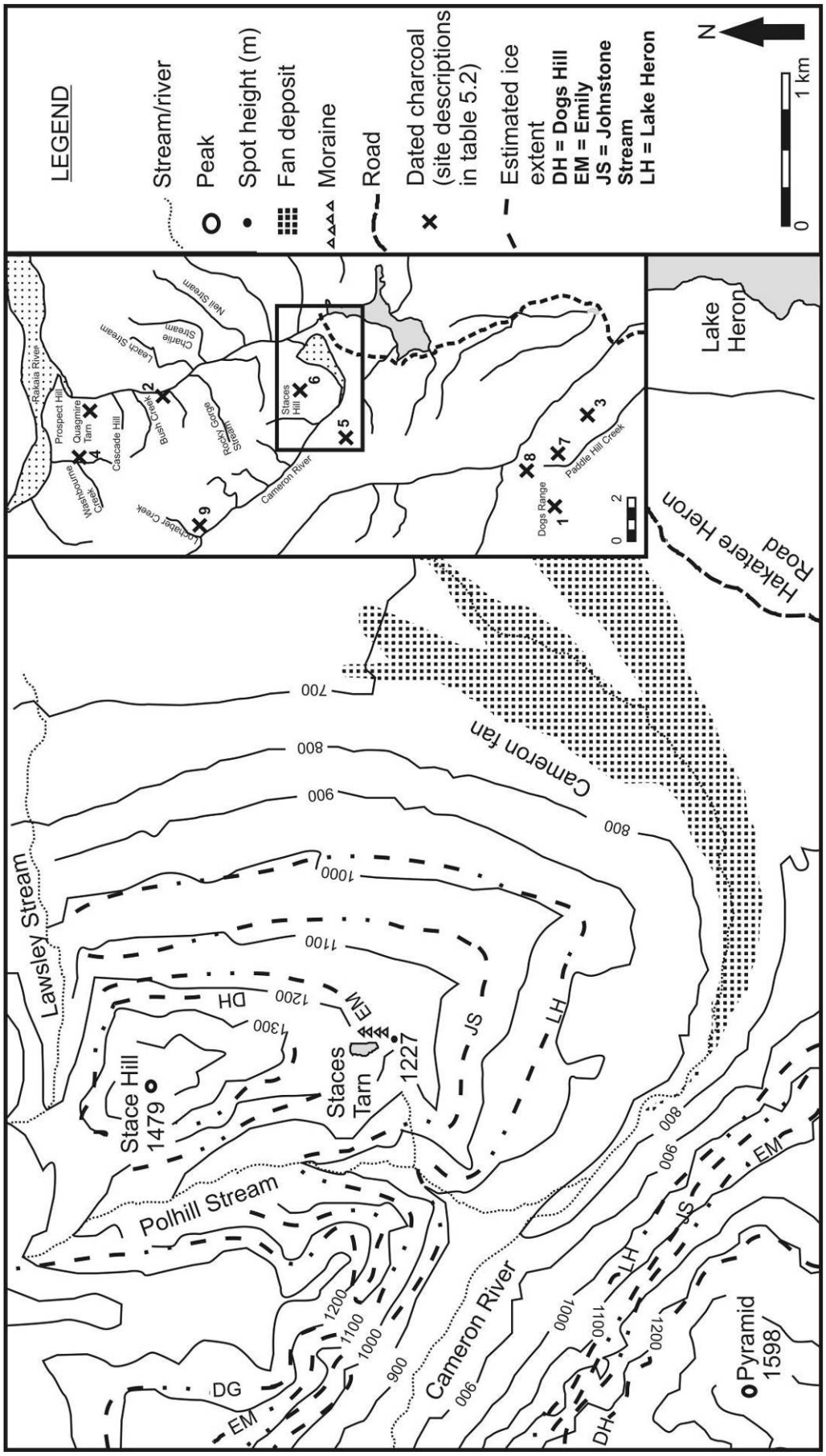

Figure 5-1 Location of Staces Tarn and sites from Table 5.2.

5.1.1 Lake formation

Staces Tarn formed following the retreat of a small offshoot of ice from the Lake Heron ice lobe (Figure 5-2). The tarn formed in the overdeepening created by the ice front, dammed behind the end moraine as the glacier stagnated. Because the topography north of the tarn rises to a ridgeline and then drops into the adjacent valley, downwasting of the glacier caused the ice lobe to be cut-off from the source. This isolated the ice lobe behind its moraine. As the ice stagnated and melted-out behind the moraine, Staces Tarn was formed (Figure 5-3). Pollen spores and invertebrates have accumulated in the tarn since then.

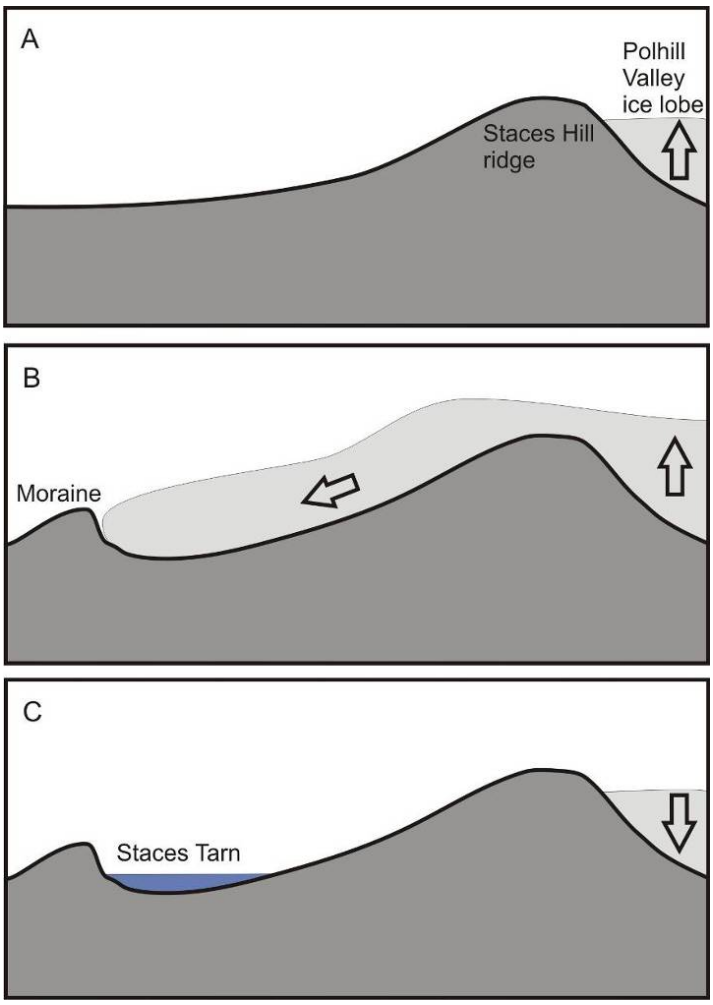

Figure 5-2 Cross section of the formation of Staces Tarn. A) Expansion of the Rakaia glacier. B) Ice flows across the divide, eroding a trough and depositing a moraine. C) Staces Tarn forms behind moraine as the glacier recedes below ridge.

At 1210 m above sea level, Staces Tarn was previously thought to reside outside the elevation of ice during the LGM (Mabin, 1980). The tarn is near the upper limit of Emily Formation lateral moraines, which were ascribed to the early Otiran Glaciation (Mabin, 1980). It was believed that the tarn formed during ice retreat from that either that or the preceding glacial advance, the Dogs Hill Formation, and could date back to the Waimean Glaciation.

Staces Tarn is located in the lee of the Southern Alps, in the path of the westerly winds and at the latitude of the Subtropical Convergence, which separates the cool southern waters from the warmer subtropical water masses. It is therefore sensitive to reorganisations of oceanic water masses (Weaver et al, 1998) and associated changes in the latitude and strength of the westerly wind flow.

Due to its elevation and the lack of a significant drainage input, the tarn has a very low sedimentation rate and is currently fed by very localised runoff. This is reflected in fact that the relatively short core (1.93 m) still yielded a significant record. In addition, the high elevation and topographic position means that the tarn is unlikely to have been compromised by catastrophic events, such as landslides, floods or variations in drainage patterns.

Figure 5-3 Panoramic view of Staces Tarn with direction of ice input indicated by arrow and terminal moraine marked.

5.2 Methods

5.2.1 Coring

Sampling was carried out at the shallow northern margin where a delta is forming into the tarn (Figure 5-3). A hand operated D-section corer with a 50 cm x 8 cm chamber was used (Figure 5-4B). The samples were extracted alternately from two holes approximately 50 cm apart to minimise down-hole contamination (Figure 5-4C). Sampling ceased at a depth of 193 cm as the corer was unable to penetrate further. Locations and elevations were determined using a handheld Garmin GPS Etrex H.

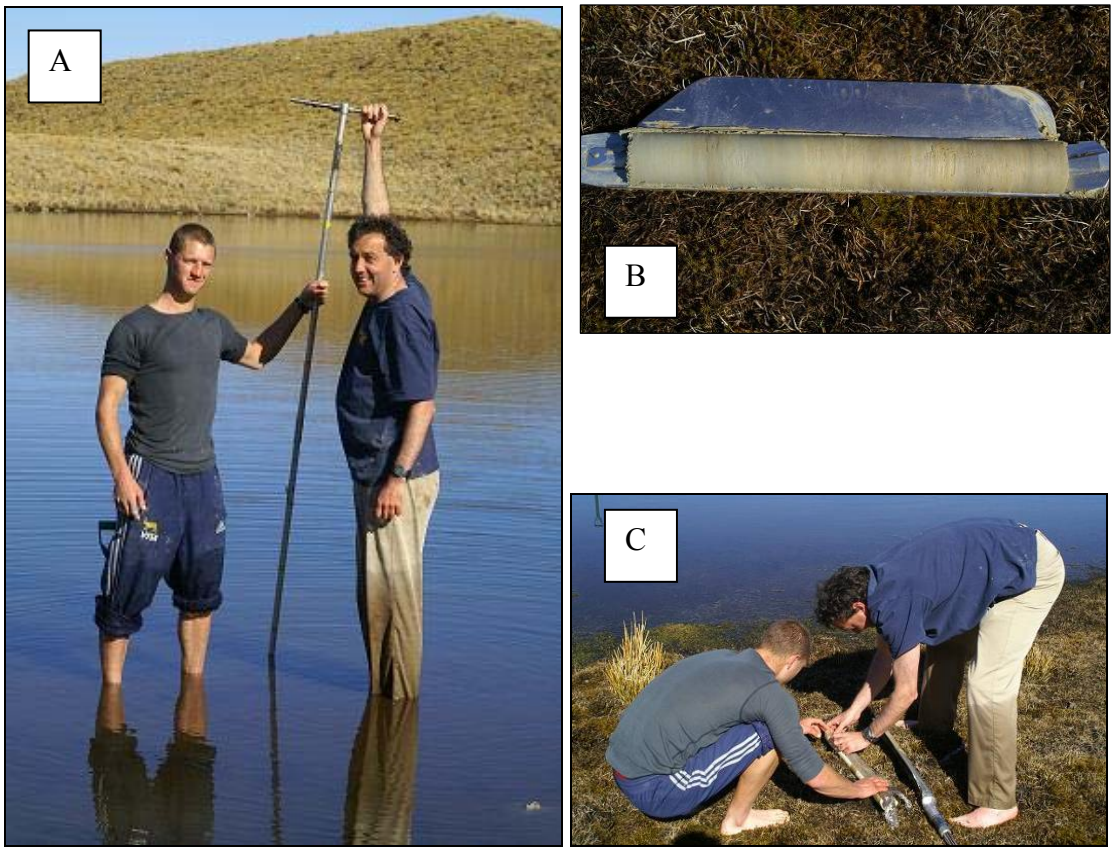

Figure 5-4 The coring procedure. (A) Acquisition of samples using D-Corer. (B) Core sample in D-corer following extraction from tarn. (C) Extraction and preservation of sample.

5.2.2 Sediment description

Description of the core is according to the Troels-Smith (1955) system (Table 5-1). The system describes the basic characteristics of the core, including the types of organic and inorganic sediments, other non-standard components, physical properties and the degree of humicity. Sixteen 1 cm³ sub-samples were removed at 10 cm intervals for the top meter of core and at 20 cm intervals from 110 cm to 190 cm for pollen and chironomid analysis. The remainder of the cores was wrapped in plastic film and archived in a cool store at 4ºC.

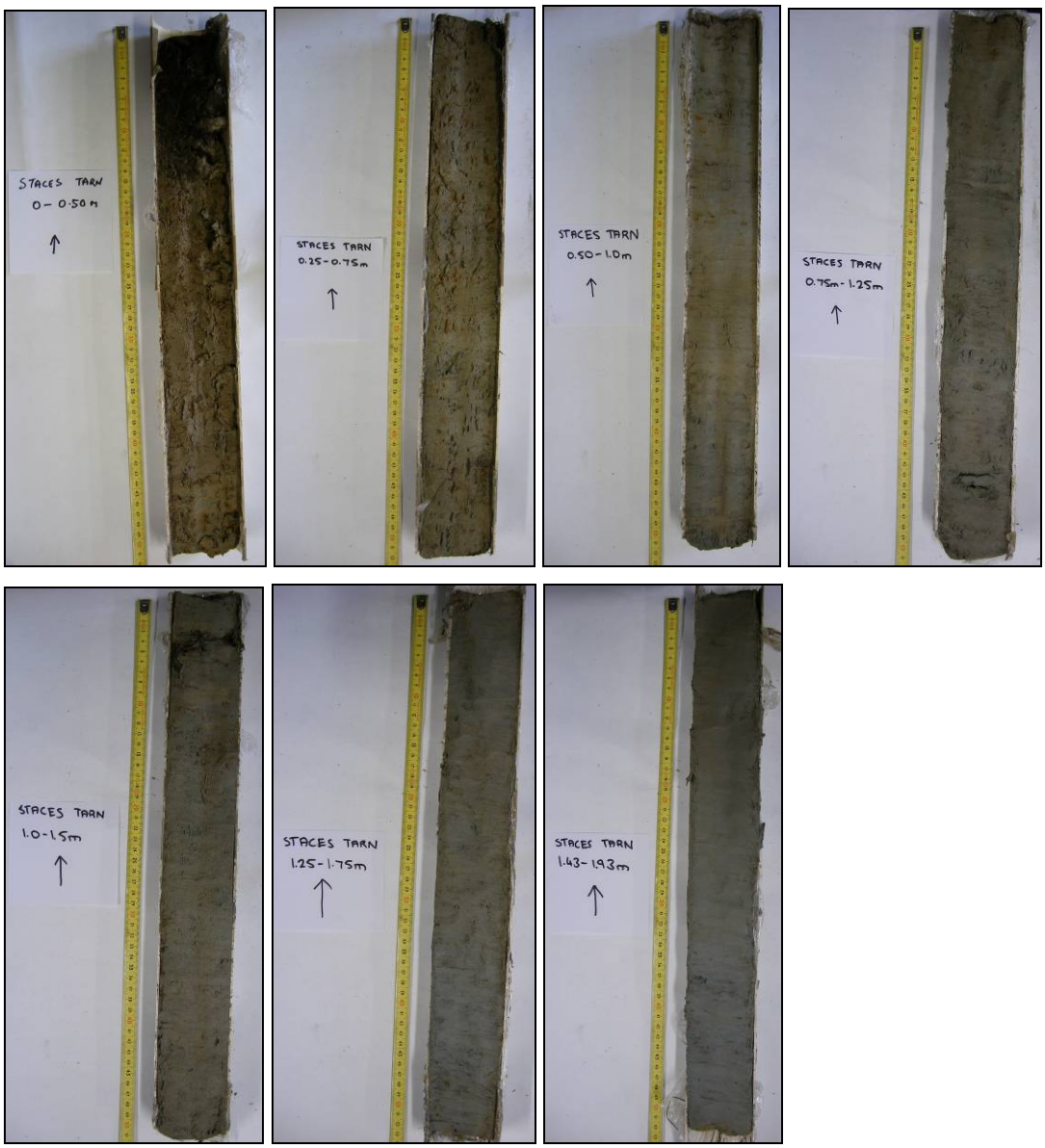

Figure 5-5 Core samples housed in 80 mm PVC pipe.

5.2.3 Pollen analysis

Pollen slides were prepared following the standard methods outlined in Moore *et al* (1991), which involved concentrating the pollen grains by digesting the samples in hydrogen peroxide to remove organic material and hydrochloric acid to remove carbonates. A lycopodium tablet added to each sample allowed the calculation of pollen concentrations. Drops of the samples were mixed with a glycerine jelly and dried on a slide. Counting was done at 400x magnification using a Leitz Diaplan comparison microscope. Publications by Moar (1993), Pocknall (1981) and Large and Braggins (1991) aided identification of palynomorphs. A target of 250 dryland pollen grains for each sample was attempted. Relatively good counts were achieved in most samples, although in a few samples the low pollen concentrations meant that the target was unable to be reached.

5.2.4 Chironomid analysis

Sediment samples were processed for invertebrates following a modified version of the chironomid processing method outlined in Hofmann (1986). Samples (1 cm^3 per sample) were deflocculated in hot 10% KOH and washed through a 93 μm mesh with distilled water. Samples were then transferred to a Bogorov counting tray and examined for invertebrate remains under a dissection microscope, at 50 x magnification. Head capsules of chironomidae larvae were handpicked with a fine picking implement and mounted on glass slides in a drop of polyvinyl lactophenol. After the initial residual water had evaporated the head capsule was covered with a No. 1 glass coverslip. Chironomid head capsules were mounted ventral side up to facilitate identification, which was carried out using a transmission light microscope with the aid of a key and figures from Woodward (2006).

5.2.5 Charcoal analysis

Charcoal analysis relies on the preservation of charcoal particles. The Staces Tarn sediments hold a record of past environmental conditions, allowing comparisons of

relative quantities of microscopic charcoal particles from which deductions about the regional fire history were made. Charcoal abundance and volume are estimated through the counting of charcoal particles in a predetermined area using a fixed and random number of points as described by Clark (1982). Charcoal values are presented in pollen diagrams as the volume of charcoal per unit volume of sediment (VR).

5.2.6 Chronology

A sediment sample was removed at 160 -170 cm and submitted for luminescence dating at Victoria University, Wellington, New Zealand. The sample comprised inorganic lake sediments and was cool-stored prior to removal. The sample (ST 160-170) yielded an age of 7.65 ± 0.55 ka.

The equivalent dose (ED) = 29.7 ± 1.5 Gy (Greys) with a total dose rate of 3.88 ± 0.20 Gy/ka. Additional data used to calculate the dose rate were radionuclide concentrations (as per gamma-spectrometry). These were U = 4.00 ± 0.26 ppm, Th = 13.7 ± 0.2 ppm, K = 2.28 ± 0.05 %. Average water content (wet/dry sample weight) equalled 1.489. The total cosmic dose rate equalled 0.1822 ± 0.0091 Gy/ka, calculated from the sediment cover thickness and from the latitude and elevation of the tarn. There is a small internal Alpha dose in the K feldspars. The Alpha efficiency (a-value) was calculated at 0.079 ± 0.007 Gy/ka; this addresses different efficiencies of Alpha and Beta radiation.

14.8 gm of sediment sample, which included the charcoal particles at 67 cm depth, was removed and sent to the Rafter Radiocarbon Laboratory at GNS Science, Wellington, New Zealand, for radiocarbon dating. The sample (NZA 29676) yielded an age of 4644 ± 40 BP (Appendix C:).

5.2.7 Results presentation

A pollen diagram was constructed using the PSIMPOLL programme (Bennett, 2002). Figure 5-6 displays the concentration of dryland taxa without swamp elements and fern spores. Had their pollen concentrations been included in the total pollen count, it may

have overwhelmed the concentrations of dryland taxa, thereby modifying and dampening changes in the dryland assemblages.

The dryland pollen results are presented in the diagrams in six ecological groups.

1. Beech forest: consisting of *Nothofagus fusca spora* type, a composite of five species, and *Nothofagus brassi.*

2. Montane podocarp forest: consists of *Halocarpus bidwillii*, *Phyllocladus spp.* and *Podocarpus nivalis.* These taxa can occur either as forest trees or as heathland elements.

3. Podocarp/broadleaf forest: consisting mainly of *Podocarpus prumnopitys type, P. totora type (*represented by both *P. hallii* and *P. traversii), P. type* and small counts of *Dacrycarpus dacrydioides*, *Dacrydium cupressinum,* and many lowland forest types. It occurs mainly below 500 m and is relatively diverse botanically. Podocarp pollen grains that were unidentifiable due to damaged sacchi or corpus are included in the total count as 'undifferentiated podocarps'.

4. Shrubland small trees and tall shrubs: dominated by *Coprosma* with smaller counts of *Muehelenmbeckia spp., Coriaria sp., Hoheria sp., Peraxilla sp, Myrsine spp., Gentiana* and *Psuedowintera traversii*.

5. Tussock/grasses: occur as the typical vegetation above the tree line, from frost hollows and also wetland margins, comprised mainly of *Poaceae* (grasses) with smaller contributions from *Apiaceae, Dracophyllum, Asteraceae, Rumex, Liliaceae, Astelia* and *Plantago.*

6. Wetland: consisting mainly of *Cyperaceae* and smaller counts of *Restionaceae, Phormium, Myriophyllum, Chenopodiaceae and Potamogeton. Trilete* and *Monolete fern* spores were included in this group.

5.3 Results

Table 5-1 Staces Tarn core description

Depth (cm)	Description (Troels-Smith, 1955)	Colour (Munsel colour system)	Comments/ description
0-10	Ld3, Th1	Dark brown (10YR 2/2)	Homogenous, consists of 10% roots (<5 cm long) of herbaceous material and trace amounts of angular detritus (<3 mm). Fairly adhesive, low cohesiveness, low H2O content, low plasticity.
10-15	Ld3, Th1	Dark brown (10YR 4/2)	Gradational boundary, roots still apparent (<1 cm long). Low H2O content, low plasticity. Wavy basal contact.
15-42	Ag4, Lf+Dg+Ga+	Dark brown (10YR 6/2)	Homogenous silt with <2 cm herbaceous roots (10% at top of zone but decreasing though core). Low H2O content, fairly plastic. Contains <2% light brown mottling (5YR 5/6). Thin (1 mm) charcoal bands at 30 and 37 cm.
42-50	Ag4, Lf+Dg+Ga+	Pale brown (10YR 6/2)	Homogenous silty clay with 5% fine root fragments and 5% light brown mottling (5YR 5/6) Low H2O content, fairly cohesive. Mottling often occurs around plant fragments. Thin (1 mm) charcoal band at 47 cm.
50-75	Ag4, Lf+Dg+Ga+	Pale brown (10YR 6/2)	Homogenous silty clay with 5% fine root fragments and 5% light brown mottling (5YR 5/6) Low H2O content, fairly cohesive. Mottling often occurs around plant fragments and thins out at base of zone. Thin (1 mm) charcoal band at 67 cm.
75-85	Ag4, Lf+Dg+Ga+	Pale brown (10YR 6/2)	Homogenous silty clay with 1% fine root fragments and 1% light brown mottling (5YR 5/6) Low H2O content, fairly cohesive.
85-125	Ag4, Lf+Dg+Ga+	Grey brown (10YR 5/2)	Fine homogenous silt with increased relative plasticity. Low H2O content. 1% herbaceous root material. Mottling very dispersed. Thin (1 mm) charcoal band at 91 cm.
125-175	Ag4, Lf+Dg+Ga+	Grey brown (10YR 5/2)	Fine homogenous silt with increased relative plasticity. Low H2O content. Only 1-2 mm herbaceous root material occurs. Mottling very dispersed and disappears at base of zone. 160-170 cm sample removed for luminescence dating.
175-193	Ag4, Lf+Dg+Ga+	Grey (10YR 5/2)	Fine homogenous silt with increased relative plasticity and cohesiveness and very low H2O content

5.3.1 Pollen results

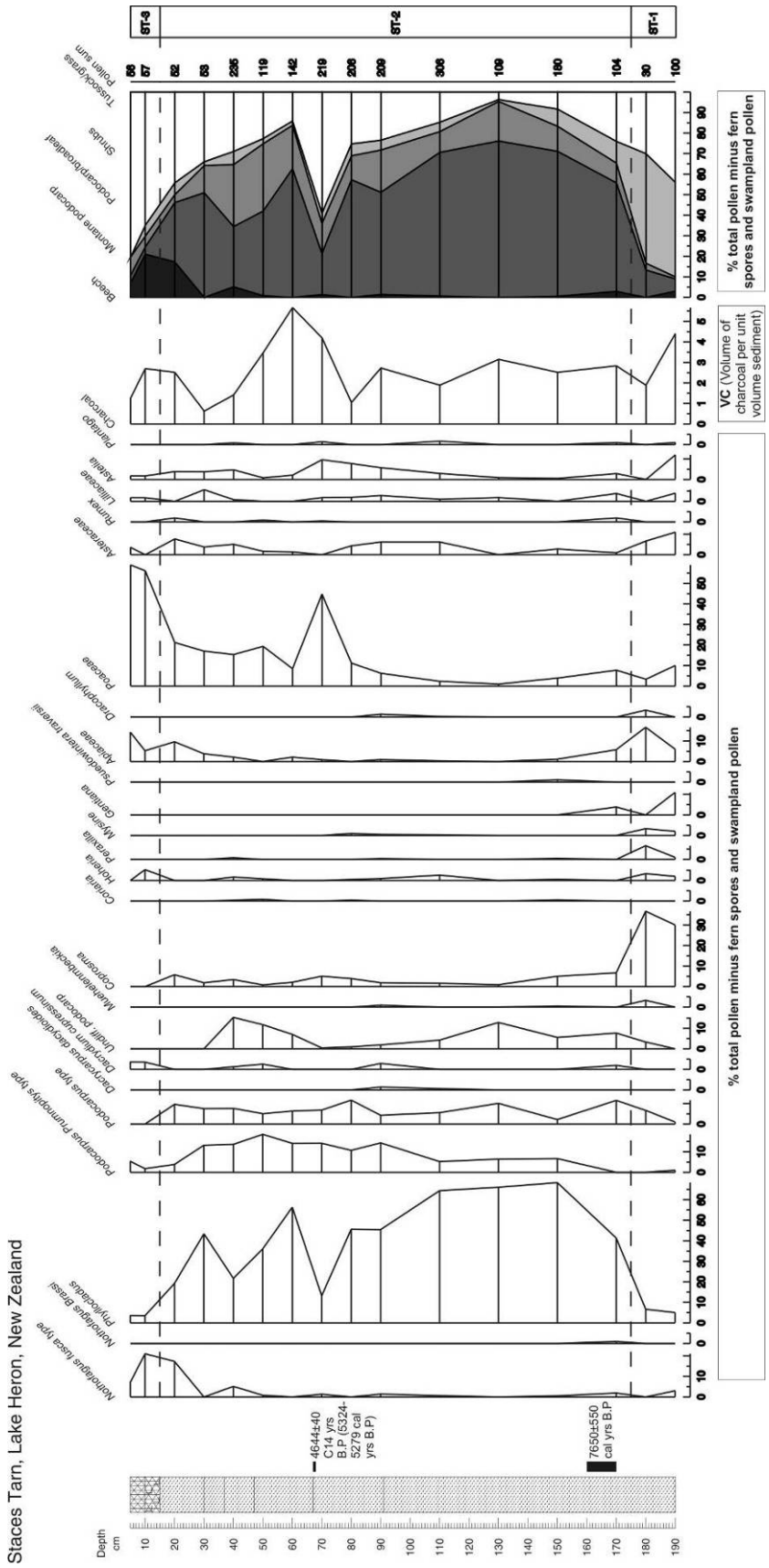

Figure 5-6 Summary pollen diagram for Staces Tarn.

The Staces Tarn dryland elements pollen diagram (Figure 5-6) is zoned according to the dominance of particular pollen types.

Zone ST-1: 190-175 cm. *Coprosma* with *Gentiana, Apiaceae, Asteraceae* and *Astelia* Zone.

Coprosma varies between 30% and 35%, with *Gentiana* decreasing from 10% to 5% at the top of the zone. Of the tussocks and grasses, *Apiaceae, Asteraceae* and *Astelia* fluctuate between 5% and 15%. *Poaceae* comprise 10% of the dryland total. At the base of the zone almost 9% cm^2/cm^3 of charcoal content is recorded, the largest count in the core.

Zone ST-1 is characterised by the dominance of shrubs and herbs (*Coprosma, Peraxilla, Gentiana, Apiaceae, Asteraceae, Astelia*).The pollen assemblage of ST-1 represents a heathland environment, comprising shrubs and herbs that are typically slow growing or stunted. Heathland occurs in the South Island in mountainous areas and on glacial outwash surfaces, including wet areas above the treeline. *Coprosma* occur in a range of environments, including alpine landscapes, and are tolerant of both poorly drained and also exposed habitats (Macphail and McQueen, 1983). *Muehlenbeckia* and *Myrsine* occur in temperate to alpine environments and are common as forest margins and grassland environments, and a similar herbfield environment has been described for *Gentiana* (Macphail and McQueen, 1983). The present characteristic habitat of *Dracophyllum* is a well-drained, cold, windswept ridge-crest, between 1200m and 1500m altitude, which carries little winter snow (Lintott and Burrows, 1973). It also occurs at lower altitudes in tussock grassland in Porters Pass and Dry Acheron (Shulmeister pers comms, 2008). It occurs in late glacial, inorganic sediments at Windwhistle, the Rakaia Gorge (Lintott and Burrows, 1973), and also in a sediment core from Kettlehole Bog in Cass (Lintott and Burrows, 1973). During full glacial times it also occurred in a site near Lake Pukaki (Lintott and Burrows, 1973). It is severely underrepresented in pollen percentages (Macphail and McQueen, 1983). Its presence is an indicator of a sub-alpine climate.

Two anomalous pollen grains occur in ST-1. The first is *Peraxilla* spp. (*c. tetrapetala*) of the genus Lorentheaceae, one of the three New Zealand “beech mistletoes”. *P.*

tetrapetala is an arboreal xylem parasite dependent on its host for water and nutrients (Ullmann *et al*, 1985). While the parasite is commonly found on *Nothofagus ssp.,* it has also been recorded on *Quintinia* (Allan, 1961). While the direct effects of *Peraxilla* spp. growth on beech trees have not been determined, Cockayne (1926) noted that young trees attacked by the parasite often died, whereas older trees seemed less affected. These mistletoe have a strong dependence on birds for pollination and dispersal, although insects may play a role for some species (Kuijt, 1969). Dispersal requires a bird to remove the pericarp from around the seed and place it on an appropriately sized branch of the correct species (Ladley and Kelly, 1996). The presence of beech mistletoe suggests that, although not prominent in the pollen count, beech trees may have been growing near Staces Tarn at this time. The second anomalous grain in ST-1 is that of *N. brassi*. Given that this pollen group has been extinct in New Zealand since the Pliocene (McQueen et al, 1968), it is likely that it is derived from another source. Possible sources include Tertiary sediments that outcrop at lower elevations in the Cameron Valley (Warren, 1967), or possibly from long distance travel from places such as tropical New Caledonia and New Guinea.

Zone ST-2: 175-15 cm. *Phyllocladus* and *P. Prumnopitys* type Zone.

Phyllocladus dominates the zone, varying between 25% and 70% of the total dryland taxa. ***P. Prumnopitys*** type increases from 1% at the bottom of the zone to 17% at the top, while undifferentiated Podocarpus pollen fluctuates between 2% and 15%. Low counts of *D. dacrydioides* (1%) and *D. cupressinum* (3%) occur. Shrubland taxa have very low counts; *Coprosma* decreases from 7% to 2% upwards through the zone. The grasses *Apiaceae* and *Poaceae* fluctuate between 1% and 5%. *Asteraceae* and *Astelia* increase from 1% to approximately 7% at the top of the zone. The charcoal content fluctuates between 2% and 6% cm^2/cm^3.

Within Zone ST-2 at 70 cm depth, *Poaceae* increases briefly to 47% with *Phyllocladus* declining to 10%. ***P. Prumnopitys*** types remain much the same at 12%. *Astelia* increases slightly to 9%. Microscopic charcoal content at this depth peaks at approximately 6 cm^2/cm^3. At 67 cm depth in the core sample a 2 mm thick band of macroscopic charcoal occurs.

Zone ST-2 is characterised by the dominance of *Phyllocladus* with prominent *Podocarpus* and is interpreted as an open forest landscape. Present distributions of *Phyllocladus* and associated Podocarpus forest occur in regions where annual precipitation ranges from at least 1250mm to 5000mm, suggesting that the region was consistently moist throughout the period. As the Lake Heron basin currently receives around 1000mm per year, it may have been wetter than it is at present. *Phyllocladus* is most prominent in wetter areas, such as the West Coast, and in mountainous areas east of the Main Divide (Wardle, 1969). Precipitation in valleys where *Phyllocladus* exists today is over twice the current annual rainfall in the basin. Because *Nothofagus* displaces it, *Phyllocladus* prefers wetter mountainous areas where *Nothofagus* is absent, such as the upper Rakaia Valley, often forming on rocky ground or as an alpine or lowland fringe to *Nothofagus* forest (Wardle, 1969).

The podocarp elements of this forest are abundant pollen producers and have long-distance dispersal capabilities. At the tarn, this means that they provide a background pollen rain. The low counts of *D. dacrydioides* and *D. cupressinum* suggest that they have been transported long distances. *D. dacrydioides* is widely distributed on West Coast of the South Island, but not currently found in inland Canterbury (Lintott and Burrows, 1973). It currently occurs in lowland montane forests up to 600 m altitude, dominating fertile, free-draining floodplains and the wet margins of the lowland swamps and bogs (Metcalf, 2002). It is an indicator of a relatively mild climate. The distribution of *Pseudowintera traversii* is currently limited to northwest Nelson from Collingwood to Westport (Patel, 1974), and is restricted to montane and sub alpine regions between about 600m and 1300m altitude (Sampson, 1980). It is a further indication of a mild, moist climate.

Casuarina made its may into Staces Tarn from Australia. Its long distance transport is evidence of the importance of westerly airflows on New Zealand's climate (Moar, 1969; Raven, 1973).

There is a small but general increase in canopy cover (*Podocarpus)* throughout ST-2, while *Phyllocladus* declines. This suggests that through ST-2, the vegetation cover progressed from a mixed shrubland-woodland environment, with some canopy cover,

to a predominantly woodland environment, in which *Phyllocladus* was the dominant understory element.

The increase at 70cm depth in *Poaceae*, and the simultaneous decline in *Phyllocladus* and a peak in the microscopic charcoal content suggests that a fire event occurred within ST-2. The event may be recorded in the sediment core as a charcoal layer at 67cm depth. Shrubs and trees recovered rapidly to their former dominance after the disturbance.

Zone ST-3: 15-0 cm. *N. fusca type* and *Poaceae* with *Hoheria* and *Apiaceae* Zone.

N. fusca type increases to 15% before dropping away to 7% in the uppermost zone. *Poaceae* is the other dominant taxa and increases from 20% to almost 60% at the top of the zone. *Hoheria* peaks at 5% and *Apiaceae* fluctuates between 6% and 15%. *Asteraceae*, *Liliaceae* and *Astelia* decrease slightly to 2%. *Phyllocladus* decreases from 15% to 2%, while *P. totora type* fluctuates between 1% and 5% and *D. cupressinum* is 4% of the dryland taxa. Charcoal values decrease upwards through the zone from 2% to 1% cm^2/cm^3.

Zone ST-3 is characterised by the emergence of the mountain beech tree *Nothofagus* of the *fusca* group and the grass *Poaceae*. The dominant forest type is *N. Fuscaspora*, which has replaced the montane podocarps. In addition, the shrub *Phyllocladus* is replaced by grasses *Apiaceae* and *Poaceae*. At present, silver beech grows up to 1100m in the South Island and mountain beech up to 1500m and it is likely that these hardy trees survived through the last glacial period. Mountain beeches are not known to disperse seeds over great distances (Burrows and Lord, 1993). This may suggest that the expansion of beech forest in ST-3 occurred from isolated stands that survived the most recent glaciation. Similar expansions of *Nothofagus* forest occur in pollen diagrams in Canterbury (Burrows and Lintott, 1973; Moar, 1971; Russell, 1980, Burrows and Russell, 1990). The pollen assemblage of ST-3 suggests a mountain beech forest cover with an increasingly dominant grass groundcover. Charcoal values are low and decrease through Zone ST-3.

5.3.2 Chironomid results

The concentrations of Chironomidae present in Staces Tarn are presented in Figure 5-7. Chironomidae was abundant in the top 10 cm of the core sample. The sample counts dramatically reduced at 15 cm depth and no more head capsules were recovered from below this depth with the exception of 55 cm depth, at which four head capsules were found. In Zone ST-1, the dominant chironomid fauna was *Chironomus* ssp, with small counts of *Paratanytarsus, Tanytarsus vespertinus* and *T. funebris*. With a diversity of only five taxa, dominated by *Chironomus* ssp, this assemblage is typical of high altitude lakes (Woodward, 2006).

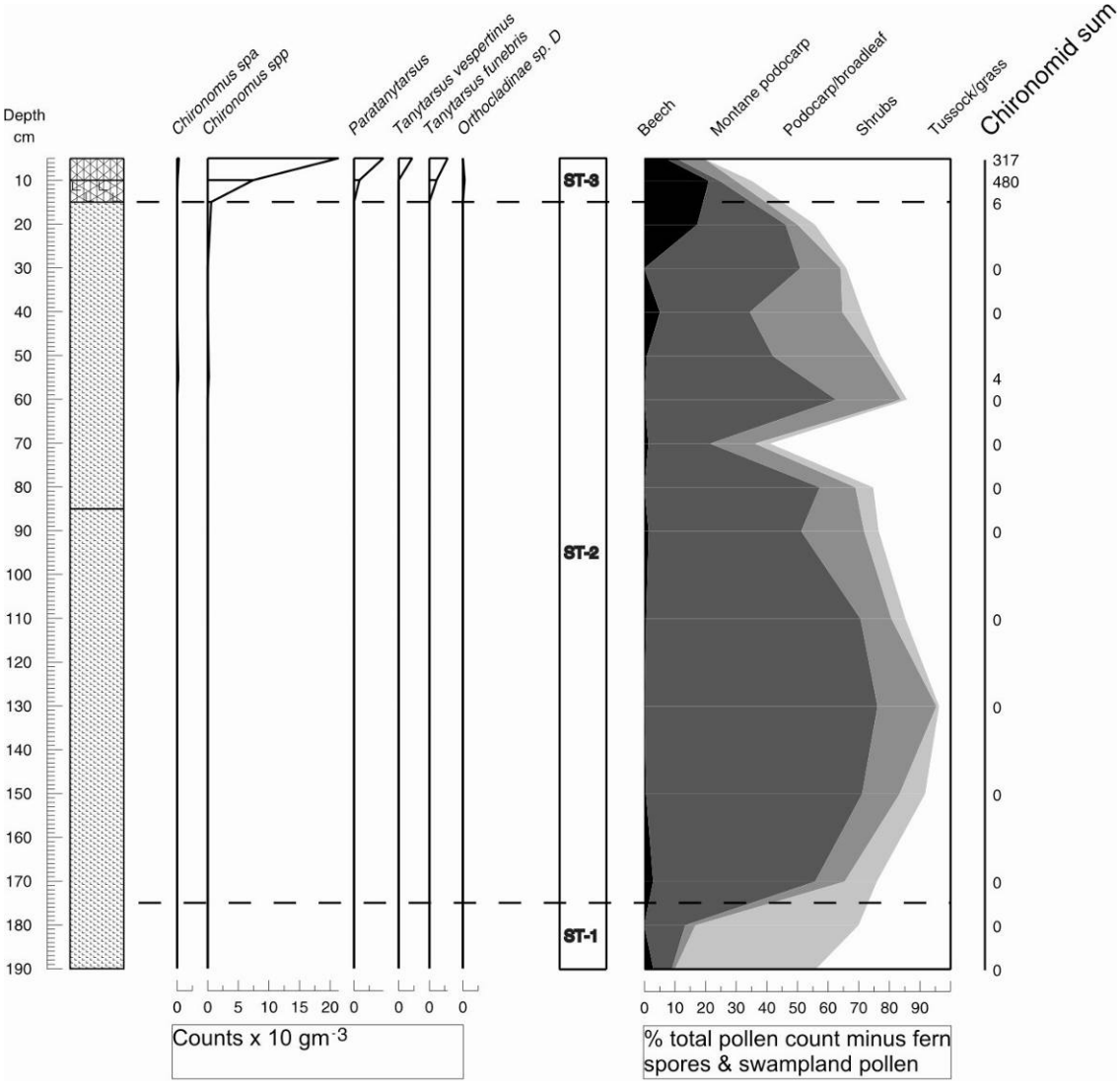

Figure 5-7 Summary diagram of Chironomid counts in Staces Tarn. Pollen zones and local vegetation summary are provided for comparison.

As the minimum target count for each sample was 50 head capsules, not enough information was recovered to infer paleoenvironmental variations. From the investigation of Chironomid fauna in 46 lakes in the South Island, Woodward (2006) calculated a positive correlation between native forest cover and the richness and diversity of taxa. He also calculated a strong negative correlation between taxa diversity and pastoral farming (Woodward, 2006). As the largest head capsule counts occur within Zone ST-1, interpreted as a grassland environment, and the lack of head capsules down the core occurs in Zone ST-2, interpreted as a dominantly forested landscape, some other variable has affected the preservation of chironomid fossils. The top 15 cm of the core contains much organic material, while inorganic lake silts occur without change below that depth. The lack of organic material is possibly explained by the very slow sedimentation rate, which, combined with the shallowness of the tarn, drastically reduced the preservation potential of fossil invertebrates.

5.4 Discussion

5.4.1 Interpretation of pollen results

The bottom of the Staces Tarn sedimentary core is dated as being older than c. 8,100 yrs B.P, representing the early Holocene. Except for the top 15cm of the sample, which is rich in organic material and poorly compacted, the sediments are uniform lake muds. Sedimentation rates are further constrained by a dated charcoal layer at 67cm depth of 4644 ± 40 yrs B.P and a luminescence age of 7.65 ± 0.5 ka from 160-170cm depth. Assuming no compaction, a sedimentation accumulation rate of 0.144 mm/yr can be derived from the 190 cm core, which is rather slow but may be explained by its high altitude and very small catchment area. As sediment at the top of the core is less compacted, the age is an overestimation and is likely to be younger.

A Holocene vegetation history has been reconstructed from pollen studies at Prospect Hill (Burrows and Russell, 1990). The close proximity of Prospect Hill to Staces Tarn enables comparisons between the two sites of different topography and elevation to be made. Burrows and Russell (1990) presented pollen diagrams from Quagmire Tarn

(740m) and Windy Tarn (750m) from the Prospect Hill plateau 13 km north of Staces Tarn. The plateau was overrun by ice during the LGM and following retreat from LGM positions a veneer of ablation till remained, within which Quagmire Tarn is located. A subsequent glacial readvance over the north-west and north sides of the plateau deposited a double-crested moraine. Windy Tarn is located up-ice of the moraine.

In contrast, Staces Tarn is located on a ridgeline almost 500 m higher. The site is far more exposed and the pollen productivity would have been much lower, raising the possibility that a greater proportion of its total input was derived from other regions. *Casuarina* is an Australian pollen type whose dispersal capabilities are well known (Moar, 1969), while *D. dacrydioides* and *D. Cupressinum* are probably derived from Westland.

Vegetation in ST-1 is characterised by the dominance of shrubs and herbs (*Coprosma, Peraxilla, Gentiana, Apiaceae, Asteraceae, Astelia*) typical of a heathland environment. The climate was colder than present and vegetation zones were depressed. The geomorphology suggests that, at the height of the LGM, the basin was sparsely vegetated and erosion was widespread; meandering rivers covered the basin floor and thick loess sheets developed. ST-1 may represent the last stages of the late Glacial period (14,000 – 10,000 yrs B.P). An abrupt change in vegetation is noted at the transition between ST-1 and ST-2 in which the heathland is replaced by woodland forest. The transition into ST-2 indicates a rising treeline, possibly in response warmer summers or to overall warming.

Zone ST-2 is a relatively long period of open forest dominance, characterised by *Phyllocladus* and *Podocarpus.* The pollen assemblage of ST-2 suggests temperatures were similar to present conditions but that there was higher precipitation. The presence of trees in the record suggests a treeline at least as high as current elevations. Stands of *Phyllocladus* often occur on poor soils where tree cover is missing, possibly because of burning. It is known that both species expand when competition is removed (Lintott and Burrows, 1973). Burrows *et al* (1990) dated the burial of *Phyllocladus alpinus* by an outwash plain in the Cameron Valley at 9,520 ± 95 yrs B.P (NZ 688). *Phyllocladus* was therefore present at least in the lower half of the Cameron Valley at this time and,

according to other dated macrofossils, was present in the Cameron Valley below approximately 1100m until at least 2,840 ± 70 yrs B.P (NZ 1880; Burrows *et al,* 1993).

At 70 cm depth within Zone ST-2, a significant grass increase occurs, along with a large peak in microscopic charcoal and a decline in montane cover. The increase in microscopic charcoal suggests the dramatic change in vegetation cover probably relates to a fire event that burned off the montane vegetation and allowed a short-lived period of grass dominance. At 67 cm depth, a 2mm thick band of macroscopic charcoal records a local fire event. Although the charcoal band occurs 3 cm higher in the sediment core, it may still be associated with the short-lived grass invasion. The delay could be attributed to the time required for the small amount of localized runoff to transport the macroscopic charcoal into the tarn. Grasses would then reoccupy the site relatively quickly after the fire, and their pollen would arrive in the sediment core earlier than the macroscopic charcoal. On the other hand, using an approximate rate of sedimentation of 0.144 mm/yr, 3 cm equates to approximately a 200 year delay. Therefore, it is more likely that two separate events are recorded; one as a peak in microscopic charcoal values and the other as macroscopic charcoal in the sediment core.

The presence of alluvial fans indicates periods of vigorous fan building in the early Holocene. The fans buried organic material that Burrows *et al* (1990) and Burrows *et al* (1993) dated. Alluvial fan development has also been dated as occurring from 7030 ± 70 yrs B.P (Wk 1782) in the South Ashburton Valley (Burrows *et al*, 1993). Rapid fan development began in the Cass River, Waimakariri valley, at 7440 ± 170 yrs B.P (NZ 5298; Burrows, 1983). Alluviation is dated to have begun in the Rangitata Gorge about 7,000 yrs B.P (Mabin, 1987). The geomorphology in the Lake Heron basin supports an early Holocene amelioration of the climate, being completely devoid of terminal moraines but having kame terraces, lateral moraines and trimlines constructed subsequent to the Lake Heron Formation (Map 1). Ice retreated as far as Prospect Hill before the Lake Stream Advance between ~12,000 and ~10,000 yrs BP (Burrows and Russell, 1990).

A late reduction in *Phyllocladus* in ST-2 marks the transition into ST-3, in which mountain beech becomes the dominant forest type, replacing montane podocarp forest.

In addition, tussock grasses replace shrubs. The decline in mountain beech forest at the top of ST-3, coinciding with an increase in tussock grasses, may be the result of fire, possibly due to anthropogenic activity. However, microscopic charcoal values decrease at the top of the sediment core. If human clearance is responsible, these charcoal values probably represent major burning during the initial clearance followed fire events of lesser severity, or at least of decrease charcoal production.

5.4.2 Late Glacial climate

Other pollen diagrams from Canterbury mountain localities have similar vegetation histories to Lake Herons. Pollen diagrams from Kettlehole bog, near Cass in the Waimakariri Catchment, Lake Henrietta and Prospect Hill, both within the upper Rakaia catchment, show a vegetation progression during the Holocene. Grasses and shrubs give way to forests, dominated initially by *Halocarpus bidwillii*. In turn, these give way to *Podocarp* forest, *Nothofagus* forest, and finally grasses. A *H. bidwillii* "spike" is not seen in the diagram for Staces Tarn and its absence at some sites has also been noted by Burrows (1990).

The natural treeline occurs at approximately 1260m in the alpine areas of Canterbury (Wardle, 1991). It varies according to temperature, which is influenced by a site's distance from the coast and by its latitude. To the south, the treeline decreases in altitude (Wardle, 1991). In the drier eastern ranges, the snowline is up to 300m higher and the grass-line lower by 150m-300m (Burrows, 1967). Tree zone limits in the central mountains and near glaciers are lower and may be altered by ancient fire events. Staces Tarn lies at 1200m, just below the current treeline. During glacial periods, the treeline is depressed as temperatures decline and forests survive by moving to lower, warmer regions. With the exception of ST-1, subalpine forest cover occurs up to the present. From the beginning of ST-2, a treeline existed at an elevation at least equal to the current location, suggesting temperatures were at least as warm as the current climate. The late arrival of *N. fusca* in the record may support the cooling temperatures in the late Holocene (McGlone, 1988).

5.4.3 Beech invasion

The formation of Beech gaps in the South Island has been the focus of discussion since the 1920s (Cockayne, 1926; Wardle, 1963; Burrows, 1965). Beech trees are one of the dominant New Zealand forest species, yet a 150 km long stretch of central Westland, and 125 km stretch of Canterbury are almost completely void of beech forest. The 'beech gap' on the West Coast is dominated by podocarp and broadleaf species, whereas vegetation in the 'beech gap' on the east coast consists mainly of grasses and stands of podocarp and very isolated beech. The generally-accepted explanation is that the gap coincides with the greatest extension of ice during the Last Glacial Maximum (LGM) (Wardle, 1963; Burrows, 1965; Leschen *et al*, 2008), although other factors indeed played a role (see below; McGlone, 1985).

The early Holocene landscape at Staces Tarn was dominated by shrubland and low-forest vegetation. *Phyllocladus* seeds are dispersed by birds and quickly occupy suitable sites following deglaciation, thus montane podocarp vegetation is typical of post-glacial records in New Zealand. McGlone (1988) estimated that *Phyllocladus* and *Halocarpus* colonised post-glacial grasslands in a period of less than a thousand years. At Staces Tarn, beech was apparent in small concentrations from the mid Holocene until beech became established the late Holocene. Isolated stands of *N. menziesii* presently occur in tributary valleys in the north of the basin, the closest being located in Rocky Gorge Stream, ~5 km north of Staces Tarn. Other stands to the north occur in Bush Creek, in an unnamed valley below Cascade Hill and in Downs Hut Stream. They also occur in tributaries in the east of the basin in Leach Stream, Charlie Stream and Neil Stream (Burrows and Russell, 1990). Outside of the basin, the closest occurrence of beech occurs above the Manuka Point Homestead (Burrows and Russell, 1990).

The mid to late Holocene tree progression at Staces Tarn is similar to that of Prospect Hill (Figure 5-1). Both record relatively low levels of *N. fusca* type pollen, which dramatically increases in the late Holocene, displacing low podocarp forest as the dominant forest cover (Burrows and Russell, 1990). *N. fusca* was present at Prospect Hill approximately 4,500 yrs B.P. However, it was not until after 2,000 yrs B.P that *N. fusca/N. menziesii* became the dominant forest type (Burrows and Russell, 1990).

Based on an inferred sedimentation rate of 0.144 mm/year, *N. fusca* did not become the dominant forest type at Staces Tarn until approximately 1,400 yrs B.P. The Lake Heron basin is likely to have favoured the spread of beech to Prospect Hill rather than to the Rakaia valley, given that much of the floor of the Rakaia valley was occupied by an unpredictable braided river, whereas the Lake Heron basin was only occupied by fans of small streams. Therefore, the time required for beech to 'cover' the ~15km to Prospect Hill along the Lake Heron basin floor was much faster (~600 yrs) than it required to "climb" the 500 vertical meters to Staces Tarn.

It has not gone unnoticed that the "South Island beech gap" occurs in the central portion of the island and that during the LGM the region subject to maximum ice thicknesses and extension. *Nothofagus* migration was initially thought to have spread from northwestern, southwestern and coastal refugia (Wardle, 1963; Burrows, 1965; Wardle, 1980). However, further research has highlighted the asynchronous nature of the late Holocene expansion of *Nothofagus* forest (Moar, 1970). Other than the northern South Island, where Nothofagus forest survived in substantial numbers, *Nothofagus* forest appears to have spread from scattered pockets. In northwest Nelson, *Nothofagus* forest may have survived throughout the LGM by migrating into refugia. Subsequent to glacial retreat, reforestation was rapid (Shulmeister *et al*, 2004). In other parts of the South Island, there were delays in the expansion of *Nothofagus* forest into recently deglaciated. In southern Westland and coastal Southland, *N. menzesii* spread between 7,000 – 6,000 yrs B.P (McIntyre and McKeller, 1970; Wardle, 1980; McGlone and Bathgate, 1983). A similar age is suggested for the spread of *N. fusca* type in northeastern South Island (Moar, 1971; Russell, 1980). In southeastern South Island and parts of Westland (Pocknall, 1980), *Nothofagus* forest expansion occurred much later, around 2,500 yrs B.P. The late arrival of beech at Staces Tarn supports theories that LGM ice in the central portion of the South Island was a major factor in the late arrival of beech.

McGlone (1988) ascertained three ecological factors common to taxa that occur in the asynchronous late Holocene spread in the South Island. Firstly, almost all taxa had wind-dispersed seeds and most form dense, even-aged stands after disturbance. Secondly, none generated well under low-light conditions, all preferring open sites. Thirdly, with the exception of *N.* fusca type, all were tolerant of poor, low fertility soils.

Three general explanations for the asynchronous rise of *Nothofagus* forest in the southern central uplands of the North Island are (Rogers and McGlone, 1989):

1. expansion at various rates from glacial refugia;
2. deterioration of soil, therefore favouring *Nothofagus* over other competitors;
3. climate change that favoured *Nothofagus* over other competitors.

Soil degradation may have a minor role in driving post-glacial forest transformations, as the slow edaphic deterioration of soil advantages *Nothofagus* over other forest species (Rogers and McGlone, 1989). Factors include leaching, inevitable loss of fertility in soils not renewed by landscape instability, and the development of large, poorly-drained areas as soil structure degenerated. In addition, the *Nothofagus* genus has a mycorrhizal association, whereby a close-fitting fungus covers the root (Baylis, 1961). A mycorrhizal association assists in the uptake of minerals and water. Baylis (1967) demonstrated that silver beech seedlings depend on the uptake of phosphorus for their growth. Furthermore, Baylis (1980) explained the limited ability of New Zealand beech dispersal on the lack of suitable fungi for mycorrhizal associations. This contrasts with the apparent ease of beeches in spreading into scrub/manuka communities which share the same ectomycorrhizal symbionts. In addition, mistletoe may have hindered beech growth, not only by killing young saplings but also by allowing rots to enter the trees (Williams and Chavasse, 1951).

The synchrony of vegetation changes between 7,500 and 2,500 yrs B.P suggests climate change is the critical influence, with a combination of factors controlling the rate of change (McGlone, 1988). Burrows and Lintott (1973) proposed that the transition represented a fundamental environmental change rather than the time required for *Nothofagus* migration. They suggested a climatic shift from mild temperatures and high rainfall to higher temperatures and lower rainfall with periodic droughts, more similar to present conditions.

In the Lake Heron basin, post-glacial beech forest spread may have been a combination of gradual creep along the basin floor from refugia further east, such as Banks Peninsula (Willet, 1950), and faster discontinuous population advance with associated backfilling. Burrows (1993) describes windblown regeneration of beech seedlings,

within 10-15km of source, in the upper Waimakariri catchment, from observations over the last fifty years. Estimated rates of spread vary. Ogden *et al* (1996) proposed 7-80m per century, whereas Rogers and McGlone (1989) calculated 6m per century for upslope migration in the southern-central uplands of the North Island.

5.4.4 Natural fire history

Natural fires have played a role in vegetation changes in the late Holocene (McGlone, 2001). Pollen diagrams in southeastern South Island record a series of fires that devastated forests and shrubland from ca. 2500 yrs B.P (McGlone, 1973). At Staces Tarn, a macroscopic charcoal layer in the sediment core is dated at 4644 ± 40 BP (NZA 29676) in the core at 67 cm. Other macroscopic charcoal layers are recognised at 30cm, 37cm, 47cm and 91 cm (Table 5-1), although throughout the core there appears to be a stable concentration of microscopic charcoal fragments (Figure 5-6), which are similar to findings from other southeastern South Island sediment cores (McGlone, 2001).

Much has been done on the fire history of the Arrowsmith Range and upper Rakaia valley region (Harvey, 1974; Rodbell, 1986; Burrows, 1989, 1990, 1996). The results indicate the widespread occurrence of fires in the region. There are difficulties in making correlations between events due to the variety of settings and the likelihood that only a few of many tens of fires are recorded. The uniformity of the Staces Tarn sediment core provides a link between the fire events recognised in other records. An approximate rate of sedimentation of 0.144 mm/yr, and assuming a constant sedimentation rate with no compaction, the macroscopic charcoal layers suggest fires occurred at c. 6,320, 3,260, 2,570 and 2,080 yrs B.P. Sedimentation rates were used to estimate the ages of charcoal layers in a sediment core from Quagmire Tarn, Prospect Hill, yielding ages of c. 5,800, 3,800, 3,500, 2,600 and 860 yr B.P (Burrows and Russell, 1990). A fire event estimated at 2,600 yrs B.P at Quagmire Tarn may correlate with the event calculated to have occurred at 2,570 yrs B.P at Staces Tarn.

Table 5-2 shows buried soil horizons with radiocarbon-dated charcoal in the Lake Heron area, illustrating the high incidence of fire events during the Holocene.

Table 5-2 Buried soil horizons with charcoal from the Lake Heron area (* indicates wood sample, inferred to date a fire).

Site number in Fig. 5.1	Laboratory number	Radiocarbon date (half life 5568 yr)	Location	Grid reference, altitude	Reference
1	NZ 1684	>40 900	Dogs Range, Paddle Hill Creek	J36/525374 1340 m	Harvey, 1974
2	Wk 2637*	8880 ± 60	Bush Creek, Lake Stream Valley	J35/587596 660 m	Burrows, 1996
3	NZ 6810	6940 ± 150	Dogs Range, Paddle Hill Creek	J36/574358 1045 m	Rodbell, 1986
2	Wk 3451*	5910 ± 60	Bush Creek, Lake Stream Valley	J35/587596 660 m	Burrows, 1996
4	NZ 3942	5830 ± 130	Washbourne Stream, Prospect Hill	S73/637833 800 m	Burrows and Russell, 1990
5	NZ 6803	5240 ± 110	Mt Pyramid, Cameron Valley	J35/559491 1580 m	Rodbell, 1986
6	NZA-29676	4644 ± 40	Staces Tarn, Staces Hill	J35/581516 1210 m	This study
5	NZ 6808	2180 ± 100	Mt Pyramid, Cameron Valley	J35/559491 1580 m	Rodbell, 1986
7	NZ 1686	1860 ± 70	Upper Paddle Hill Creek	J36/548371 609 m	Harvey, 1974
8	NZ 1687	1820 ± 70	Upper Paddle Hill Creek	J36/544392 731 m	Harvey, 1974
4	NZ 3941	860 ± 50	Washbourne Stream, Prospect Hill	S73/637833 800 m	Burrows and Russell, 1990
9	NZ 3943	620 ± 60	Lochaber Creek, Cameron valley	J35/511574 1200 m	Burrows *et al*, 1990

Of particular significance to this study are dated charcoal fragments from Mt Pyramid (Rodbell, 1986). Two fire events at this location have been dated; at 5,240 ± 110 and 2,180 ± 100 yrs B.P (see Table 5-2). While the first event is not identified in the sediments at Staces Tarn, the event at ~2,180 yrs B.P may correlate with the charcoal layer estimated to have occurred at 2,080 yrs B.P. If this is the case, the fire must have been very large given that it occurred on both sides of the Cameron River; at the

relatively high elevations of Mt Pyramid and at Staces Tarn, 3 km to the northeast (Figure 5-1). Few other estimated fire events from Staces Tarn correlate with dated events in the area, and this may suggest a high frequency of relatively localized events. Lightning strikes are the only source of natural fires in the South Island and McGlone (2001) calculated the total area burnt under present conditions to be no more than 80km². Whether pre-deforestation trees and shrubs were more susceptible to fire is not known, but McGlone (2001) suggests that this is possible given New Zealand's dry, drought-prone, unique bioclimatic zone.

Peaks in microscopic charcoal concentrations (VR) in the pollen diagram occur at the base of the core, at 70 cm depth and also there is a small peak at the ST-2 to ST-3 transition. This last peak mirrors the increase of *Nothofagus* in ST-3. Natural fires are often contemporaneous with vegetation changes; a connection is made between fire events and N- fusca type expansion in southwestern South Island (McGlone and Bathgate, 1983). McGlone (1988) interpreted the changes as an intensification of wind flow across the southern half of the South Island, disturbing forest structure in the west and encouraging the spread of *N.* fusca type forest.

5.4.5 Human impact

The top 15 cm of the sediment core, which is highly fibrous, may represent the effects of human impact on vegetation. Lake Heron basin has been used since the 19th century for farming. Most devastating to vegetation was setting fires to the vegetation, or "burning the run" (Barker, 1870: 194). It involved seasonally setting fire to tussock, and left "vast tracts of perfectly black and barren country, looking desolate and hideous to a degree hardly to be imagined" (Barker, 1870: 196). These fires would probably have engulfed Staces Tarn. The present vegetation around Staces Tarn is predominantly *Chionochloa* sp. *cf. rigid*a. At lower elevations, *Kunzea ericoides* and *Leptospermum scoparium* occur near where the Cameron River enters the Lake Heron basin (Burrows, 1993). This is likely to be regrowth from the burning. However, although microscopic charcoal occurs in ST-3, a predicted large increase is not recorded.

5.5 Conclusion

The Staces Tarn vegetation history shows an amelioration of the climate in the early Holocene. The vegetation cover following glacial retreat progressed from a herbland and shrubland environment into low montane-forest, dominated initially by *Phyllocladus* but eventually replaced by *Nothofagus* forest. The historical presence of trees at the site indicates a treeline at least as high as current elevations, which suggests temperatures were at least as warm as present. Despite isolated stands of beech forest probably surviving the last glaciation, a range of factors may have contributed to the delayed dominance of forest as forest cover. These include slow beech dispersal rates, unsuitable soils, competition with other pre-existing taxa but most importantly climate change. An increase in fire events in the late Holocene may have assisted in the spread of beech forest, which migrated by both slowly advancing up the basin floor and by spreading from pre-existing isolated stands. The top of the core is characterised by a relatively large organic content and by a change in vegetation cover to grasses. This may be due to human activity, although this is not represented as large increases in microscopic charcoal content. Sediment in the sample core is predominantly lake silts with little organic content except for the top 15 cm. This meant that the chironomid study was somewhat inhibited.

6 Discussion and conclusion

The Lake Heron basin proved to be an excellent area for a very high-resolution study on climate change spanning the Last Glacial Maximum (LGM) through to the present. During full glaciation, a lobe of the Rakaia Glacier flowed through from the upper Rakaia Valley and deposited numerous moraines and ice marginal features during retreat. Because the elevation of the basin is higher than the Rakaia valley floor, and no major drainage occupied the basin subsequent to ice retreat, the glacial features are well preserved.

This study also presents the first systematic surface exposure dating (SED) campaign in the basin, and thus helps to address the problem of poor knowledge of age constraints on the timing of late Quaternary glaciations in New Zealand.

Although the lack of developed drainage resulted in few sedimentological outcrops, sediments exposed along the southern shores of Lake Heron demonstrate the nature of glacial and paraglacial sedimentation at the later stages of ice retreat. The sediments show that ice fronts oscillated across several hundred metres, which complements the geomorphological study.

The Staces Tarn sediment core provided detailed reconstruction of local Holocene vegetation change, providing an evaluation of Holocene climate change.

This chapter considers the implications of the nature and timing of glacial advances and the postulated mechanisms of climate change.

6.1 Implications for the Last Glacial Maximum

6.1.1 MIS 2 larger than MIS 4

The two erratic boulders from the Emily Formation moraine yielded ages of 23.3 ± 1.6 and 24.6 ± 1.8 ka B.P. The moraine is thus the earliest Late Otiran (MIS 2) advance dated in the Lake Heron basin. The Dogs Hill and Pyramid Formations are correlated with MIS 6 and 8 glaciations. It is probable therefore, that MIS 2 was a larger advance than the MIS 4 advance and that the younger ice advance destroyed the earlier glacial deposits. In the South Island, moraines of the LGM are often a similar to or of larger extent than MIS 4 advances. In the adjacent lower Rakaia valley, there are no preserved MIS 4 moraines between the Woodlands (MIS 6) and Tui Creek (LGM) limits (Shulmeister et al, in prep). In fact, there are no dated MIS 4 end moraines in the South Island. It may be that other moraines previously associated with MIS 4 are actually MIS 2, as seems to be the case in the Lake Heron basin. This is not to say that there were not sizable glacial advances during the last glaciation prior to the LGM. Speleothems from Aurora Cave, near Lake Te Anau, record significant MIS 4 ice (Williams, 1996) and the effects of MIS 4 glaciation definitely show up in long-term marine records, such as DSDP 594. In other areas, LGM moraines and outwash drape over earlier glacial deposits, such as in the lower Rakaia valley (Shulmeister et al, unpub data) and Westland (Preusser et al, 2005).

6.1.2 Position of MIS 2/3 transition

The SED age for the Emily Formation was 24.6 ± 1.8 ka B.P. This sample was taken from an erratic boulder resting on a lateral moraine on Emily Hill at an elevation that suggests the ice pushed several kilometers into the Stour River valley. Corresponding moraines in the west of the basin occur on the north bank of the Ashburton River and several Emily Formation lateral moraines occur at higher elevations than the one dated, such as those below Dogs Hill (see Figure 3-8 and map 1). These lateral moraines formed when the Lake Heron glacier coalesced with Lake Clearwater glacier and extended several kilometers into the Ashburton Gorge and Trinity Valley (mapped as

Trinity Formation, Oliver and Keene, 1990), at the full extent of the LGM. Therefore, it is probable that the lateral moraine dated on Emily Hill is slightly postdates the local LGM culmination and that maximum MIS 2/3 ice in this basin dates to 25 or 26 ka or earlier.

There is a growing body of evidence in New Zealand for glacial advances occurring either late in MIS 3 or during an extended Last Glacial Maximum (eLGM). In the adjacent Rakaia valley, Shulmeister *et al* (in prep) noted that although they SED dated the LGM to between 23-21 ka B.P, "a slightly older age for the largest LGM in the Rakaia is likely as the ages do not come from the furthest downvalley moraine ridge". MIS 3 glacial advances also occur in South Westland (Suggate and Almond, 2005). The la1/M51 from South Westland ranged from 34 – 28 ka B.P, and although no glacial advance is currently dated in the Lake Heron basin that corresponds to this advance, it is possible that the aforementioned higher lateral moraines relate to this period. Difficulty exists, however, in correlating the two glacial systems. The glacial advances in South Westland were constrained by radiocarbon dating of organic material at the base and top of outwash gravels, therefore the ages represent the period from initial glacier advance to the onset of retreat. In contrast, SED ages represent the culmination of an ice advance and not the preceding period during which ice is advancing. While this complicates correlations between the two dating techniques, it suggests the Lake Heron glacier was advancing prior to 24.5 ka. Two LGM advances are identified in Westland: the la2/M52 advance (24.5 to 21.5 cal yrs B.P) and the mn/M6 advance, (20.5 to 19 cal yrs B.P). These glacial advances were separated by a significant period in which coverbed sequences formed. The Emily and Johnstone Stream Formation advances in the Lake Heron basin correlate well with the former Westland advances, except that numerous recessional moraines in the Lake Heron basin suggest only minor readvances during overall retreat and no great hiatus as seen in South Westland.

In summary, while Mix et al (2001) preferred an age range of 23,000 to 19,000 cal years ago (for the LGM), Suggate and Almond suggest the period began at 28,000 and ended at 19,000 cal years ago. More circumstantial evidence includes a lowering of global sea levels from 27,000 to 20,000 cal years ago (Lambeck et al, 2002) and regional climatic inferences from Antarctica, which show a maximum cold period from 26,000 to 18,000 cal years ago (Petit et al, 1999). In addition, recent pollen studies have

shown apparent climate change beginning prior to the LGM. Smith et al (2008) used the Kawakawa tephra (c.27,000 cal yrs B.P) as a chronostratigraphic marker in determining the timing of a climate amelioration within an eLGM. Newnham *et al* (2007) proposed an eLGM from a Late Otiran vegetation study in the Auckland region. They recommended that the term 'eLGM' be employed by the New Zealand region. Although this data may support Suggate and Almond's extended LGM, the LGM represent the lowest sea-level period and not regional temperatures. It therefore would be unwise to interpret these findings as representing a longer LGM. The pre-LGM age of the Emily Formation suggests that the regional glacial maxima in New Zealand started earlier than the generally accepted LGM, which is in line with other regional evidence.

6.1.3 Last Glacial Maximum ice thickness

Two erratic boulders from the moraine that impounds Staces Tarn returned surface exposure dates (SED) of 18,700 ± 800 and 21,300 ± 500 cal yrs B.P. Again, assuming that the older SED age best represents the 'true' age of the moraine, the c. 21,300 yrs B.P age best represents the age of the moraine. The ages suggest the presence of ice at Staces Tarn for several thousand years at culmination of the LGM but after the largest local ice, suggested to be sometime prior to 24,500 yrs B.P. This tarn sits just below the Dogs Hill (MIS 6) ice limits and suggests that LGM ice was much thicker than previously considered. Ice thickness at the culmination of the LGM was at least 150m thicker than previously believed (Figure 3-10). Assuming a linear relationship to ELAs in the proximal accumulation areas, this equates to the LGM being colder (or colder and wetter) than previously estimated (Porter, 1975).

6.2 Climate variations during Last Glacial ice recession

New Zealand's responses to the last deglaciation were complex. This is attributable to its isolated location in the mid-latitudes of the Southern Hemisphere and its position within the zone of south westerlies winds. Also, it is influenced by the Sub-Tropical Convergence Zone (STCZ). These factors contribute to make New Zealand sensitive to

changes in atmospheric and oceanic circulation. While much of the current interest in deglaciation centers on changes during the Younger Dryas Chronozone/Antarctic Cold Reversal and interhemispheric connections, a few New Zealand studies have looked at the possibility of climate variation during glacier recession from the LGM (Alloway *et al*, 2007). Recent records have shown the importance of decadal and inter-annual climate variation, and although past changes have been identified in tree-rings, ice cores and laminated lake sediments (Shulmeister *et al*, 2004), their effects prior to the Holocene are poorly understood.

The geomorphological map (Map 1) illustrates that LGM glacier recession was broken up by numerous minor still stands or minor readvances. At least twenty fragmented moraine ridges occur between the SED-dated Emily Formation and Johnstone Stream Formation moraines (Figure 6-1), suggesting a nearly steady-state retreat punctuated by decadal-scale readvances. It may be that, in addition to overall ice retreat, the Lake Heron glacier was responding to smaller-scale climate variations. One such variation recently described is the Pacific Decadal Oscillation (PDO; Mantua et al., 1997), a pattern of Pacific climate variability that persists for 20 to 30 years, the causes of which are not fully understood. From 1977 through to the mid-1990's a long-lasting shift in New Zealand's climate occurred (Salinger and Mullan, 1999), characterised by more persistent than average westerly air-flows. As a result, the west and south of the South Island were wetter and cloudier. This period coincided with a readvance of the Franz Josef Glacier in South Westland. A similar effect has been noted in Australian rainfall during this period (Power *et al*, 1998).

In addition, this change coincided with an eastward movement in the longitude of the South Pacific Convergence Zone and more frequent El Niño Southern Oscillation (ENSO) events. ENSO is a major systematic global climate fluctuation that occurs with an interval of about 2 to 7 years and persists for about a year. It is associated with unusually warm ocean waters along the tropical South American coast and out along the Equator to the dateline (Gagan *et al,* 2004). During an El Niño event, New Zealand experiences stronger or more frequent westerly winds during the summer and winds that are more southerly during the winter. This results in droughts on the east coast areas and more rain in the west (Fitzharris *et al,* 1992). Overall, temperatures during El Niño are colder both on land and in the surrounding ocean. La Niña events have the

reverse effect on New Zealand's climate; moister, wet conditions occur in northeast parts of the North Island as the winds tend more northeasterly. The effects of El Niño during the LGM has been described by Rein *et al* (2004). They interpreted stronger El Niño activity about 17,000 yrs B.P based on a marine sediment record off the coast of Peru. It may be that the recessional moraines in the Lake Heron basin reflect a terrestrial-based response to LGM small-scale climate variations in the LGM.

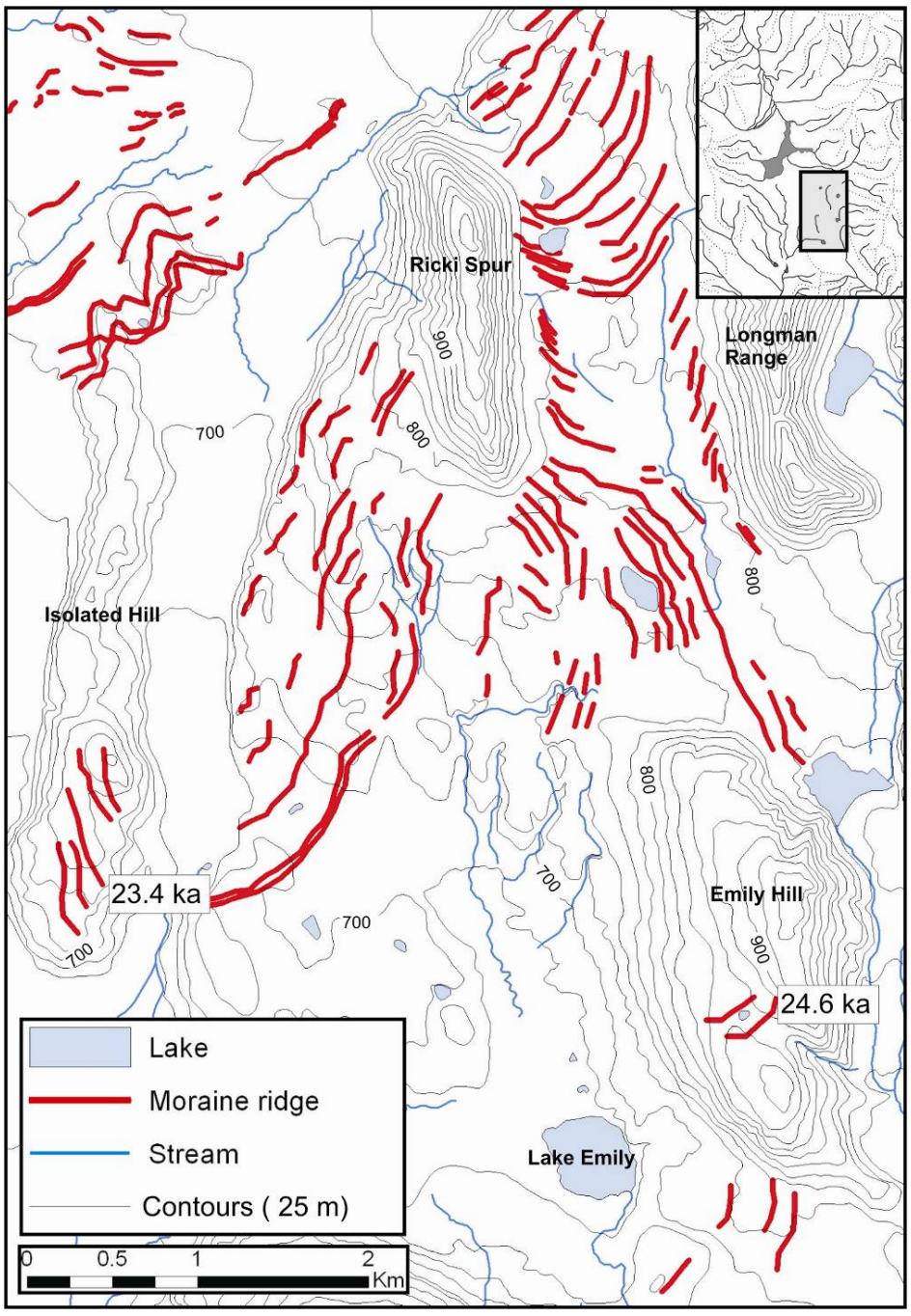

Figure 6-1 Moraine ridges in the east of the Lake Heron basin. At least 20 ridges occur between the SED dated samples from the Emily Formation (24.6 ka) and Johnstone Stream Formation (23.4 ka).

6.3 Seasonality variations during the Holocene

6.3.1 Early Holocene

The herb and shrubland in the lower part of the Staces Tarn pollen diagram (Figure 5-6) are typical of the late-glacial period in inland Canterbury (Burrows and Russell, 1990; McGlone et al, 2003). The fine sediment throughout the Staces Tarn core reflects the high elevation of Staces Tarn, which meant there was only patchy vegetation present and that the site was often subject to winter frosts.

An improving climate promoted the spread of forest onto the site and the Late Glacial herbland and shrubland vegetation was replaced by low, montane forest about 7,500 years B.P. The presence of trees at Staces Tarn at this time suggests that temperatures were at least as warm as at present, as the site is located near the modern treeline. An early Holocene thermal optimum is suggested for the New Zealand region approximately 7,000 yrs B.P (Wilmshurst *et al,* 2007). Wilmshurst quantified predeforestation pollen rain-vegetation-climate relationships with fossil pollen sites and suggested a thermal optimum between 1.5°C and 3°C warmer than present lasted from about 9,000 to 7,000 yrs B.P. Marine cores off the North Island suggest sea surface temperatures between 12,000 and 7,000 yrs B.P were 2-3°C higher than those at present (Weaver *et al,* 1998). At Prospect Hill (13 km north and 470 m lower) low-montane forest replaced shrubland at 10,000 yrs B.P. However, forest arrival at Staces Tarn contradicts the presumed early Holocene warmer temperatures, as trees are not dominant at the site until 7,500 yrs B.P, which is somewhat late in the so-called thermal optimum. Podocarp trees disperse and colonise sites quickly if temperatures are warm enough (Macphail and McQueen, 1983). For this reason, it would have been expected that podocarps would have colonised the site earlier in the thermal optimum. Hence, some other factor or factors must have been inhibiting forest spread. The upper limit of tree growth is closely associated with the summer 10°C isotherm (Koeppen, 1923), and West (1977) noted that at least three months with mean temperatures greater than 10°C are required for forests to dominate. The mean monthly temperature in January for the Lake Coleridge Climatological Station in the Rakaia valley is 15.3°C. At 364m asl, this climatological station is 836m below the elevation of Staces Tarn (1200m). Using an

environmental lapse rate of 0.6°C/100m, mean January temperature at Staces Tarn would be approximately 10.3°C. Therefore, small changes in the mean monthly temperatures could result in noticeable changes in vegetation cover. It is proposed that low seasonality, resulting in milder winters and cooler summers, delayed the forest colonisation of Staces Tarn area. This is despite the fact that annual temperatures were at least as warm as they are today. McGlone (1988) suggested the change to a mild, drought-free, and weakly seasonal climate was the most significant factor controlling vegetation at that time.

At Staces Tarn, montane forest cover steadily declines after about 7000 years B.P, coeval with a gradual increase in grasses. McGlone and Wilmshurst (1999) suggested that a southward displacement of the subtropical high during the early Holocene would have produced drier climates with relatively frosty winters, and stable summers moderated by mist and fog coming from an enhanced northeasterly airflow. They went on to suggest that as the subtropical high retreated northwards from its early Holocene position, temperatures gradually declined. The westerlies also increased through the Holocene (Shulmeister *et al*, 2004) and the gradual decline of podocarp forests may reflect both a gradual cooling and an increase in the occurrence of droughts as eastern areas dried out under the enhanced westerly flow.

6.3.2 Mid Holocene

Increasing charcoal indicate that from about 5,000 yrs B.P there were an increase in the frequency of fire events. McGlone *et al* (1995) reported a similar time for the outbreak of fires in Central Otago. Fires in east Otago are dated as having occurred slightly later (McGlone and Wilmshurst, 1999). The increase in fire events may also have reduced montane forest cover. Throughout the Holocene, summer insolation had gradually been strengthening, and by 3,200 yrs B.P had achieved values close to those of the present (Berger, 1978). The appearance of beech in the pollen assemblage, estimated at about 3,300 yrs B.P, may reflect a shift from warm winters with wet summers to cooler winters and drier summers. McGlone *et al* (1992) suggested an increased summer insolation and intensification of westerly wind flow over southern New Zealand at this time. Beech forest is more tolerant than montane forest of low winter insolation and

low summer humidity and is also favoured by disturbance. The relatively minor mid Holocene expansion of beech forest may be contemporaneous with the natural fires. Beech is recorded at Quagmire Tarn about 4,000 yrs B.P (Burrows and Russell, 1990) and some 700 years later at Staces Tarn. This suggests that although fire events may have assisted beech spread by compromising the condition of its competitors, it is more likely that slow rates of beech migration from the nearest local forests were the most significant factor.

Fire history data provide information on the role of fire as a long term ecological process and the changes in fire activity that have occurred in response to variations in climate, vegetation and human activity. The fire history of Staces Tarn was reconstructed using charcoal records and it is evident that fire has been an important element in the environment since the early Holocene. Fire events occurred at Staces Tarn about 6320, 4644 ± 40 (NZA 29676), 3260, 2570 and 2080 C14 yrs B.P, while a lower level but stable concentration of microscopic charcoal fragments occur throughout the whole record. Charcoal counts suggest the incidence of fire events increased about 5,000 years B.P, which is similar to the time suggested by McGlone (1995). Many fires occurred in the region during the Holocene and lightning strikes are the probable cause. A connection may exist between natural fires and vegetation changes, most notably small beech increases and large grass increases, and these may reflect an intensification of wind flow across the South Island. Large variations in climate are associated with periods of drought, strong winds and high lightning activity. A wet season before a dry fire year allows burnable material to accumulate and then desiccate. Such alterations of wet and dry years are characteristic of areas that are strongly influenced by recent variations in the ENSO phenomenon. High seasonality from the mid Holocene may reflect an increase in ENSO related events. The stronger and more frequent summer westerly winds would cause higher temperatures and less precipitation at Staces Tarn, and thus an increase in fire events. In the winter, the colder southerly winds would bring colder temperatures, which may have favoured beech forest over other forest types (McGlone, 1988). The onset of fire events and the spread of beech forest roughly coincide with renewed glacial advances in the Southern Alps about 5,000 yrs B.P after a long period of inactivity (Gellatly *et al*, 1988). At least eleven episodes of glacial expansion have been recorded since about 5,000 yrs B.P and may be due to ENSO events bringing more southerly/southwesterly airflows and cooler

temperatures and an increase in cloud cover to the Southern Alps (McGlone and Wilmshurst, 1999).

6.3.3 Late Holocene

At about 1,400 years B.P, a pronounced vegetation change occurs as beech replaces the low-montane forest as the dominant forest cover. While the relatively slow beech expansion may be the result of a range of factors, including slow dispersal rates, unsuitable soils and competition with other pre-existing taxa, climate change is probably the most important factor. Beech became the dominant forest type at Quagmire Tarn about 2,000 yrs B.P. Ongoing local declining temperatures and increasing precipitation, in conjunction with the increased overall precipitation and higher summer temperatures, may have caused an increase in fire events (McGlone *et al*, 1995). Beech regenerates faster than its competitors do, and frequent disturbances caused by fire to the already weakened forest will have encouraged its growth.

6.4 Suggestions for further research

The Lake Heron Formation needs to be dated in order to complete the SED campaign in the basin and to make this one of New Zealand's best-dated sequences from LGM though to deglaciation. In addition, the higher Pyramid and Dogs Hill surfaces need more work done; their genesis is not well understood and have poor age constraints. With better dating, the nature of deglaciation processes may be more fully understood. It may also be possible to use the moraine sequence to identify linkages with regional and global climate variations, such as PDO and ENSO signals.

The Staces Tarn sedimentary core did not reach the bottom of the tarn. With better equipment it is probable that the record could be extended into the late glacial period. In addition, other small tarns and bogs exist in the basin which could be cored and used in corroboration. The tarn on Emily Hill is impounded by the moraine dated at 24.6 ka B.P and is another site that has potential to yield a record through the late LGM. As it is

at lower altitude and further east in the basin, it may help resolve some of the mysteries surrounding post-glacial forest expansion, and particularly the spread of *Nothofagus*.

From the evidence, it seems the Lake Heron area has been more affected by natural fires than other South Island inter-montane basins. This may be the case. Molloy (1977) posed several questions in his review of the fire history of the Cass basin. He pondered the relationship between natural fires and possible trends and landscape instability. Understanding of the latter has been contributed to by Burrow (1996), who showed a strong connection between fire events and alluvial fan development. Molloy also noted how little is known about the frequency of natural fires and the amount of land affected. The fire history at Staces Tarn helps answer these questions by providing evidence of at least five mid-late Holocene fires. However, it may be that the apparent increase in events is because the area has received greater attention and that research in other intermontane basins would contribute to the broader picture. In addition, the apparent abundance of charcoal from ancient fires is either a reflection of an increase in fire events or possibly a product of the good preservation of datable material already noted in the Lake Heron basin. These issues require further research.

6.5 Concluding summary

In summary, the Lake Heron area offers an outstanding opportunity to investigate climate and environmental change for the post-LGM period. This thesis has provided the context for future work. The possibilities of getting decadal-scale change from the moraine ridges and for investigating ecological change at the treeline are particularly important.

7 Acknowledgments

Firstly, I would like to thank Jamie Shulmeister, my Super-visor, for his unyielding support and encouragement throughout the entire process, despite being a crazy Irishman. When times got rough, all I ever had to do is look at the amount of work piled up on your desk to realize that I didn't have it so bad. Also, thanks to Kari Bassett, my associate supervisor. To the geomorph and sediment supremo Liv Hyatt, I owe you a huge debt of gratitude as you always showed me an open door and listened to my ridiculous geological theories. Best of luck with the PhD and for your future with Dr Nick. To my parents for bringing me lunch and listening to me babble on about glaciology, even if you happened to be sleeping at the time (Dad). Especially my mum for joining me on some days in the field (Figure 3-1) and for proof reading. HUGE thanks to Nana and Puppa for supporting me through six long years at uni. To Puppa, I can't thank you enough for all the advice you've offered. And Nana, gluten-intolerance will never stop me from eating your truffles. To the best support-crew ever…my sisters, Penny and Ally, and my brother, Kong, thanks for giving me an escape from university when it all got too much. Thanks to Greer and Myf, my roommates, for putting up with the smell of sweaty training clothes and my choice in music. One day you will come around to the sweet sweet sound that is four boys singing in harmony (I know you wanna borrow my Westlife albums). To Rob, Kerry and the entire tech team, a huge thanks for helping me through all the nitty gritty science parts (and for fast-tracking my samples!). This includes you too Henrik, it was very much appreciated. In addition, huge thanks to the high county station holders, the Todhunters and the Watsons, for letting me walk all over your land. Last, but definitely not least, to Pat and Janet, the two most gorgeous and important girls in the department. Without you the whole department would fall apart.

8 References

Allan, H. H. 1961: Flora of New Zealand. Vol. 1. Wellington, Government Printer.

Alloway, B. V., Lowe, D. J., Barrell, D. J. A., Newnham, R. M., Almond, P.C., Augustinus, P.C., Bertler, N. A. N., Carter, L., Litchfield, N.J., McGlone, M.S., Shulmeister, J., Vandergoes, M. J., Williams, P. W. and members, N. Z. I., 2007: Towards a climate event stratigraphy for New Zealand over the past 30,000 years (NZ-INTIMATE project). *Journal of Quaternary Science, 22 (1):* 9-35.

Anderson, B. and Mackintosh, A. 2006: Temperature change is the major driver of late-glacial and Holocene glacier fluctuations in New Zealand. *Geology 34 (2):* 121-124.

Applegate, P. J., Lowell, T. V., Alley, R. B. 2008: Comment on "Absence of Cooling in New Zealand and the Adjacent Ocean During the Younger Dryas Chronozone". *Science 320:* 746d.

Barker, 1870: *Station life in New Zealand*. London: Macmillan.

Baylis, G. T. S. 1980: Mycorrhizas and the spread of beech. *New Zealand journal of ecology 3:* 151 - 153.

Barrows, T. M., Stone, J. O., Fifield, L. K., Cresswell, R. G., 2001: Late Pleistocene glaciation of the Kosciuszko Massif, Snowy Mountains, Australia. Quaternary Research 55: 179–189.

Barrows, T. M., Stone, J. O., Fifield, L. K., Cresswell, R. G., 2002: The timing of the last glacial maximum in Australia. Quaternary Science Reviews 21, 159–173.

Barrows, T. T, Lehman, S. J., Fifield, L. K., Deckker, P. D. 2008: Absence of Cooling in New Zealand and the Adjacent Ocean During the Younger Dryas Chronozone. *Science 318:* 86-89.

Basher, L. R., and McSaveney, M. J. 1989: An early Aranuian glacial advance at Cropp River, central Westland, New Zealand. *Journal of the Royal Society of New Zealand: 19 (3)*, 263–268.

Benn, D. I. 2002: Clast fabric development in a shearing granular material: implications for subglacial till and fault gouge- Discussion. *Bulletin of the Geological Society of America. 114:* 382-383.

Benn, D. I., and Evans, D. J. A. 1998: Glaciers & glaciation: Wiley, New York.

Bennett K. D. 2002: Psimpoll 3.10: C Programs for Plotting Pollen Diagrams and Analysing Pollen Data. Uppsala University, Sweden, 117 pp.

Bennett, M. R., Glasser., N.F. 1996: Glacial Geology: ice sheets and landforms. Chichester, Wiley.

Berryman, K. R., Beanland, S., Cooper, A. F., Cutten, H. N., Norris, R. J., and Wood, P. R. 1992: "The Alpine Fault, New Zealand: variations in Quaternary structural style and geomorphic expression." Annals Tectonicae 6: 126-163.

Birkeland, P. W. (1982). Subdivision of glacial deposits, Ben Ohau Range, using relative-dating methods. *Bulletin of the Geological Society of America*, 93: 433-449.

Bishop, D. G., Bradshaw, J. D., and Landis, C. A. 1985: "Provisional Terrane map of the South Island, New Zealand." Circum Pacific Council of Energy Minerals and Earth Sciences. Series 1.

Bowden, M. J. 1983: The Rakaia River and catchment - a resource survey. North Canterbury Catchment Board and Regional Water Board, Christchurch, New Zealand (4 vols.). 593 p.

Bradshaw, J. D. 1989: Cretaceous geotectonic patterns in the New Zealand region. *Tectonics 8:* 810.

Burrows, C. J. 1965: Some discontinuous distributions of plants within New Zealand and their ecological significance. II: disjunctions between Otago- Southland and Nelson-Marlborough and related distribution patterns. *Tuatara 13:* 9-29.

Burrows, C. J. 1969: Forest distribution and the forest and scrub flora. *In:* G. A.: Knox *ed.* The Natural History of Canterbury. Wellington. A. H. & A. W. Reed. 226-254.

Burrows, C. J. 1977a: Forest and scrub flora of the upper Rangitata, Rakaia and Wilberforce Valleys. *Canterbury botanical society journal. 10:* 1-8.

Burrows, C. J. 1977b: Forest vegetation. *In:* C. J. Burrows *ed* Cass: history and science in the Cass district, Canterbury, New Zealand. Department of Botany, University of Canterbury. Pp. 233-257.

Burrows, C. J. 1979: A chronology for cool-climate episodes in the Southern Hemisphere 12 000-1000 yr B.P. *Palaeogeography, palaeoclimatology, palaeoecology 27:* 287-347.

Burrows, C. J. 1980: Radiocarbon dates for post-Otiran glacial activity in the Mount Cook region. *New Zealand Journal of Geology and Geophysics, 23:* 239-248.

Burrows, C. J. 1983: Radiocarbon dates from Late Quaternary deposits in the Cass District, Canterbury, New Zealand. *New Zealand journal of botany 21*: 443 - 454.

Burrows, C. J. 1988: Late Otiran and early Aranuian radiocarbon dates from South Island localities. *New Zealand natural sciences 15:* 25-36.

Burrows, C. J. 1996: Radiocarbon dates for Holocene fires and associated events, Canterbury, New Zealand. *New Zealand Journal of Botany, 34:* 111-121.

Burrows, C. J., Russell, J. B. 1975: Moraines of the upper Rakaia Valley. *Journal of the Royal Society of New Zealand 5: 463 – 477.*

Burrows, C. J. and Gellatly, A. F. 1982: Holocene glacier activity in New Zealand. *Striae*, *18:* 41-47.

Burrows, C. J.; Russell, J. B. 1990: Aranuian vegetation history of the Arrowsmith Range, Canterbury. 1. Pollen diagrams, plant macrofossils and buried soils from Prospect Hill. *New Zealand journal of botany 28:* 323 - 345.

Burrows, C. J.; Duncan, K. W.; Spence, J. R. 1990: Aranuian vegetation history of the Arrowsmith Range, Canterbury II. Revised chronology for moraines of the Cameron Glacier. *New Zealand Journal of botany 28:* 455-66.

Burrows, C. J., and Lord, J. M. 1993: Recent colonisation of Nothofagus Fusca at Cass, Canterbury. *New Zealand Journal of Botany, 31:* 139- 146.

Carol, H. 1947: The formation of roches moutonees. *Journal of Glaciology 1:* 57-59.

Carter, R. M., and Gammon, P. 2004: New Zealand maritime glaciation: Millenial-scale southern climate change since 3.9 MA. *Science 304:* 1659-1662.

Chinn, T. J. H. 1996: New Zealand glacier responses to climate change of the past century. *New Zealand Journal of geology and geophysics 39:* 415-428.

Clark R. 1982: Point count estimation of charcoal in pollen preparations and thin sections. *Pollen Spores 24:* 523–525.

Clayton, L. 1968: Late Pleistocene glaciations of the Waiau Valleys, North Canterbury. *New Zealand journal of geology and geophysics 11:* 757–767.

Cockayne, 1926: Monograph on the New Zealand Beech Forests. Part I. The Ecology of the Forests and Taxonomy of the Beeches. *N.Z. State Forest Bull*., No. 4. Govt. Printer. Wellington.

Colhoun, E., and Shulmeister, J. 2006: Late Pleistocene of the SW Pacific region. *In:* Elias, S. *ed.* Encyclopaedia of Quaternary Sciences. Elsevier, Amsterdam. Pp. 1066-1075.

Cooke, P. J. 1988: The late Quaternary stratigraphy and micropaleontology of DSDP site 594, Southwest Pacific. Unpublished M.Sc. thesis, lodged in the Library, University of Waikato, Hamilton, New Zealand.

Cranwell, L. M; von Post, L. 1936: Post Pleistocene pollen diagrams from the southern hemisphere. 1, New Zealand. *Geografiska Annaler 3-4:* 308-347.

Delteil, J., Collot, J-Y., Wood, r., Herzer, R., Calmant, S., Christoffel, D., Coffin, M., Ferriere, J., Lamarche, G., Lebrun, J-F., Mauffret, A., Pontoise, B., Popoff, M., Ruellan, E., Sosson, M., and Sutherland, R. (1996). "From strike-slip faulting to oblique subduction: a survey of the Alpine Puysegar trench transition, New Zealand, Results of Cruise Geodynz-Sud Leg 2." *Marine Geophysical Researches 18:* 383-399.

Denton, G. H., and Hendy, C. H. 1994: Younger Dryas age advance of Franz Josef Glacier in the Southern Alps, New Zealand. *Science:* 264: 1434.

Dowdeswell, J. A., Hambry, M. J. and Wu, R. 1985: A comparison of clast fabric and shape in Late Precambrian and modern glacigenic sediments. *Journal of Sedimentary Petrology* 55: 691-704.

Easterbrook, D. J. 2003: Global, double, Younger Dryas, glacial fluctuations in ice sheet and alpine glaciers. XVI INQUA Congress Preograms with Abstracts. 73 pp.

Eden, D. N.; Hammond, 2003: A. P. Dust accumulation in the New Zealand region since the last glacial maximum. *Quaternary Science Reviews 22*, 18-19, p. 2037-2052.

Evans, D. J. A., Salt, K. E., Allen, C. S. 1999: Glacitectonized lake sediments, Barrier Lake, Kananaskis Country, Canadian Rocky Mountains. *Can. J. Earth Sci. 36:* 395-407.

Evans, D. J. A. and Benn, D. I. 2004: *A Practical Guide to the Study of Glacial Sediments*. Edward Arnold Publishers Ltd. London. 266 pp.

Evans, D. J. A., Phillips, E. R., Hiemstra, J. F., and Auton, C. A. 2006: Subglacial till: Formation, sedimentary characteristics and classification. *Earth-Science Reviews Volume 78, Issues 1-2,* 115-176.

Evans, D. J. A., Hiemstra, J F., O'Cofaigh, C. 2007: An assessment of clast macrofabrics in glacigenic sediments based on A/B plane data. *Geografiska Annaler, Series A: Physical Geography 89 (2),* 103–120.

Evans, M. 2008: A geomorphological and sedimentological investigation into the glacial deposits of the Lake Clearwater Basin, Mid Canterbury, New Zealand. Unpublished MSc thesis, University of Canterbury.

Eyles, N., Eyles, C.H., Miall, A.D. 1983: Lithofacies types and vertical profile models; an alternative approach to the description and environmental interpretation of glacial diamict and diamictite sequences. *Sedimentology, 30:3*, 393-410.

Eyles, N. 2006: The role of meltwater in glacial processes. *Sedimentary Geology 190:* 257-268.

Field, B. D., Brown, G. H. 1986: Lithostratigraphy of Cretaceous and Teritary sediments, southern Canterbury, New Zealand. New Zealand Geological Survey record, *New Zealand Geological Survey report. 14:* 55.

Field, B. D., Uruski, C.I., Beu, Brown, G., Crampton, J., Funnel, R., Killops, S., Laird, M., Mazengarb, C., Morgans, H., Rait, G., Smale, D. and Strong, P. 1997: Cretaceous and Cenozoic development and hydrocarbon geology of a plate margin: East Coast region, New Zealand. Lower Hutt, New Zealand, Inst. *Geol. Nucl. Sci: 301*.

Fitzharris, B. B., Hay, J. E., Jones, P. D. 1992: Behaviours of New Zealand glacier and atmospheric circulation changes over the past 130 years. *The Holocene 2*: 97-106.

Fitzsimons, S. J. 1997: Late-glacial and early Holocene glacier activity in the Southern Alps, New Zealand. *Quaternary International 38/39:* 69–76.

Fowke, N. C. 1974: Tertiary rocks of the Rakaia Catchment. Geology. Dunedin, University of Canterbury. Unpublished B.Sc (Hons).

Gagan, M. K., Hendy, E. J., Haberle, S. J., Hantoro, W. S. 2004. Post-glacial evolution of the Indo-Pacific Warm Pool and El Niño-Southern Oscillation, *Quaternary International: 118-119*, 127-143.

Gage, M. 1958: Late Pleistocene glaciations of the Waimakariri Valley, Canterbury, New Zealand. *New Zealand Journal of Geology and Geophysics 1:* 123-155.

Gage, M. 1977: Glacial geology. *In:* Burrows, C. J. *ed.* Cass: history and science in the Cass District, Canterbury. Department of Botany, University of Canterbury. Pp. 67-78.

Gellatly, A. F., Chinn, T. J. H., and Ro¨thlisberger, F. 1988: Holocene glacier variations in New Zealand. *Quaternary Science Reviews 7,* 227–242.

Gibbard, P. L. 1986: Comparison of the clast lithological composition of the gravels in the Middle Thames using canonical variates and principal components analysis. In: Bridgland, D,R, (ed.) *Clast lithological analysis*. Technical Guide 3, Quaternary Research Association: Cambridge, 153-164.

Griffiths, G. A., and McSaveney, M. J. 1983: "Distribution of mean annual precipitation across some steepland regions of New Zealand." *New Zealand Journal of Science 26:* 197 - 209.

Hart, J. K. 1996: Proglacial glaciotectonic deformation associated with glaciolacustrine sedimentation, Lake Pukaki, New Zealand. *Journal of Quaternary Science, 11:* 149-160.

Harvey, M. D. 1974: Soil studies in a high country catchment, Paddle Creek, South Canterbury. Unpublished MAgSc thesis, Lincoln College, University of Canterbury, New Zealand.

Henderson, R. D., and Thompson, S. M. 1999: "Extreme rainfalls in the Southern Alps of New Zealand." Journal of Hydrology 38(2): 309 - 330.

Heusser, L. E., van de Geer, G., 1994: Direct correlation of terrestrial and marine paleoclimatic records from four glacial-interglacial cycles—DSDP site 594 southwest Pacific. Quaternary Science Reviews 13, 273–282.

Hofmann W. 1986: Chironomid analysis. In: Berglund B.E. (ed.), Handbook of Holocene Palaeoecology and Palaeohydrology. J. Wiley and Sons, Chichester, pp. 715–727.

Hooyer, T. S., Iverson, N. R. 2000: Diffusive mixing between shearing granular layers: constraints on bed deformation from till contacts. *Journal of Glaciology. 46*: 641-651.

Hyatt, O., Shulmeister, J., Thackray, G.D., Rother, H., Evans, D.J.A., Evans, M. 2007: The nature of glacial advances in a hyper-humid climate: Morphological and sedimentological evidence from selected New Zealand glacial valleys. *Abstracts/Quaternary International vol. 176-168*, 185 pp.

Ildefonse, B., Mancktelow, N.S. 1993: Deformation around rigid particles: the influence of slip at the particle/matrix interface. *Tectonophysics 221*, 345-359.

Ivy-Ochs, S., Schlu¨chter, C., Kubik, P. W., and Denton, G. H. 1999: Moraine exposure dates imply synchronous Younger Dryas glacier advances in European Alps and in the Southern Alps of New Zealand. *Geografiska Annaler 81 A*: 313–323.

Kirkbride, M. P. 1993: The temporal significance of transitions from melting to calving termini of glaciers in central Southern Alps. *The Holocene 3*: 232-240.

Klein, E. and Davis, D. 2002: Surface Sample Bias and Clast Fabric Interpretation Based on Till, Ditch Plains, Long Island, April 2002, Long Island Geologists, State University of New York. http://www.geo.sunysb.edu/lig/Conferences/abstracts_02/klein/klein.htm.

Koeppen, W. 1923: Die climate der Erde Grundriss der Klimakunde. Berlin. Walter de Gruyter (Summerised, in 1937, by the Committee of the Geophysical Association) in *Geography 22 (4):* 252-282.

Kuijt, J. 1969: The biology of flowering parasitic plants. Berkeley, University of California Press.

Ladley, J., Kelly, D. 1996: Dispersal, germination and survival of New Zealand mistletoes (Loranthaceae): dependence on birds. *New Zealand journal of ecology 20:* 69-79.

Laird, M. G., Bradshaw, J.D. 1994: Geological aspects of the opening of the Tasman Sea. Rotterdam, Balkema.

Laird, M. G., Bradshaw, J.D. 2004: The break-up of a long-term relationship: the Cretaceous separation of New Zealand from Gondwana. *Gondwana Research 7:* 273-286.

Lambeck, K., Yokoyama, Y., Purcell, T., 2002: Into and out of the last glacial maximum: sea level change during Oxygen Isotope Stages 3 and 2. *Quaternary Science Reviews 21:* 343–360.

Large M. F. and Braggins J. E. 1991: Spore Atlas of New Zealand Ferns & Fern Allies. SIR Publishing, Wellington, New Zealand, 167 pp.

Lawson, D. E. 1979: A comparison of pebble orientations in ice and deposits of the Matanuska Glacier, Alaska. *Annals of Glaciology 2*: 78-84.

Lewis, W. V. 1947: "The formation of roches moutonness: some comments of Dr H. Carol's article." *Journal of Glaciology 1:* 60-63.

Lintott, W. H., Burrows, C. J. 1973: A pollen diagram and macrofossils from Kettlehole Bog, Cass, South Island, New Zealand. *New Zealand journal of botany 11:* 269-282.

L.I.N.Z 1999: Map 260 J35 Arrowsmith. Wellington, Land Information New Zealand.

Locke, W. 1995: Modeling of icecap glaciation of the northern Rocky Mountains of Montana. *Geomorphology 14:* 123-130.

Locke, W. 1996: Teaching geomorphology through spreadsheet modelling: *Geomorphology,16:* 251-258.

Locke, W. 2007: GlacPro computer spreadsheet model, http://www.homepage.montana.edu/~ueswl/spreadsheet.html, accessed March 5.

Luyenduk, B. P. 1995: "Hypothesis of Cretaceous rifting of east Gondwana caused by subducted slab capture." Geology 23(373).

McGlone, M. S. 1988: New Zealand. *In:* Huntley, B.; Webb, T.III. Vegetation history. London, Kluwer Academic publishers. Pp. 557—599.

McGlone, M. S., Mark, A. F., Bell, D. 1995: Late Pleistocene and Holocene vegetation history, Central Otago, South Island, New Zealand. *Journal of The Royal Society of New Zealand, 25:* 1-22.

McGlone, M. S., and Wilmshurst. 1999: A Holocene record of climate, vegetation change and peat bog development, east Otago, South Island, New Zealand, *Journal of Quaternary science, 14:* 239-254.

McIntyre, R. 2007: Historic heritage of high-country pastoralism: South Island up to 1948. Published by Science & Technical Publishing Department of Conservation. Wellington. New Zealand. 172 pp.

McQueen, D. R., Mildenhall, D. C., Bell, C. J. E., 1968: Paleobotanical evidence for changes in the Tertiary climates of New Zealand. *Tuatara 16 (1):* 49-56.

McSaveney, M.J. and Whitehouse, I.E. 1989: An early Holocene glacial advance in the Macauley river valley, central Southern Alps, New Zealand. *New Zealand Journal of Geology and Geophysics, 32:* 235-241.

Mabin, M. C. G. 1980: Late Pleistocene glacial sequences in the Rangitata and Ashburton Valleys, South Island, New Zealand. Unpublished Ph.D. thesis, University of Canterbury.

Mabin, M. C. G. 1983: Late Otiran sedimentation and glacial chronology in the Warwick Valley, south east Nelson. *New Zealand journal of geology and geophysics 26:* 186-195.

Mabin, M. C. G. 1987: Early Aranuian sedimentation in the Rangitata Valley, Mid Canterbury. *New Zealand journal of geology and geophysics 30:* 87-90.

Macphail, M. K.; McQueen, D. R. 1983: The value of New Zealand pollen and spores as indicators of Cenozoic vegetation and climate. *Tuatara 26:* 37-59.

Mager, S., Fitzsimons, S., 2007: Formation of glaciolacustrine Late Pleistocene end moraines in the Tasman Valley, New Zealand. *Quaternary Science Reviews 26:* 743-758.

Mantua, N.J.; Hare, S.R.; Zhang, Y.; Wallace, J.M.; Francis, R.C. 1997: A Pacific interdecadal climate oscillation with impacts on salmon production. *Bulletin of the American Meteorological Society 78*: 1069–1079.

Martinson, D. G., Pisias, N. G., Hays, J.D., Imbrie, J., Moore, T. C., Shackleton, N. J., 1987: Age dating and orbital theory of the ice ages: development of a high-resolution 0 to 300,000-year chronostratigraphy. *Quaternary Research 27:* 1-29.

Mason, B. 1948: Middle Tertiary strata at Smite River, Lake Heron, New Zealand. *N.Z Journal of Science and Technology 30 (B) 1:* 55-58.

Metcalf, Lawrie. 2002: Trees of New Zealand. Auckland: New Holland.

Mix, A.C., Bard, E., Schneider, R., 2001: Environmental processes of the ice age: land, oceans, glaciers (EPILOG). *Quaternary Science Reviews 20:* 627 - 657.

Moar, N. T. 1966: Plant fragments from Kettlehole Bog, Cass. *New Zealand journal of botany 4:* 596-598.

Moar, N. T. 1969: Possible long-distance transport of pollen to New Zealand *New Zealand Journal of Botany 7:* 424-6.

Moar, N. T. 1970: Recent pollen spectra from three localities in South Island, New Zealand. *New Zealand journal of botany 8:* 210-221.

Moar, N. T. 1971: Contributions to the Quaternary history of the New Zealand flora. 6. Aranuian pollen diagrams from Canterbury, Nelson and North Westland, South Island. *New Zealand journal of botany 9:* 80-145.

Moar, N. T. 1973: Contributions to the Quaternary history of the New Zealand flora. 7. Two Aranuian pollen diagrams from central South Island. *New Zealand journal of botany 11:* 291-304.

Moar N. T. 1993: Pollen Grains of New Zealand Dicotyledonous Plants. Manaaki Whenua Press, Lincoln, New Zealand, 200 pp.

Moore P. D., Webb J. A. and Collinson M. E. 1991: Pollen Analysis. Blackwell Scientific Publications, Oxford, England, 216 pp.

Molloy, B. P. J.; Burrows, C. J.; Cox, J. E.; Johnston, J. A.; Wardle, P. 1963: Distribution of subfossil forest remains, eastern South Island, New Zealand. *New Zealand Journal of Botany 1*: 68–77.

Molloy, B. P. J. 1977: The fire history. *In:* C. J. Burrows *ed.* Cass: history and science in the Cass district, Canterbury, New Zeal and. Department of Botany, University of Canterbury. Pp. 157-70.

Molloy, B. P. J., Cox, J. E. 1972: Subfossil forest remains and their bearing on forest history in the Rakaia Catchment, Canterbury, New Zealand. *N.Z Journal of Botany 10:* 267-276.

Nelson, C. S., Cooke, P. J., Hendy, C. H., Cuthbertson, A. .M., 1993: Oceanographic and climatic changes over the past 160,000 years at Deep-sea Drilling Project site 594 off southeastern New Zealand, southwest Pacific Ocean. *Paleoceanography 8:* 435–458.

Newnham, R. M., Lowe, D. J., Giles, T. and Alloway, B. V. 2007: Vegetation and climate of Auckland, New Zealand, since ca. 32 000 cal. yr ago: support for an extended LGM. *Journal of Quaternary Science 22:* 517-534.

Newnham, R.M., Vandergoes, M.J., Hendy, C.H., Lowe, D.J. and Preusser, F. 2007: A terrestrial palynological record for the last two glacial cycles from southwestern New Zealand. *Quaternary Science Reviews 26:* 517-535.

Norris, R. J., Koons, P.O., and Cooper, A.F. (1990). "The obliquely convergent plate boundary in the South Island of New Zealand: Implications for ancient collision zones." *Journal of Structural Geology 12:* 715-725.

Oerlemans, J., 1994: Quantifying global warming from the retreat of glaciers. *Science 264:* 243-245.

Ogden, J., Stewart, G. H., Allen, R. B. 1996: Ecology of New Zealand Nothofagus forests. In: Veblen T. T., Hill, R. S., Read, J. ed. *The ecology and biogeography of Nothofagus forests.* New Haven, Yale University Press. Pp. 25–82.

Oliver, P. J. 1977: The Mesozoic geology of the Mount Somers area, Canterbury. Geology. Unpublished Ph.D. thesis, University of Canterbury

Oliver, P. J., Keene, H. W. 1990: Sheet J36 BD and part sheet J35—Clearwater. Geological map of New Zealand 1:50 000. Wellington, Department of Scientific and Industrial Research.

Patel, R. N. 1974: Wood anatomy of the Dicotyledons indigenous to New Zealand 4. Winteraceae. *New Zealand journal of botany 12:* 19 – 32.

Petit, J. R., Jouzel, J., Raynaud, D., Barkov, N. I., Barnola, B, I., Benders, M., Chappellaz, J., Davis, M., Delmotte, M., Kotlyakov, V.M., Legrand, M.,

Lipenkov, Lorius, C., Pe´ pin, L., Ritz., C., Saltzman, E., Stievenard. 1999: Climate and atmospheric history of the past 420,000 years Vostok ice core, Antarctica. *Nature 399:* 429–436.

Pettinga, J., Yetton, M.D., Van Dissen, R.J., and Downes, G., 2001, Earthquake Source Identification and Characterisation for the Canterbury Region, South Island, New Zealand. *Bulletin of the New Zealand Society for Earthquake Engineering 34:* 282-317.

Pillans, B. 1991: New Zealand Quaternary stratigraphy: an overview. *Quaternary science reviews 10:* 405-418.

Pocknall D. T. 1981. Pollen morphology of the New Zealand species of Dacrydium Solander, Podocarpus L'Heritier, and Dacrycarpus Endlicher (Podocarpaceae). *New Zealand Journal of Botany 19:* 67–95.

Porter, S. C., 1975, Equilibrium-line altitudes of late Quaternary glaciers in south Alps, New Zealand. *Quaternary Research, 5 (1):* 27-47.

Power, S., Tseitkin, F., Torok, S., Lavery, B., Dahni, R., McAvaney, B. (1998). Australian temperature, Australian rainfall and the Southern Oscillation, 1910–1992: coherent variability and recent changes. *Australian Meteorological Magazine 47*: 85–101.

Preusser, F., Andersen, B.G., Denton, G.H. and Schluchter, C., 2005. Luminescence chronology of Late Pleistocene glacial deposits in North Westland, New Zealand. *Quaternary Science Reviews, 24 (20-21):* 2207-2227.

Putkonen, J., and Swanson, T. 2003: Accuracy of cosmogenic ages of moraines. *Quaternary Research: 59 (2)*, 255-261.

Raven, P. H. 1973: Evolution of subalpine and alpine plant groups in New Zealand. *New Zealand Journal of Botany 11:* 177-200.

Rein, B., Luckage, A., Reinhardt, L, Sirocko, F., Wolf, A,. and Dullo., W-C. 2005: El Niño variability off Peru during the last 20,000 years, *Paleoceanolography, 20*. PA4003, doi:10.1029/2004PA001099.

Ricker, K. E.; Chinn, T. J.; McSaveney, M. J. 1992: A late Quaternary moraine sequence dated by rock weathering rinds, Craigieburn Range, New Zealand. *Canadian journal of earth sciences 30 (9):* 1861-1869.

Rodbell, D. T. 1986: The use of lichenometry, rock weathering and soil development to estimate ages of moraines and fluvial terraces in the upper South Branch,

Ashburton Valley, South Island, New Zealand. Unpublished M.Sc. thesis, University of Colorado, Boulder.

Rogers, G. M., McGlone, M. S. 1989: A postglacial vegetation history of the southern central uplands of North Island, New Zealand. *Journal of the Royal Society of New Zealand 19:* 229-248.

Rother, H., Shulmeister, J., 2005: Synoptic climate change as a driver of late Quaternary glaciations in the mid-latitudes of the Southern Hemisphere. *Climate of the Past, 2:* 11-19.

Rother, H., Late Pleistocene glacial geology of the Hope-Waiau valley system in North Canterbury, New Zealand. 2006. Unpublished Ph.D. thesis, University of Canterbury.

Rother, H., Fink, D., Shulmeister, J., Evans, M., Mifsud, C. 2008. 10Be / 26Al exposure age chronologies from mid-latitude Southern Hemisphere glacial sequences in the Southern Alps, New Zealand. *Geophysical Research Abstracts, Vol. 10,* EGU2008-A-01973.

Rudberg, S. 1988: "Gross geomorphology of Fennoscandia: six complementary ways of explanation." *Geografiska Annaler 70a (3):* 135-167.

Russell, J. B. 1980: Aranuian pollen diagrams from montane Canterbury, New Zealand. Unpublished Ph.D. thesis, University of Canterbury.

Salinger, M.J.; Mullan, A.B. 1999: New Zealand climate: temperature and precipitation variations and their link with atmospheric circulation 1930-1994. *International Journal of Climatology 19*: 1049–1071.

Samson, F.B. 1980: Natural hybridism in *Psuedowintera* (Winteraceae). *Journal of the Royal Society of New Zealand 18:* 43- 51.

Santamaria Tovar, D., Shulmeister, J., Davies, T. R. 2008: Evidence for a landslide origin of New Zealand's Waiho Loop moraine. *Nature Geoscience (in press).*

Sara, W. A. 1979: Glaciers of Westland National Park, New Zealand. Department Of Scientific and Industrial Research Information Series, 79 (2nd Edition).

Schilling, D. H., and Hollin, J. T. 1981: Numerical reconstruction of valley glaciers and small ice caps. In T. Hughes and G. H. Denton (eds.), "The Last Great Ice Sheets", p 207-221, John Wiley and Sons, New York.

Sharp, M. J. 1982: Modification of clasts in lodgement tills by glacial erosion. *Journal of Glaciology 28:* 475-481.

Shulmeister, J.P., Goodwin, I., Renwick, K., Armand, L., McGlone, M.S., Cook, E., Dodson, J., Hesse, P.P., Mayewski, P., Curran, M. 2004: The Southern Hemisphere westerlies in the Australasian sector over the last glacial cycle: A synthesis. *Quaternary International 118-119:* 23-53.

Shulmeister, J., Fink, D. and Augustinus, P.C. 2005: A cosmogenic nuclide chronology of the last glacial transition in North-West Nelson, New Zealand - new insights in Southern Hemisphere climate 70 forcing during the last deglaciation. *Earth and Planetary Science Letters. 233:* 455-466.

Shulmeister, J.P., Rieser, U., Fink, D., Thackray, G.D, Hyatt, M.H., Rother, H. 2007: Luminescence and surface exposure dating chronology from 5e to YD in the Rakaia Valley, Canterbury, New Zealand and insights for the timing and forcing of NZ glaciation. *Abstracts/Quaternary International vol. 176-168*, 383 pp.

Sissons, J. B. 1958: "The deglaciation of part of East Lothian." Transactions of the Institute of British Geography 25: 59-78.

Smith, C., Almond, P., and Shanhun, F. 2008: Vegetation at the extended LGM interstadial: evidence from the phytolith record across biogeographical zones of northern South Island, New Zealand. AUS-INTIMATE 2008 abstract.

Soons, J. M. 1963: The glacial sequence in part of the Rakaia Valley, Canterbury, New Zealand. *New Zealand journal of geology and geophysics 6:*735-756.

Soons, J. M. 1996: Changes in geomorphic environments in Canterbury-during the Aranuian. *New Zealand Journal of Botany. 32:* 365–372.

Soons, J. M. and Gullentops, F. W. 1973: Glacial advances in the Rakaia Valley, New Zealand. *New Zealand Journal of Geology and Geophysics, 16:* 425-438.

Soons, J. M. and Burrows, C. J. 1978: Dates for Otiran deposits including plant microfossils and macrofossils, from Rakaia Valley. *N.Z Journal of Geology and Geophysics 21 (5):* 607-615.

Speight, R. 1919: The Older Gravels of North Canterbury. *Trans. N.Z. Inst., 51:* 269–281.

Speight, R. 1934: The Rakaia Valley. *Trans. N.Z. Inst.*, vol. lxii, pp. 457–496.

Speight, R., Cockayne, L., and Laing, R. M, 1910: The Mount Arrowsmith District; a Study in Physiography and Plant Ecology. *Trans. N.Z. Inst., 43:* 315–378.

Storey, B. C., Leat, P.T., Weaver, S.D., Pankhurst, R.J., Bradshaw, J.D. and Kelley, S. 1999: "Mantle plumes and Antarctica-New Zealand rifting: evidence from

Mid-Cretaceous mafic dykes." *Journal of the Geological Society of London 156:* 659-671.

Sugden, D. E., Glasser, N.F. and Clapperton, C.M. (1992). "Evolution of large roches moutonees." Geografiska Annaler 74a: 253-264.

Suggate, R. P. 1961: The upper boundary of the Hawera Series. *Transactions of the Royal Society of New Zealand (Geology) 1:* 11-6.

Suggate, R. P. 1965: Late Pleistocene geology of the northern part of the South Island, New Zealand. *New Zealand Geological survey bulletin (new series) 77.*

Suggate, R. P., 1990: Late Pliocene and Quaternary glaciations of New Zealand. *Quaternary Science Reviews 9,* 175–197.

Suggate, R. P. 2004: South Island, New Zealand; Ice advances and marine shorelines. In Quaternary Glaciations—Extent and Chronology, Part III (J. Ehlers and P. L. Gibbard, Eds.), pp. 285–291, Elsevier, Amsterdam.

Suggate, R. P, and Almond, P.C. 2005: The Last Glacial Maximum (LGM) in western South Island, New Zealand: implications for the global LGM and MIS 2. Quaternary Science Reviews 24: 1923 – 1940.

Troels-Smith J. 1955: Characterization of unconsolidated sediments. Geological Survey of Denmark 10: 1–73.

Ullmann, I.; Lange, O. L.; Ziegler, H.; Ehleringer, J.; Schulze, E.-D.; Cowan, I. R. 1985: Diurnal courses of leaf conductance and transpiration of mistletoes and their hosts in central Australia. *Oecologia 67:* 577-587.

Von Haast, J. 1877: Notes on the geology of the Clent Hills and Mt. Somers Districts in the Province of Canterbury. *N.Z Geological Survey Report of Geological Exploration No. 8:* 1-19.

Von Haast, J. 1879: Geology of the Provinces of Canterbury and Westland, New Zealand. The Times, Christchurch.

Waight, T. E., Weaver, S.D., Muir, R.J., Maas, R. and Elby, G.N. 1998: "The Hohonu Batholith of North Westland, New Zealand: Granitoid compositions controlled by source H2O contents and generated during tectonic transition." Contributions to mineralogy and petrology 130(225 - 239).

Walker, I. R. 2001: Chironomids as indicators of past environmental change. In: Armitage P. Cranston PS and Pinder LCV (eds), The Chironomidae: The biology and Ecology of Non-Biting Midges. Chapman and Hall, London. Pp 405-422.

Wardle, J. A. 1984: New Zealand beeches. Christchurch, New Zealand Forest Service.

Wardle, P. 1969: Biological flora of New Zealand. 4. *Phyllocladus alpinus* Hook f. (Podocarpaceae) Mountain Toatoa, Celery Pine. *New Zealand journal of botany 7:* 76 - 95.

Wardle, P. 1991: Vegetation of New Zealand, Cambridge Press, Cambridge.

Warren, G. 1967: Sheet 17-Hokitika. Geological map of New Zealand 1:250,000. Wellington, New Zealand. Department of Scientific and Industrial Research.

Weaver A. J, M. Eby, A. F. Fanning, and E. C. Wiebe. 1998: Simulated influence of carbon dioxide, orbital forcing and ice sheets on the climate of the Last Glacial Maximum. *Nature,* 394, 847–853.

Weaver, S. D., Bradshaw, J.D., Pankhurst, R.J., Muir, R.J., Storey, B.C., Waight, T. E, and Ireland, T. R. 1996: "Cretaceous magmatism, make-up and break-up of the SW Pacific Gondwana margin." *Geological Society of Australia 43:* 548-556.

West, R. G. 1977: *Pleistocene Geology and Biology.* Longman Group Limited, London.

Williams, P. W., 1996. A 230 k cal. yr record of glacial and interglacial events from Aurora Cave, Fiordland, New Zealand. New Zealand Journal of Geology and Geophysics 39, 225–241.

Wilmshurst, J. M., McGlone, M. S., Charman, D. J. 2002: Holocene vegetation and climate change in southern New Zealand: linkages between forest composition and quantitative surface moisture reconstructions from an ombrogenous bog. *J. Quaternary Sci., 17:* 653-666.

Wilmshurst, J. M., McGlone, M. S., Leathwick, J. R., Newnham, R. M. 2007: A pre-deforestation pollen-climate calibration model for New Zealand and quantitative temperature reconstructions for the past 18,000 years BP. *J. Quaternary Sci. 22:* 535-547.

Woodward, C. 2006: Development of chironomid-based transfer functions for surface water quality parameters and temperature, and their application to Quaternary sediment records from the South Island, New Zealand. Unpublished PhD thesis, University of Canterbury.

9 Appendix A: GLACPRO data

Pyramid advance

Up-ice dist. (m)	Bedrock elevation (m)	Shape factor	Basal shear (bar)	Step Length (m)	Change (m)	Calculated Elevation (m)	Centerline Thickness (m)	Moraine crest (m)	Ice thickness (m)
0	500					1000	500	1000	
1000	510	0.9	0.3	1000	15	1020	510	1020	
2000	515	0.9	0.3	1000	14.444	1040	525	1040	
3000	530	0.9	0.3	1000	14.032	1060	530	1060	
4000	545	0.9	0.3	1000	13.899	1080	535	1080	535
5000	555	0.9	0.5	1000	22.949	1102.949	547.9491	1100	545
6000	565	0.9	0.7	1000	31.369	1134.319	569.3186	1140	575
7000	572	0.9	0.7	1000	30.192	1164.511	592.5107	1170	598
8000	580	0.9	0.5	1000	20.722	1185.232	605.2323		-580
9000	595	0.9	0.5	1000	20.286	1205.518	610.5183	1200	605
10000	605	0.9	0.6	1000	24.132	1229.651	624.6508	1220	615
11000	615	0.9	0.6	1000	23.587	1253.237	638.2373	1240	625
12000	623	0.9	0.7	1000	26.932	1280.169	657.1692	1260	637
13000	628	0.9	0.7	1000	26.156	1306.325	678.3251	1280	652
14000	633	0.9	0.7	1000	25.34	1331.665	698.6653	1300	667
15000	637	0.9	0.7	1000	24.602	1356.268	719.2678	1320	683
16000	642	0.9	0.8	1000	27.312	1383.579	741.5795		-642
17000	650	0.9	0.7	1000	23.179	1406.758	756.7582		-650
18000	660	0.9	0.7	1000	22.714	1429.472	769.4721		-660
19000	675	0.9	0.7	1000	22.339	1451.811	776.8106		-675
20000	690	0.9	0.7	1000	22.128	1473.938	783.9382	1480	790
21000	695	0.9	0.7	1000	21.926	1495.864	800.8645	1500	805
22000	693	0.9	0.6	1000	18.397	1514.261	821.2613	1520	827
23000	691	0.9	0.6	1000	17.94	1532.201	841.2012	1540	849
24000	691	0.9	0.6	1000	17.515	1549.716	858.7158	1560	869
25000	691	0.9	0.6	1000	17.157	1566.873	875.8732	1575	884
26000	691	0.9	0.6	1000	16.821	1583.695	892.6945	1590	
27000	691	0.9	0.5	1000	13.754	1597.448	906.4481	1605	
28000	691	0.9	0.5	1000	13.545	1610.993	919.9931		
29000	690	0.9	0.5	1000	13.346	1624.339	934.3386		
30000	689	0.9	0.5	1000	13.141	1637.479	948.4792		
31000	685	0.9	0.5	1000	12.945	1650.424	965.4239		
32000	680	0.9	0.5	1000	12.717	1663.141	983.1414		
33000	678	0.9	0.5	1000	12.488	1675.63	997.6297		
34000	674	0.9	0.5	1000	12.307	1687.937	1013.937		
35000	668	0.9	0.5	1000	12.109	1700.046	1032.046		
36000	665	0.9	0.5	1000	11.897	1711.942	1046.942		
37000	661	0.9	0.5	1000	11.727	1723.669	1062.669		
38000	655	0.9	0.5	1000	11.554	1735.223	1080.223		
39000	645	0.9	0.5	1000	11.366	1746.589	1101.589		
40000	640	0.9	0.5	1000	11.146	1757.735	1117.735		
41000	630	0.9	0.5	1000	10.985	1768.719	1138.719		
42000	620	0.9	0.5	1000	10.782	1779.501	1159.501		
43000	612	0.9	0.5	1000	10.589	1790.09	1178.09		
44000	605	0.9	0.5	1000	10.422	1800.512	1195.512		
45000	615	0.9	0.5	1000	10.27	1810.782	1195.782		
46000	630	0.9	0.5	1000	10.268	1821.049	1191.049		
47000	650	0.9	0.5	1000	10.308	1831.358	1181.358		

Dogs Hill advance

Up-ice dist. (m)	Bedrock elevation (m)	Shape factor	Basal shear (bar)	Step Length (m)	Change (m)	Calculated Elevation (m)	Centerline Thickness (m)	Moraine crest (m)	Ice thickness (m)
0	545					860	315	860	315
1000	555	0.8	0.3	1000	26	880	325	880	325
2000	565	0.8	0.3	1000	25.5	900	335	900	335
3000	572	0.8	0.3	1000	24.739	920	348	920	348
4000	580	0.8	0.3	1000	23.815	940	360	940	360
5000	595	0.8	0.3	1000	23.021	960	365	960	365
6000	605	0.8	0.3	1000	22.705	980	375	980	375
7000	615	0.8	0.27	1000	19.89	999.89	384.89	1000	385
8000	623	0.8	0.27	1000	19.379	1019.269	396.2689	1020	397
9000	628	0.8	0.3	1000	20.914	1040.183	412.1827	1040	412
10000	633	0.8	0.3	1000	20.106	1060.289	427.2891		
11000	637	0.8	0.3	1000	19.396	1079.685	442.6846		
12000	642	0.8	0.3	1000	18.721	1098.406	456.4056		
13000	650	0.8	0.4	1000	24.211	1122.617	472.6166	1120	470
14000	660	0.8	0.4	1000	23.38	1145.997	485.997	1140	480
15000	675	0.8	0.4	1000	22.737	1168.734	493.7338	1160	485
16000	690	0.8	0.4	1000	22.38	1191.114	501.1143	1180	490
17000	695	0.8	0.4	1000	22.051	1213.165	518.1651		
18000	693	0.8	0.4	1000	21.325	1234.49	541.4904		
19000	691	0.8	0.4	1000	20.407	1254.897	563.897		
20000	691	0.8	0.4	1000	19.596	1274.493	583.4928		
21000	691	0.8	0.4	1000	18.938	1293.43	602.4305		
22000	691	0.8	0.4	1000	18.342	1311.773	620.7729		
23000	691	0.8	0.4	1000	17.8	1329.573	638.5732		
24000	691	0.8	0.4	1000	17.304	1346.877	655.8774		
25000	690	0.8	0.4	1000	16.848	1363.725	673.7251		
26000	689	0.8	0.4	1000	16.401	1380.126	691.1265		
27000	685	0.8	0.4	1000	15.988	1396.115	711.1148		
28000	680	0.8	0.4	1000	15.539	1411.654	731.6538		
29000	678	0.8	0.4	1000	15.103	1426.757	748.7566		
30000	674	0.8	0.4	1000	14.758	1441.514	767.5144		
31000	668	0.8	0.4	1000	14.397	1455.912	787.9115		
32000	665	0.8	0.4	1000	14.024	1469.936	804.9359		
33000	661	0.8	0.4	1000	13.728	1483.664	822.6637		
34000	655	0.8	0.4	1000	13.432	1497.096	842.0957		
35000	645	0.8	0.4	1000	13.122	1510.218	865.2177		
36000	640	0.8	0.4	1000	12.771	1522.989	882.9891		
37000	630	0.8	0.4	1000	12.514	1535.503	905.5034		
38000	620	0.8	0.4	1000	12.203	1547.707	927.7066		
39000	612	0.8	0.4	1000	11.911	1559.618	947.6177		
40000	605	0.8	0.4	1000	11.661	1571.278	966.2785		
41000	615	0.8	0.4	1000	11.436	1582.714	967.7141		
42000	630	0.8	0.4	1000	11.419	1594.133	964.1328		
43000	650	0.8	0.4	1000	11.461	1605.594	955.5938		

Emily advance

Up-ice dist. (m)	Bedrock elevation (m)	Shape factor	Basal shear (bar)	Step Length (m)	Change (m)	Calculated Elevation (m)	Centerline Thickness (m)	Moraine crest (m)	Ice thickness (m)
0	595					660	65	660	65
1000	605	0.8	0.1	1000	43	700	95	700	95
2000	615	0.8	0.1	1000	29.079	740	125	740	125
3000	623	0.8	0.1	1000	22.1	790	167	790	167
4000	628	0.8	0.1	1000	16.542	840	212	840	212
5000	633	0.8	0.1	1000	13.031	860	227	860	227
6000	637	0.8	0.2	1000	24.339	890	253	890	253
7000	642	0.8	0.3	1000	32.757	922.7569	280.7569		-642
8000	650	0.8	0.3	1000	29.518	952.2753	302.2753		-650
9000	660	0.8	0.3	1000	27.417	979.6924	319.6924		-660
10000	675	0.8	0.3	1000	25.923	1005.616	330.6157	990	315
11000	690	0.8	0.3	1000	25.067	1030.683	340.6826	1015	325
12000	695	0.8	0.3	1000	24.326	1055.009	360.0088	1035	340
13000	693	0.8	0.3	1000	23.02	1078.029	385.029	1060	367
14000	691	0.8	0.3	1000	21.524	1099.553	408.5534	1090	399
15000	691	0.8	0.3	1000	20.285	1119.838	428.8384	1115	424
16000	691	0.8	0.3	1000	19.325	1139.164	448.1638	1135	444
17000	691	0.8	0.3	1000	18.492	1157.656	466.656		
18000	691	0.8	0.3	1000	17.759	1175.415	484.4153		
19000	691	0.8	0.3	1000	17.108	1192.524	501.5236		
20000	690	0.8	0.25	1000	13.771	1206.294	516.2941		
21000	689	0.8	0.25	1000	13.377	1219.671	530.6707		
22000	685	0.8	0.25	1000	13.014	1232.685	547.6849		
23000	680	0.8	0.25	1000	12.61	1245.295	565.2948		
24000	678	0.8	0.25	1000	12.217	1257.512	579.5118		
25000	674	0.8	0.25	1000	11.917	1269.429	595.4292		
26000	668	0.8	0.2	1000	9.279	1278.708	610.7082		
27000	665	0.8	0.2	1000	9.0469	1287.755	622.7551		
28000	661	0.8	0.2	1000	8.8719	1296.627	635.627		
29000	655	0.8	0.2	1000	8.6922	1305.319	650.3192		
30000	645	0.8	0.2	1000	8.4958	1313.815	668.815		
31000	640	0.8	0.2	1000	8.2609	1322.076	682.0759		
32000	630	0.8	0.2	1000	8.1003	1330.176	700.1761		
33000	620	0.8	0.2	1000	7.8909	1338.067	718.067		
34000	612	0.8	0.2	1000	7.6943	1345.761	733.7613		
35000	605	0.8	0.2	1000	7.5297	1353.291	748.291		
36000	615	0.8	0.2	1000	7.3835	1360.674	745.6745		
37000	630	0.8	0.2	1000	7.4094	1368.084	738.0839		
38000	650	0.8	0.2	1000	7.4856	1375.569	725.5695		

Johnstone Stream advance

Up-ice dist. (m)	Bedrock elevation (m)	Shape factor	Basal shear (bar)	Step Length (m)	Change (m)	Calculated Elevation (m)	Centerline Thickness (m)	Moraine crest (m)	Ice thickness (m)
	650					680	30	680	30
1000	660					720	60	720	60
2000	675					760	85	760	85
3000	690	0.8	0.1	1000	32.5	792.5	102.5	790	100
4000	695	0.8	0.1	1000	26.951	819.4512	124.4512	810	115
5000	693	0.8	0.1	1000	22.197	841.6487	148.6487	820	127
6000	691	0.8	0.1	1000	18.584	860.2328	169.2328	840	149
7000	691	0.8	0.1	1000	16.324	876.5564	185.5564	860	169
8000	691	0.8	0.15	1000	22.331	898.8879	207.8879	880	189
9000	691	0.8	0.15	1000	19.933	918.8205	227.8205	900	209
10000	691	0.8	0.15	1000	18.189	937.0092	246.0092	920	229
11000	691	0.8	0.15	1000	16.844	953.8531	262.8531		
12000	690	0.8	0.15	1000	15.765	969.6176	279.6176		
13000	689	0.8	0.15	1000	14.819	984.4369	295.4369		
14000	685	0.8	0.15	1000	14.026	998.4628	313.4628		
15000	680	0.8	0.15	1000	13.219	1011.682	331.682		
16000	678	0.8	0.15	1000	12.493	1024.175	346.1752		
17000	674	0.8	0.15	1000	11.97	1036.145	362.1453		
18000	668	0.8	0.15	1000	11.442	1047.588	379.5875		
19000	665	0.8	0.15	1000	10.916	1058.504	393.504		
20000	661	0.8	0.15	1000	10.53	1069.034	408.0344		
21000	655	0.8	0.15	1000	10.155	1079.19	424.1897		
22000	645	0.8	0.15	1000	9.7686	1088.958	443.9584		
23000	640	0.8	0.15	1000	9.3336	1098.292	458.292		
24000	630	0.8	0.15	1000	9.0417	1107.334	477.3337		
25000	620	0.8	0.15	1000	8.681	1116.015	496.0148		
26000	612	0.8	0.15	1000	8.3541	1124.369	512.3689		
27000	605	0.8	0.15	1000	8.0874	1132.456	527.4563		
28000	615	0.8	0.15	1000	7.8561	1140.312	525.3124		
29000	630	0.8	0.15	1000	7.8882	1148.201	518.2006		
30000	650	0.8	0.15	1000	7.9964	1156.197	506.197		

Lake Heron advance

Up-ice dist. (m)	Bedrock elevation (m)	Shape factor	Basal shear (bar)	Step Length (m)	Change (m)	Calculated Elevation (m)	Centerline Thickness (m)	Moraine crest (m)	Ice thickness (m)
0	675	0.8	0.1	1000		710	35	710	20
1000	690	0.8	0.1	1000	79	730	40	730	35
2000	695	0.8	0.1	1000	69.063	760	65	760	67
3000	693	0.8	0.1	1000	42.5	790	97	790	99
4000	691	0.8	0.1	1000	28.479	818.4794	127.4794	810	119
5000	691	0.8	0.1	1000	21.67	840.1496	149.1496	840	149
6000	691	0.8	0.1	1000	18.522	858.6712	167.6712	860	169
7000	691	0.8	0.1	1000	16.476	875.1469	184.1469	880	189
8000	691	0.8	0.1	1000	15.002	890.1485	199.1485	900	209
9000	691	0.8	0.1	1000	13.872	904.0201	213.0201		
10000	690	0.8	0.1	1000	12.968	916.9883	226.9883		
11000	689	0.8	0.1	1000	12.17	929.1586	240.1586		
12000	685	0.8	0.1	1000	11.503	940.6614	255.6614		
13000	680	0.8	0.1	1000	10.805	951.4667	271.4667		
14000	678	0.8	0.1	1000	10.176	961.6429	283.6429		
15000	674	0.8	0.1	1000	9.7394	971.3823	297.3823		
16000	668	0.8	0.1	1000	9.2894	980.6717	312.6717		
17000	665	0.8	0.1	1000	8.8351	989.5068	324.5068		
18000	661	0.8	0.1	1000	8.5129	998.0197	337.0197		
19000	655	0.8	0.1	1000	8.1968	1006.217	351.2166		
20000	645	0.8	0.1	1000	7.8655	1014.082	369.0821		
21000	640	0.8	0.1	1000	7.4848	1021.567	381.5669		
22000	630	0.8	0.1	1000	7.2399	1028.807	398.8068		
23000	620	0.8	0.1	1000	6.9269	1035.734	415.7337		
24000	612	0.8	0.1	1000	6.6449	1042.379	430.3785		
25000	605	0.8	0.1	1000	6.4188	1048.797	443.7973		
26000	615	0.8	0.1	1000	6.2247	1055.022	440.022		
27000	630	0.8	0.1	1000	6.2781	1061.3	431.3001		

Lake Stream advance

Up-ice dist. (m)	Bedrock elevation (m)	Shape factor	Basal shear (bar)	Step Length (m)	Change (m)	Calculated Elevation (m)	Centerline Thickness (m)	Moraine crest (m)	Ice thickness (m)
0	605					680	75	680	75
1000	615	0.8	0.1	1000	37	740	125	740	125
2000	630	0.8	0.1	1000	22.1	800	170	800	150
3000	650	0.8	0.1	1000	16.25	820	170	820	820

10 Appendix B: till fabric data

Trend	Plunge
140	15
90	26
150	18
84	24
334	60
142	1
235	5
140	12
161	0
100	20
213	7
40	56
278	23
120	6
340	30
287	12
155	22
2	24
340	8
122	18
310	30
137	18
348	30
110	60
124	20

Trend	Plunge
157	0
40	20
15	32
147	5
45	43
54	42
165	20
199	1
142	22
312	60
58	50
170	0
58	32
62	32
345	80
153	32
69	30
189	3
135	60
316	45
153	0
182	51
116	42
105	18
61	29

11 Appendix C: SED and C14 data

SAMPLE SITE : Emily Hill, Lake Heron
COLLAB/COLLECTOR : Jeremy and Helen Pugh DATE : 19/10/07

SAMPLE ID	**HER-EH-1-1**	**HER-EH-1-2**
Geographic Locality	Emily Hill 2 moraine in saddle on Emily Hill	Emily Hill 2 moraine in saddle on Emily Hill
Grid Ref (Lat/Long)	E2367736 / N5738867	E2367777 / N5738944
Altitude (asl)	859m	872m
Rock Type / Lithology	Greywacke	Greywacke
Glacial Stage / Age	LGM	LGM
Site Description	Terminal moraine ridge	Latero-terminal moraine ridge
Surface position	On crest	On crest
Depth / Thickness	4-5 cm	4-5 cm
Boulder dimensions	390 x 420 x 200 cm	510 x 800 x 490 cm
Topographic Shading	340-360 = 2º / 360-40 = 5º / 40-100 = 10º / 100-200 = 4º / 200-340 = 1º	360-20 = 6º / 20-40 = 10º / 40-60 = 11º / 60 – 100 = 2º / 100-190 = 1º / 190-200 = 2º / 200-360 = 1º
Comment	Sample retrieval focused on quartz veins.	Broken and fractured surface. Sample retrieval focused on quartz veins.

SAMPLE SITE : Staces Tarn, Lake Heron
COLLAB/COLLECTOR : Jeremy and Penny Pugh DATE : 22/11/07

SAMPLE ID	**LH-ST-1-1**	**LH-ST-1-2**
Geographic Locality	Staces Tarn terminal moraine	Staces Tarn terminal moraine
Grid Ref (Lat/Long)	E2358238 / N5751559	E2358212 / N5751632
Altitude (asl)	1207m	1200m
Rock Type / Lithology	Greywacke	Greywacke
Glacial Stage / Age	120,000?	120,000?
Site Description	Terminal moraine ridge	Terminal moraine ridge
Surface position	On crest	On crest
Surface character	Smoothed, rounded, weathered, fractured, covered in lichen. Grainy surface.	Smoothed, rounded, weathered, fractured, covered in lichen. Grainy surface.
Depth / Thickness	4-5 cm	4-5 cm
Boulder dimensions	300 x 350 x 100 cm	100 x 100 x 400 cm
Topographic Shading	20-160 = 1º / 160-210 = 2º / 210-280 = 1º / 280-320 = 5º / 320-20 = 6º	40-230 = 1º / 230-20 = 7º / 20-40 = 3º

SAMPLE SITE : Johnstone Stream moraine, Lake Heron
COLLAB/COLLECTOR : Henrik Rother and Jeremy Pugh DATE : 17/10/06

SAMPLE ID	**Ran – LE – I - 1**	**Ran – LE – I - 3**
Geographic Locality	Rangitata, Lake Emily Moraine (I), opposite Isolated Hill	Rangitata, Lake Emily Moraine (I), opposite Isolated Hill
Grid Ref (Lat/Long)	E2362756 / N5740319	E2362447 / N5739890
Altitude (asl)	665 m	683 m
Rock Type / Lithology	Greywacke	Greywacke
Glacial Stage / Age	LGM	LGM
Site Description	Moraine ridge	Moraine ridge
Surface position	Near crest	At crest
Depth / Thickness	5 cm	5 cm
Boulder dimensions	160 x 130 x 220 cm	350 x 190 x 110
Topographic Shading	Uniform horizon shielding 6º	Uniform horizon shielding 6º

SAMPLE SITE : Johnstone Stream moraine, Lake Heron
COLLAB/COLLECTOR : Henrik Rother and Jeremy Pugh DATE : 17/10/06

SAMPLE ID	**Ran – LE – I - 4**
Geographic Locality	Rangitata, Lake Emily Moraine (I), opposite Isolated Hill
Grid Ref (Lat/Long)	E2362470 / N5739901
Altitude (asl)	682 m
Rock Type / Lithology	Greywacke
Glacial Stage / Age	LGM
Site Description	Moraine ridge
Surface position	On upper slope
Surface character	
Depth / Thickness	5 cm
Boulder dimensions	210 x 120 x 100 cm
Topographic Shading	Uniform horizon shielding 6º

RAFTER
GNS SCIENCE

Accelerator Mass Spectrometry Result

NZA	**29676**
R	29835
Job No	64305
Measured	23-May-08
TW No	2266
Issued	28-May-08
	Page 1 of 1

Sample ID	Charcoal sample (Stacey's Tarn)
Description	Charcoal
Fraction Dated	charcoal
Submitter	Jeremy Pugh Department of Geological Sciences, University of Canterbury

* **Radiocarbon Age**		**4644 ± 40 BP**		$\delta^{13}C$ =	-26.5 ‰
** **Per cent modern** =	55.7 ± 0.28	$\delta^{14}C$ =	-444.7 ± 2.8 ‰	$\Delta^{14}C$ =	-443 ± 2.8 ‰

* Reported age is the conventional radiocarbon age before present (BP)

** Per cent modern means absolute per cent modern relative to the NBS oxalic acid standard (HOxI) corrected for decay since 1950.

Age, $\Delta^{14}C$, $\delta^{14}C$ and absolute per cent modern are as defined by Stuiver Polach, Radiocarbon 19:355-363 (1977)

Sample Treatment Details

Sample consisted of 3 big chunks of pale gray soil, and small amount of black charcoal can be seen. A lot of small whit "ball" on surface. Microscopic exam revealed big chunks of pale gray soil, a lot of plant materials were visible, and a lot of white ball-like stuff, might be"eggs, shells or forams or…" Most charcoal were buried in the soil and really hard to separate them. Picked out charcoal as many as possible with tweezers. Treated with A/A/A and dried in vacuum oven.

Stored	remainder
Comments	There is not enough charcoal in the remainder, but plenty of plant material can be dated.

The reported errors comprise statistical errors in sample and standard determinations, combined in quadrature with a system error component based on the analysis of an ongoing series of measurements on an oxalic acid standard.
For the present result the system error component is conservatively estimated as 0% (= ± 0 radiocarbon years).

National Isotope Centre, Institute of Geological and Nuclear Sciences Ltd (GNS Science)
PO Box 31-312 Lower Hutt, New Zealand Fax +64 4 570 4657 Phone +64 4 570 4644
www.RafterRadiocarbon.co.nz

INSTITUTE OF GEOLOGICAL AND NUCLEAR SCIENCES LTD.
PO Box 31312, Lower Hutt, New Zealand
Phone (+64 4) 570 4671, Fax (+64 4) 570 4657

RADIOCARBON CALIBRATION REPORT

NZA-29676 CONVENTIONAL RADIOCARBON AGE 4644 ± 40 years BP

Southern Hemisphere Atmospheric data from McCormac et al (2004);
FG McCormac, AG Hogg, PG Blackwell, CE Buck, TFG Higham, and PJ Reimer (2004)
Radiocarbon 46, 1087-1092

CALIBRATED AGE in terms of confidence intervals (Smoothing parameter: 0, Offset: 0)

68% confidence interval is	3495 BC to 3455 BC 5444 BP to 5404 BP (18.9% of area)
plus	3375 BC to 3330 BC 5324 BP to 5279 BP (28.7% of area)
plus	3213 BC to 3185 BC 5162 BP to 5134 BP (10.5% of area)
plus	3154 BC to 3125 BC 5103 BP to 5074 BP (9.8% of area)
95% confidence interval is	3509 BC to 3424 BC 5458 BP to 5373 BP (26.3% of area)
plus	3380 BC to 3263 BC 5329 BP to 5212 BP (36.1% of area)
plus	3239 BC to 3102 BC 5188 BP to 5051 BP (32.3% of area)